THE EFFECTS OF ADDITIVES ON RADIATION INDUCED DAMAGE TO

DEOXYRIBONUCLEIC ACID.

thesis submitted for the degree of

Doctor of Philosophy

at the University of Leicester

by

Stephen Robert Langman BSc (Leicester)

Department of Chemistry

University of Leicester

June 1993

UMI Number: U058877

UMI
Dissertation Publishing

ProQuest

This thesis is dedicated to my beloved parents Patricia and David without whose love this work would not have been attempted, and to my partner Victoria without whose love it would never have been completed.

ACKNOWLEDGEMENTS.

CONTENTS

CHAPTER 1. INTRODUCTION.

1.1. Preview.

The effects of exposing living systems to radiation have been subject to intense research for many years. The results of such exposure are complex and of serious consequence to whole organisms and to individual cells. Exposure may result in cell death, mutagenesis and carcinogenesis.

Human beings are not only exposed to natural sources of radiation but also to radiation from nuclear weapons testing and nuclear industrial accidents such as the tragedy in Chernobyl. The long term effects of such exposure are still not entirely known. It seems likely that nuclear weapons will continue to proliferate and that nuclear power will play an increasing rôle as an energy source as other fuel stocks are exhausted. To ensure the future safety of workers in these industries and of society in general, a full understanding of the effects of radiation on living systems is clearly important.

The use of radiation in radio-therapy is a tremendously important method of treating certain types of cancer. Research into the mechanisms of radiation damage to the cell and the repair processes that may follow is vital to the future development of this life saving technique.

In light of these factors, the study of the effects of radiation on living systems is not simply of academic interest.

The structural integrity of cellular deoxyribonucleic acid (DNA) is vital for normal cell function. Whilst radiation induced damage to the cell is believed to be harmful in

general, it is now believed that radiation induced damage to the DNA leads to such phenomena as cell death, mutagenesis and carcinogenesis.

The studies presented here centre on both the effects of ionizing radiation on DNA and also the *radioprotective* and *radiosensitizing* effects additive compounds may have upon these. The ultimate aim is to contribute to the development of drugs which may either provide protection to living systems from the harmful effects of radiation or selectively enhance cancer radio–therapy techniques.

1.2. An overview of the effects of ionizing radiation on living systems.

The effects of exposing living systems to ionizing radiation are extremely complex and may be expressed over a wide time scale (Figure 1–1). Ionizing radiation may be defined as any radiation consisting of either directly or indirectly ionizing particles or electromagnetic quanta. Exposure of biological systems to such radiation results in the physical processes of energy deposition (timescales of 10^{-18} to 10^{-12}s). Initially energy deposition from ionizing radiation results in primary ionizations. The products of these ionizations, such as emitted electrons, may in turn cause further or secondary ionizations. The complex nature of the fundamental processes governing energy deposition and dose, and variations in these with radiation quality for a wide range of ionizing radiations is discussed by *Keifer*[1] and *Faharaziz and Rodgers*[2]. Computer models of ionization 'tracks' have been used to study the nature and variations in the density of ionization for DNA models and several radiation qualities[3]. Such areas are still subject to intense research.

The products of ionization undergo chemical reaction via radical chemistry

resulting in chemical changes to the DNA (timescales of 10^{-8}s to 10ms). Such

changes lead to biological responses within the cell. Radiation induced damage repair

may occur in two ways. Firstly 'fast' (timescales of 10ms) chemical repair of DNA

radical species by for example free thiol groups such as that of glutathione[4-5].

However the mechanisms and nature of all possible 'fast' chemical repair responses of

the cell are not completely understood. Secondly, enzymic repair of chemical

alterations to the DNA structure (described below) also occur (timescales of

minutes-hours).

Exhaustion of these repair processes by overwhelming doses of radiation may lead

to cell death (timescales of hours to days), where the ability to produce viable

progeny by mitosis is lost (this may not be expressed for several cell divisions).

However the distinction must be made that a single damage event can result in cell

death even when repair mechanism exist and function within the cell. The incorrect

repair of DNA lesions or chemical alterations may also be expressed as cell death, but

also may result in mutagenesis or carcinogenesis (timescale of years).

1.3. The chemical structure and organisation of DNA within the cell.

An understanding of the structure of DNA, not only of the isolated molecule but

also of its quaternary structure and organisation within the cell is essential to a full

understanding of the effects of radiation upon it and hence the consequences to cell

function. As initially proposed by Watson and Crick, DNA consists of two Figure
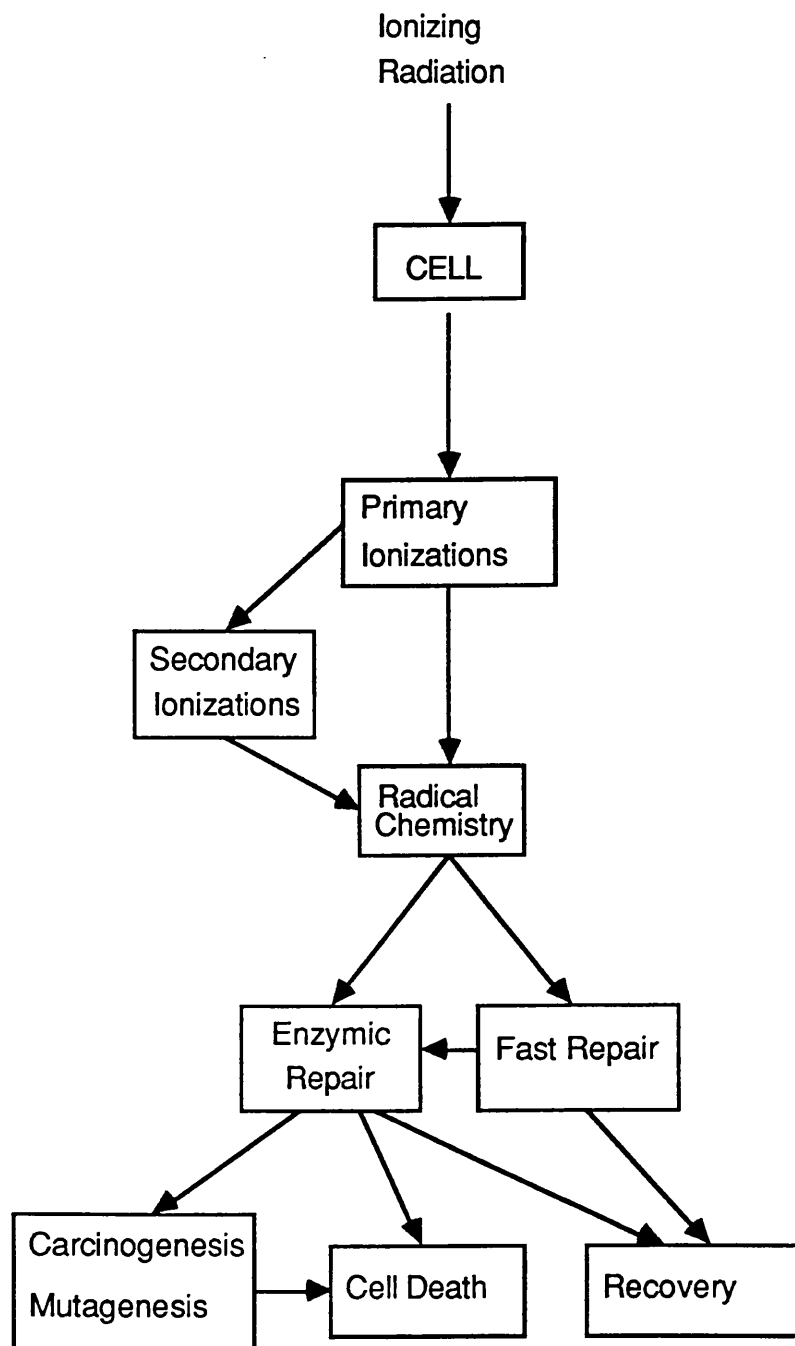
1-1. A schematic representation of the processes which occur following exposure of the cell to ionizing radiation.

anti-parallel polynucleotide chains coiled in a duplex about a common axis. The

backbone of each strand consists of deoxyribose sugar residues linked by

phosphodiester bridges between the 3'-carbon atom of one sugar residue and the

5'-carbon atom of the next (Figure 1–2i). Each deoxyribose residue is bonded to one

of four bases; guanine[G], adenine[A] (purines), thymine[T] and cytosine[C]

(pyrimidines) at the 1'-carbon atom of the deoxyribose residue via an N-glycosylic

bond. The bases are complementary between the two polynucleotide chains; the two

strands are held together by hydrogen bonding between the complementary guanine

and cytosine, and adenine and thymidine base residues. The structure and hydrogen

bonding of these base pairs is illustrated below (Figure 1–2ii).
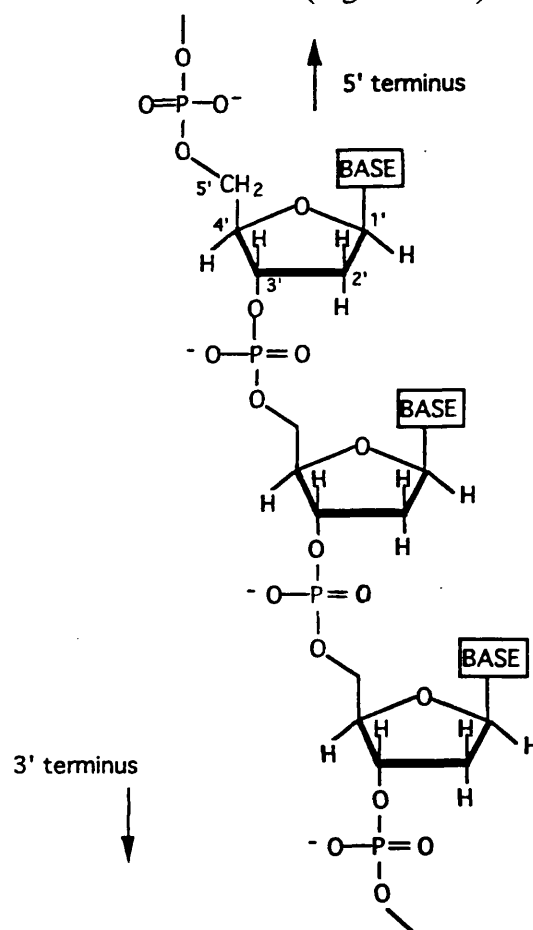
Figure 1–2. i) The primary structure of DNA, illustrating the phosphodiester chain of

the sugar phosphate backbone.

Adenine [A]   Thymine [T]

1'-C deoxyribose

1'-C deoxyribose

Guanine [G]   Cytosine [C]

1'-C deoxyribose

1'-C deoxyribose
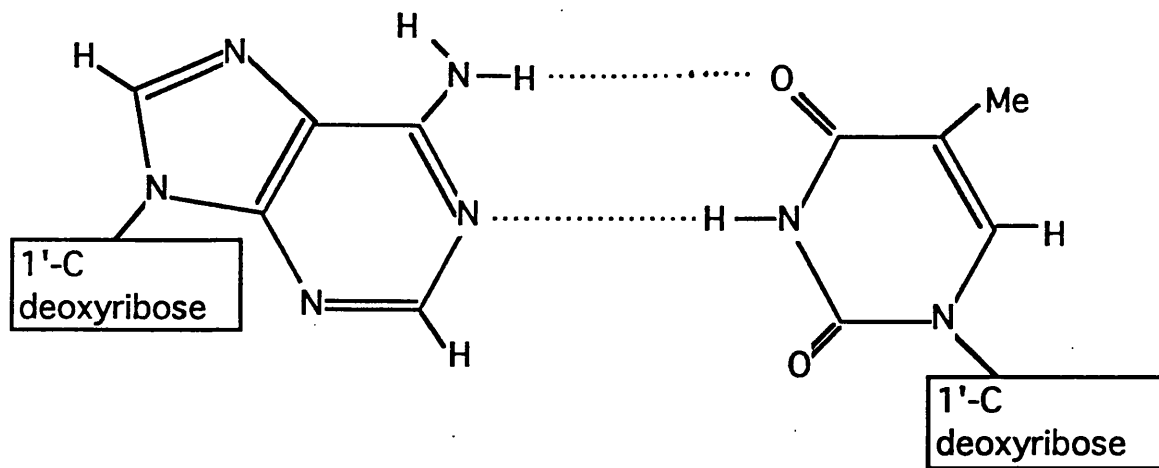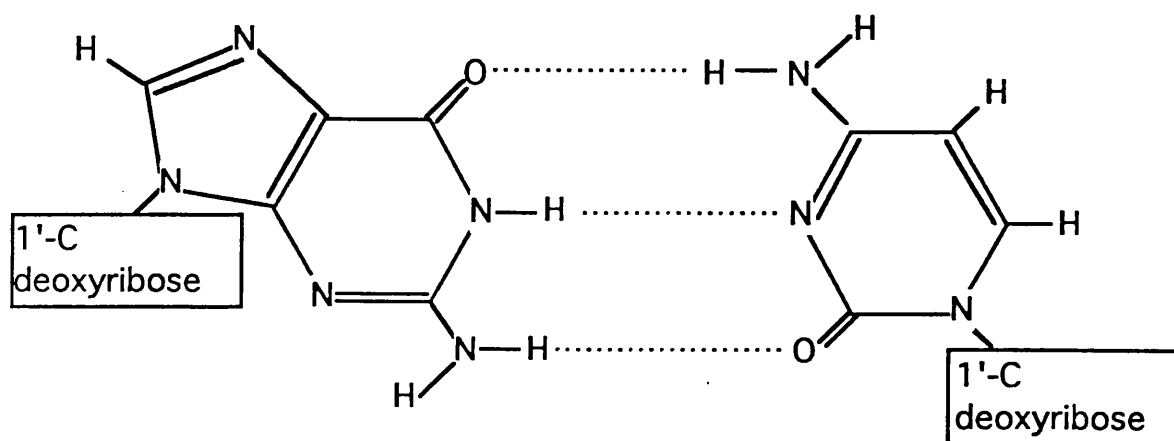
ii) The structure and hydrogen bonding of the DNA base pairs.

The resulting duplex has its base pairs stacked in parallel forming the core of the

helix, the strands being anti-parallel as the 5'-P terminus of each strand is adjacent to

the 3'-OH terminus of the complementary strand.

DNA has been shown to exist in several helical forms termed the A, B, C and D

forms. The Z form has also been determined in which the sugar-phosphate backbone

exists as a left-handed helix. The A, C and D forms predominate in low ionic strength

or at specific relative humidities; the B form is thought to be the native form[6].

In the cell, the DNA's higher order structure is highly organised since in

mammalian cells each chromosome consists of approximately 8×10^8 base pairs so

these huge molecules must not simply be accommodated within the cell nucleus but

must be arranged in such a way as to allow the genetic information of any section to

be readily copied during transcription. Within the cell the DNA exists as complexes

with protein molecules to give chromatin.

DNA is closely associated with many types of DNA binding protein which may be

subdivided into histone and non-histone chromosomal proteins. Whilst non-histone

proteins may influence DNA folding in specific regions, it is DNA binding to the

histone proteins which induces the bulk folding of the DNA into chromatin. Histone

proteins have relatively small molecular weights and contain a high proportion of the

positively charged lysine and arginine amino acid residues which facilitate

electrostatic binding to the DNA. Five types of histone protein are involved in

chromatin. The histones H2A, H2B, H3 and H4 are bound with DNA into

nucleosomes which are the fundamental repeating units of chromatin. The DNA is

bound to the outer surfaces of a histone complex which contains a pair of each of the

histones. Each nucleosome unit contains approximately 150 DNA base pairs.

Nucleosomes are linked continuously to each other via short sections of unbound

DNA of around 60 base pair units which are termed 'linker' DNA. The remaining

histone protein H1 is believed to bind adjacent nucleosomes together, further

compacting the DNA molecule. DNA-protein complexes have been reviewed by

Champoux[7] and Von Hippel[8].

1.4. Initial interaction of gamma-radiation and matter.

Ionizing radiation may be defined as any radiation consisting of directly, or indirectly ionizing particles or photons. Whilst high energy photons interact sparsely with matter, occasional interactions of these photons with an atomic nucleus or an orbital electron results in an ionization event. The principle ionizing radiation sources used for the studies presented here were ^{60}Co 1.17 and 1.31 MeV gamma-rays. The interaction of a photon of gamma-radiation with an orbital electron is thought to result in the majority of the photon's energy being given to the electron, causing the electron to be ejected from the atom. These high energy electrons may give rise to further ionizations and excitations by collision with other orbital electrons. Such emitted electrons are responsible for the majority of damage induction with indirectly ionizing radiations.

1.5. The radiation chemistry of DNA.

In order to discuss the molecular level effects of ionizing radiation, a distinction is usually drawn between the *direct* and *indirect* effects of radiation upon DNA.

The simplest view is that 'direct' effects are due to the absorption of radiation by the DNA molecule itself. 'Indirect' effects are due to the reaction of the DNA with diffusible radical products formed by the radiolysis of the DNA's solvent environment. Both indirect and direct processes may result in damage to the DNA structure. (As shown below, this simple definition leaves open an important method of damage and is therefore somewhat ambiguous.)

The radiation chemistry of DNA itself is complex, since ionizing radiation is not selectively absorbed by DNA alone. In isolated DNA systems conditions may be modified to allow the study of specific mechanisms of DNA damage by ionizing radiation. Within the cell, the environment of the DNA is dramatically more complex, however there is a large and growing body of evidence and it is now generally believed that DNA double strand breaks are the important lesion leading to most cellular effects and to cell death.

Radiation induced chemical alterations to DNA structure may take several forms;

i) **Single Strand Breaks**, ssb.

These are scissions in the sugar phosphate back bone of one strand of the duplex, and may be quantified in a number ways; the mechanisms by which such lesions may occur is discussed below.

ii) **Double Strand Breaks**, dsb.

These may be the result of a single energy deposition or the interaction of two single strand breaks formed in close proximity to each other. The contribution of these two processes are reflected by dose response curves. Frey and Hagen[9] demonstrated that direct formation of dsb in dilute aqueous solution is of very minor importance, the formation of dsb being quadratic and a result of OH derived ssb. However within the cell, for doses of above 10Gy, the dose response is linear indicating the direct formation of dsb is of far greater importance, *Radford* demonstrated that dsb may be linearly related to lethal lesions strongly supporting the belief that dsb are the important lesions leading to cell death[10]. This linear relationship has also been demonstrated by *Prise et al*[11].

11

Both single and double strand break yields have been used in the studies reported here.

iii) **Base Damage and Base Loss.**

Exposure of aqueous DNA to ionizing radiation results in a dose dependent reduction in optical absorbance at 265nm. This has been attributed to base damage and base loss.

iv) **Intramolecular and DNA-protein cross links.**

Intramolecular DNA cross link formation results in large changes in DNA melting profiles and may interfere with DNA transcription should they not be correctly repaired. DNA-protein cross links may also occur since DNA within the cell is closely associated with many proteins. Such cross links have been studied by *Oleinick*[12&13].

It must be stressed that these types of DNA damage are not mutually exclusive, in fact often quite the contrary, for example base loss or damage may induce local denaturing and strand breaks are often accompanied by base loss.

1.6. The indirect effects of ionizing radiation.

Water accounts for between 80 to 90% of the total weight of the cell, thus for indiscriminately ionizing radiation such as the gamma-radiation used in these studies, water radiolysis may also account for at least 40% of the total ionization events within the cell. The highly mobile and reactive water radiolysis products may react with the cell's biomolecules including the DNA. Thus the indirect mechanism must be

significant. An understanding of the indirect component of DNA damage can only be gained with a full understanding of the radiation chemistry of water.

In the absence of oxygen, the absorption of ionizing radiation by a water molecule results either in excitation or ionization (Reaction 1). The excited molecules undergo homolytic splitting yielding hydrogen atoms, H·, and hydroxyl radicals, OH· (Reaction 2).

$$H_2O \;\;----> \;\; H_2O^+ + e^- \qquad (1)$$

$$H_2O \;\;----> \;\; H_2O^* \;\;----> \;\; H· + OH· \qquad (2)$$
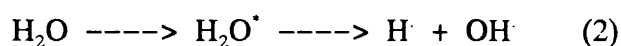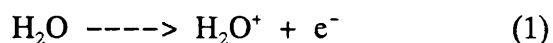
Thus the initial deposition of energy results in the formation of H·, OH·, H_2O^+ and e^-. The lifetime of the H_2O^+ species is extremely short (of the order 10^{-14}s); further reaction with water molecules results in the formation of hydronium ions, H_3O^+ and further hydroxyl radicals (Reaction 3), although a small number of electron–transfer processes may occur prior to this (Reaction 4).

$$H_2O^+ + H_2O \;\;----> \;\; H_3O^+ + OH· \qquad (3)$$

$$H_2O^+ + H_2O \;\;---- \;\; H_2O + H_2O^{+·} \qquad (4)$$
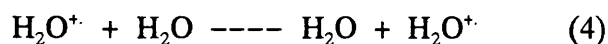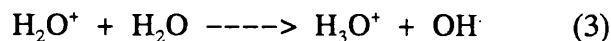
The emitted electrons may cause further excitations or ionizations or become hydrated to form aqueous electrons, e_{aq}^-, which are less reactive. Such energy dissipation results in the formation of small localised regions containing high

13

concentrations of ions and free radicals known as *spurs, blobs* or *track ends*. The

concentration of these reactive units rapidly diminishes due to dispersive diffusion,

during which further reactions may occur. Solvated electrons may react in a number

of ways (Reactions 4–8):

$$e_{aq}^- + H_3O^+ \longrightarrow H^\cdot + H_2O \qquad (5)$$

$$e_{aq}^- + H^\cdot + H_2O \longrightarrow H_2 + OH^- \qquad (6)$$

$$2e_{aq}^- + 2H_2O \longrightarrow H_2 + 2OH^- \qquad (7)$$

$$e_{aq}^- + H_2O_2 \longrightarrow OH^- + OH^\cdot \qquad (8)$$
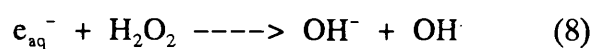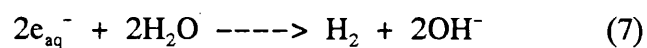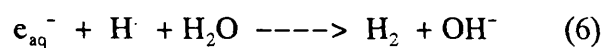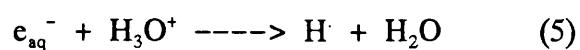
Some recombination reactions are also possible (Reactions 9–11):

$$OH^\cdot + OH^\cdot \longrightarrow H_2O_2 \qquad (9)$$

$$H^\cdot + H^\cdot \longrightarrow H_2 \qquad (10)$$

$$H^\cdot + OH^\cdot \longrightarrow H_2O \qquad (11)$$
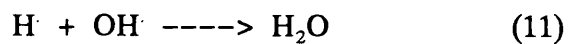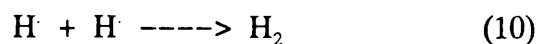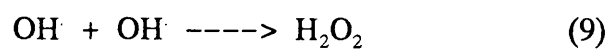
Thus overall, energy deposition within the solvent results in the formation of

hydrogen atoms, solvated electrons and hydroxyl radicals. The probabilities of these

reactions is largely dependent on the local concentrations of the reacting species

14

within the individual tracks or spurs. It must be stressed that interaction with solutes

may occur only if they are themselves within the spurs. However the reactive

hydrolysis products H·, OH· and e_{aq}^- are able to escape these spurs or tracks, and may

react with solute molecules located in close proximity. Thus cellular DNA damage

may only occur if these spurs or tracks are in relatively close proximity to the DNA.

The likelihood of such DNA damage is discussed below.

In the cell under normal circumstances, oxygen is present. The radiobiological

effects of oxygen are profound and complex, and are not discussed here. However the

reaction of molecular oxygen with solvated electrons or hydrogen atoms yields further

diffusible and reactive products which may subsequently cause DNA damage

(Reactions 12-14):

$$O_2 + H· ----> HO_2· \qquad (12)$$

$$O_2 + e_{aq}^- ----> O_2^- \qquad (13)$$

$$HO_2· + HO_2· ----> H_2O_2 + O_2 \qquad (14)$$
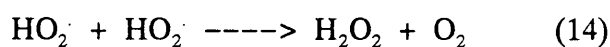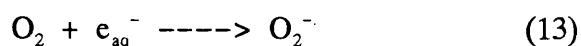
Studies using dilute aqueous DNA irradiated at room temperature have

demonstrated that OH· radicals are the principal cause of DNA damage. Extensive

studies using model compounds have shown that OH· radicals attack DNA in a

relatively unselective way.

Hydrogen atom abstraction from the sugar residues is believed to account for

approximately 20% of OH· radical attack on DNA; the most significant and well

characterised mechanism for this being H–atom abstraction from the 4' C–atom of the

deoxyribose residue. The resulting sugar radical may undergo β–elimination resulting

in a scission of the sugar–phosphate backbone, commonly termed as a strand break (

Figure 1–3).
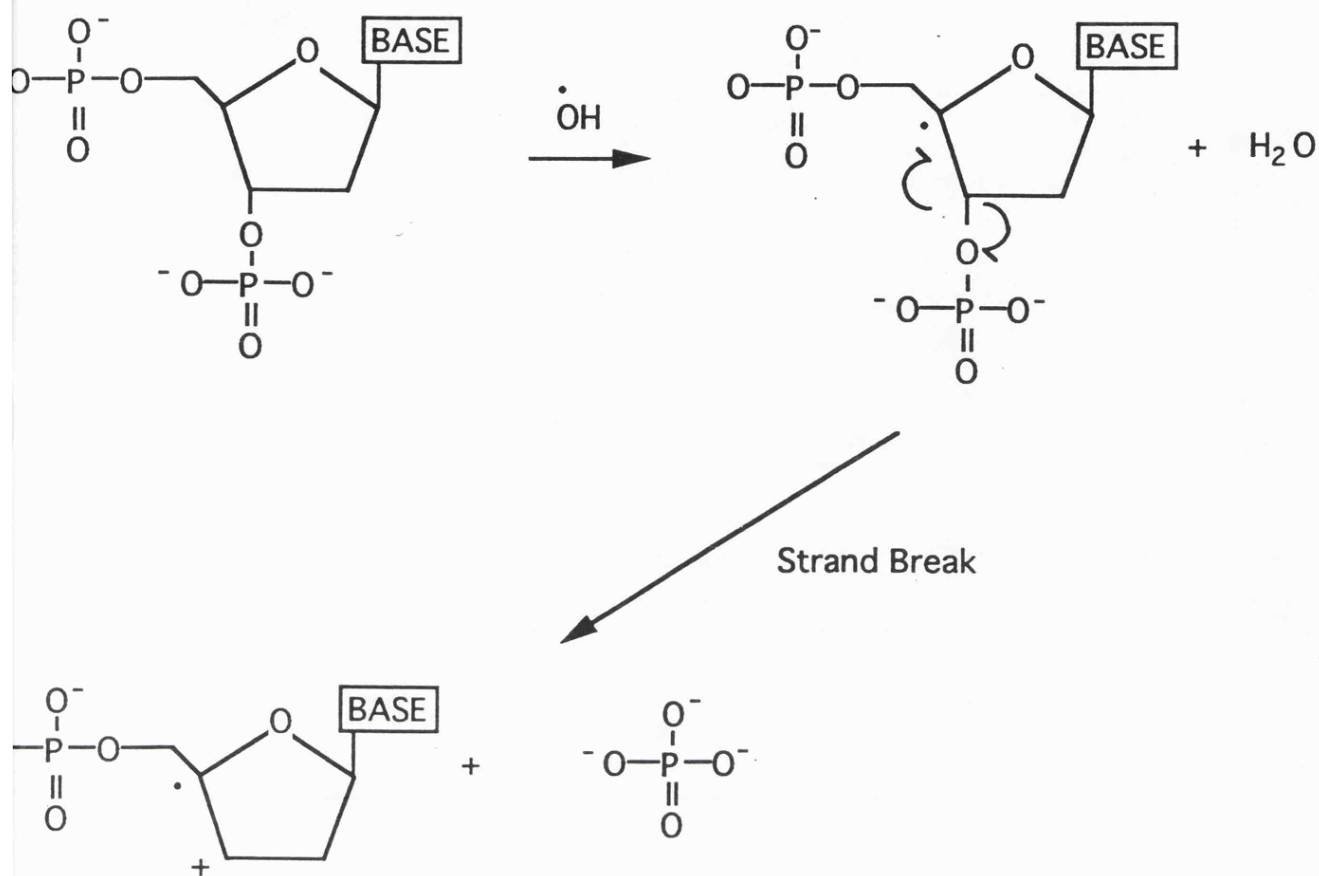
Figure 1–3. The β–elimination mechanism by which 4' C–atom centred sugar radicals may yield strand breaks.

Base–OH radical adduct formation has also been shown to lead to strand breakage and is believed to account for the majority of OH radical damage to DNA. Intramolecular H–atom transfer from the sugar residue to the base–OH radical centre with the subsequent loss of H_2O again results in sugar radical formation. The resulting sugar radical may also undergo β–elimination as described above.

DNA damage may also result from reaction with solvated electrons (e_{aq}^-), which may form radical cations centred on the pyrimidine base residues. Similar reactions to those described below for the direct effects may occur, again resulting in strand

17

breakage. The radiation chemistry of water is discussed in detail by *Faharaziz and*

Rogers[2].

1.7. The direct effects of ionizing radiation.

Direct irradiation results in absorption of energy by DNA and yields electron–loss and electron–gain centres within the molecule itself (DNA ––––> DNA^+ + DNA^-). Partial π–orbital overlap within the DNA's central base stack is believed to allow both 'hole' and electron migration by charge transfer. The precise mechanism of this process is not fully understood. Various mechanisms for charge transfer processes are discussed by Baverstock and Cundall[14]. Such electron–loss and electron–gain centres may be studied by electron spin resonance (esr) spectroscopy.

Early esr studies of irradiated *dry* oriented DNA fibres were carried out by Gräslund *et al*[15,16]. Studies of frozen aqueous DNA samples irradiated at low temperatures (usually 77K) have been carried out by Hüttermann *et al*[17], Gregoli *et al*[18] and Symons *et al*[19].

Frozen aqueous DNA samples are used in the studies presented here and it is necessary to consider the nature of this system in order to understand the results. During freezing, ice crystallite formation occurs with the exclusion of solute molecules. These crystallites bind most of the water molecules of the system. In studies using $HOD-D_2O$, ice crystallite water molecules are observed as a narrow band at *ca.* 3280 cm^{-1} superimposed over a weak broad band assigned to solvating water. The solvating water has a glass like structure. The water molecules strongly interact with both the $(RO)_2PO_2^-$ residues of the DNA and their sodium counter ions, and the base residues are also strongly solvated. Under these conditions irradiation results in direct irradiation of DNA which is phase separated from the bulk ice phase. Hydroxyl radicals formed within the ice phase are trapped and may not cause DNA

damage. Annealing of samples to 130K results in the irreversible loss of these radicals; this corresponds with the loss of OH radicals in pure ice. The product H_2O_2 remains trapped within the ice phase until melting. The great advantage of this system is that additive compounds are incorporated into the DNA solvating regions and their effects upon direct DNA damage can be studied. Studies incorporating hydrogen peroxide into the DNA solvating region have demonstrated that DNA damage from OH radicals formed within the DNA solvating region does occur, to give primarily, sugar centred radicals[20]. Such sugar radicals are not observed in pure aqueous samples, supporting the premise that the observed OH radicals are trapped within the ice crystallites and do not enter the DNA phase.

Early esr studies characterised the primary electron loss and electron gain centres as being guanine cations [G^+] and thymine anions [T^-][18,21]. The electron loss centre is still thought to be localised on guanine [G^+] (Figure 1–4i.), however recent publications have suggested that electron capture, whilst being largely centred on the pyrimidine bases, is not a selective process and that cytosine [C^-] (Figure 1–4ii.) and thymine [T^-] (Figure 1–4iii.) radical anions are formed[22-24]. Although a strong case for electron capture by thymine residues has been put forward[25], the site of electron localisation remains unresolved.

FIG 1-4.i.

FIG 1-4.ii.

C^{-} ·
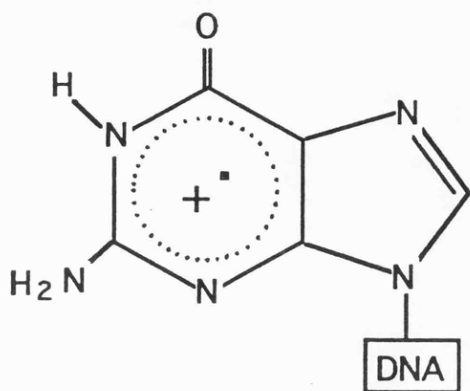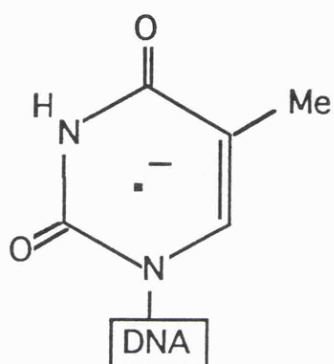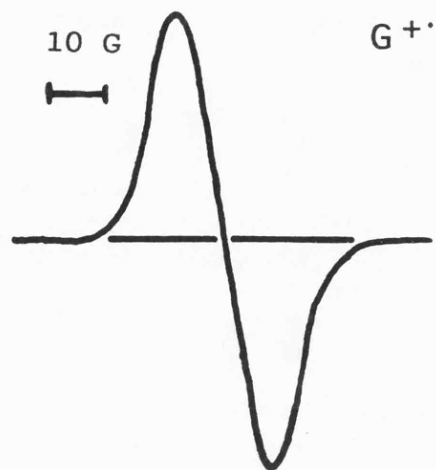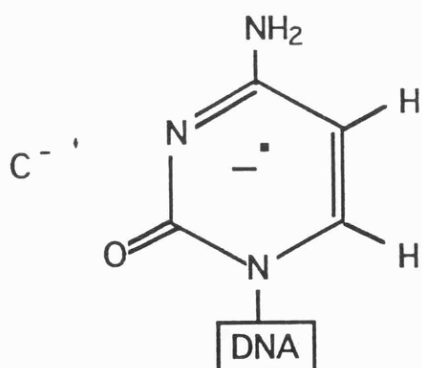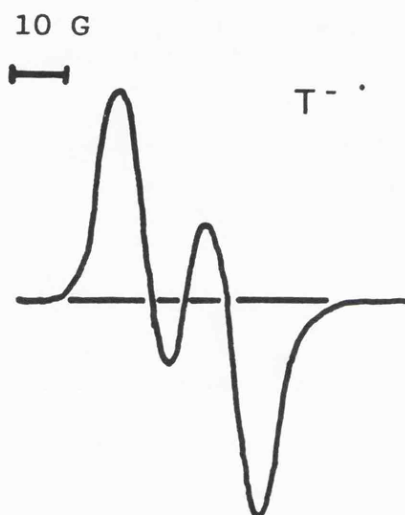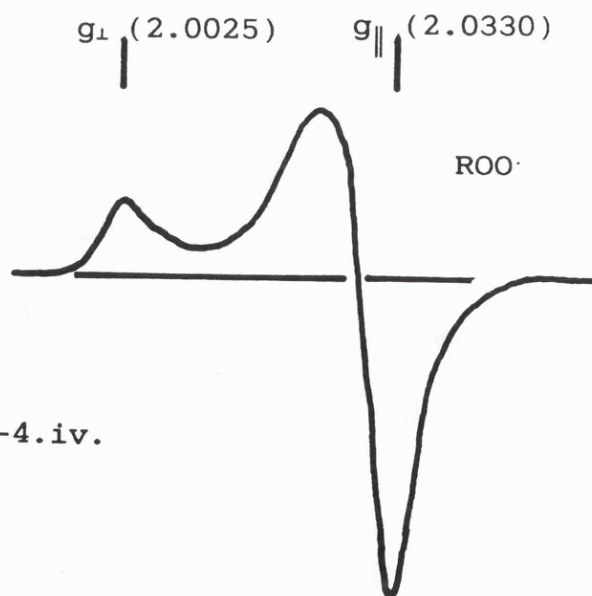
FIG 1-4.iii.

FIG 1-4.iv.

Figure 1-4.

i) The structure and first derivative X–band esr spectrum of G^{+}·.

ii) The structure C^{-}·.

iii) The structure and first derivative X–band esr spectrum of T^{-}·.

iv) The first derivative X–band esr spectrum of RO_2·.

The primary DNA radical ions G^+ and C^-/T^- are stable at 77K. Their esr spectra

are seen as a composite of the G^+ singlet (25 G) and the indistinguishable doublets

(17 G) of C^-/T^-. In addition to these features, the 1st derivative spectrum at 77K also

contains the parallel and perpendicular features of OH radicals which are trapped

within the ice crystallites (Figure 1–5). Annealing to 130K results in the irreversible

loss of hydroxyl radicals (the product H_2O_2 remaining trapped in the ice crystallites

until thawing), leaving equal yields of G^+ and pyrimidine anions C^-/T^-. On further

annealing, T^- is readily protonated from the solvent at the 6' C–atom, forming TH

(Figure 1–6i.). TH gives rise to an unambiguously assigned octet esr spectrum

(Figure1–6ii.) with the corresponding loss of the doublet feature from the central

DNA composite feature. TH continues to increase in intensity until a maximum at *ca.*

210K. A plot of the intensities of these radicals versus temperature demonstrates their

behaviour on annealing (Figure 1–7.).

The presence of oxygen results in the formation of the uncharacterised RO_2^-

species by reaction at the anion centre which results in reduction in TH yield on

annealing (Figure 1–4iv.).

The mechanism by which these radical centres give rise to strand breakage has not

been revealed by esr studies. DNA strand breaks may be quantified in supercoiled

plasmid DNA. After exposure to ionizing radiation single strand breaks result in the

relaxation of supercoiling in the plasmid pBR 322, resulting in an open circular form.

Double strand breaks result in relaxation into a linear form. The three forms of the

this DNA may be separated by gel electrophoresis and from the relative intensities of

the resulting bands, the yield of these two types of lesions may be quantified. This is

represented schematically in figure 1-8.
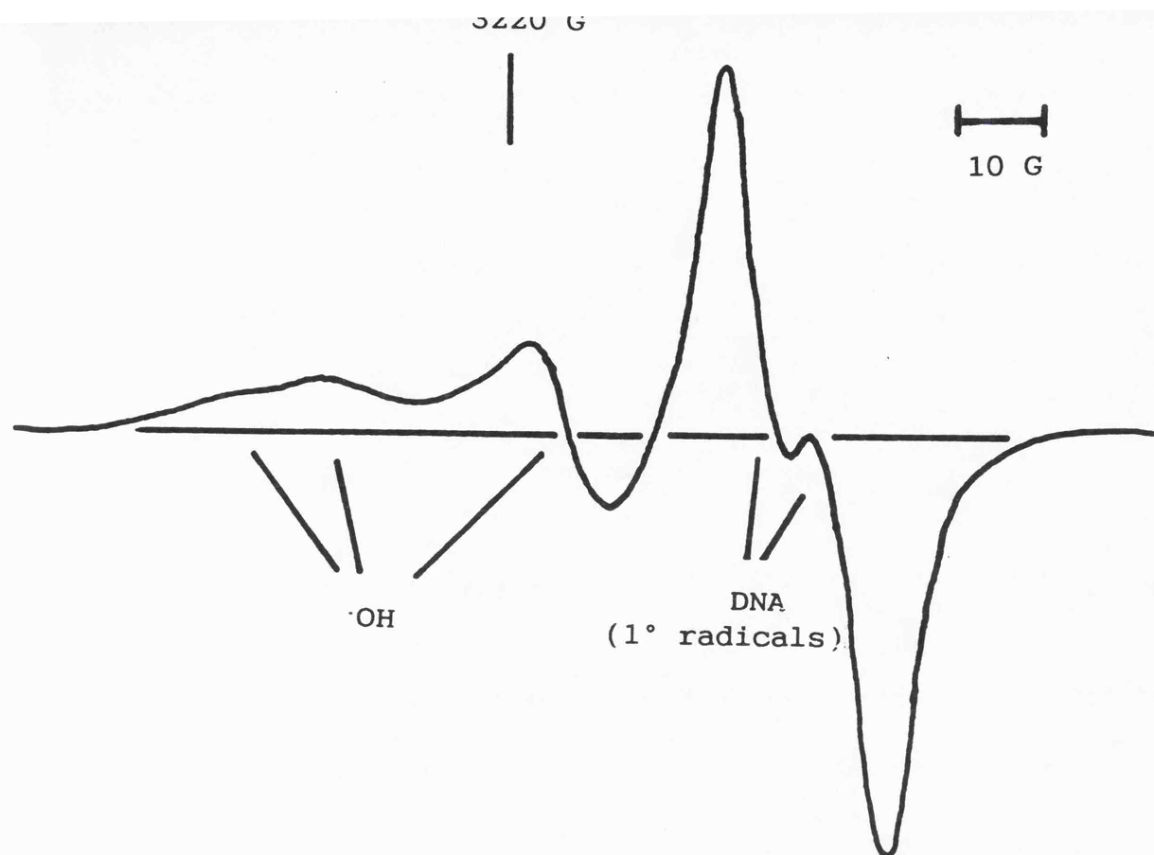
Figure 1-5. First-derivative X-band esr spectrum of deoxygenated aqueous DNA after exposure to ^{60}Co gamma-rays at 77K, showing features assigned to OH radicals and composite features of DNA primary radicals, guanine cations [G$^+$] and pyrimidine anions [C$^-$/T$^-$].
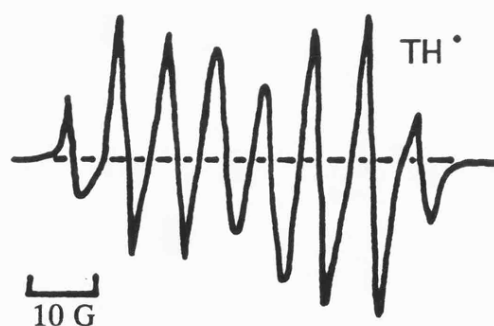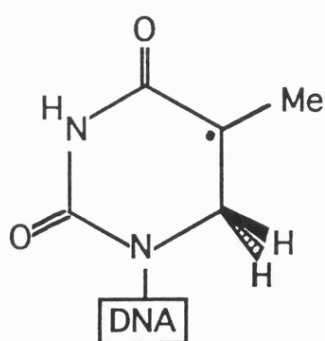
Figure 1-6. The structure and first derivative esr spectrum of TH radicals containing the characteristic octet feature.

24
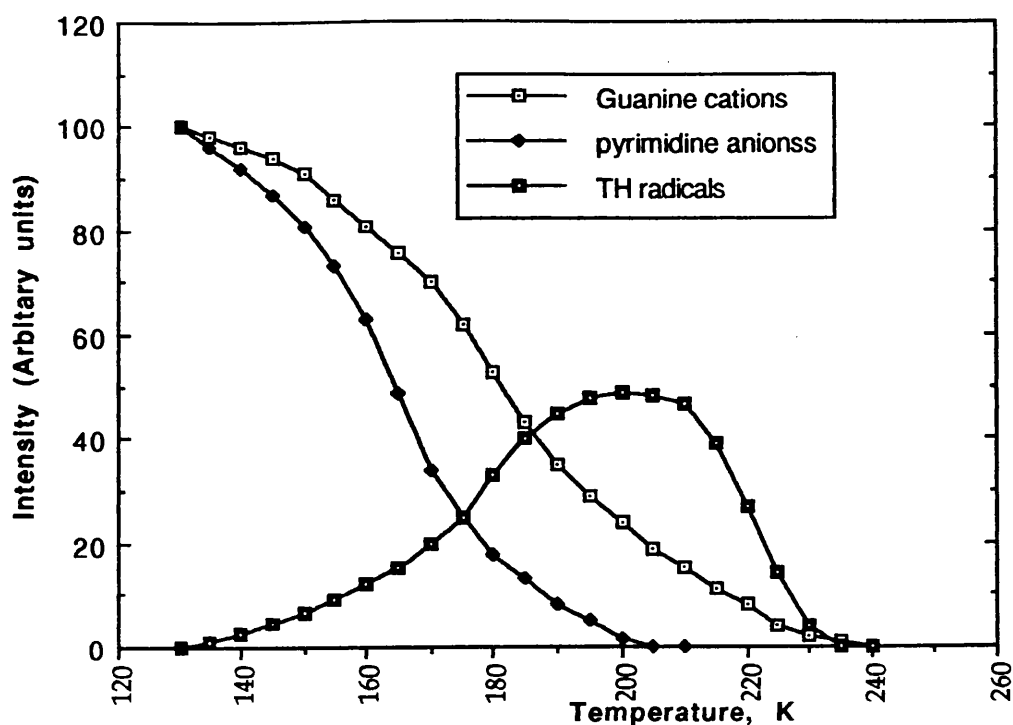
Figure 1-7. A plot of the intensities of DNA primary and secondary radical features versus temperature.

Conditions of direct damage may be produced by irradiation at 77K. Such studies have demonstrated that *ca.* 25% of the DNA primary radicals formed under direct damage conditions give rise to strand breakage[26,27].

It has been suggested that strand breakage occurs via neutral sugar residue centred radicals, and that this is likely to occur as a result of hydrogen atom transfer from the sugar residues positioned close to the base centred radicals[28,29]. In fact several such sugar C-H units are `poised' close to base radical centres, and for TH this seems a likely mechanism to form sugar centred radicals which may in turn decay to yield strand breaks (Figure 1-9). This mechanism has been further supported by the report that TH_2 residues are a major product of aqueous DNA irradiation at 77K[30].

The mechanism by which G⁺ centres may yield strand breaks is less clear, reaction with water molecules may give rise to G˙OH or G˙ centres which may in turn yield sugar radicals by the same route as TH˙ above.
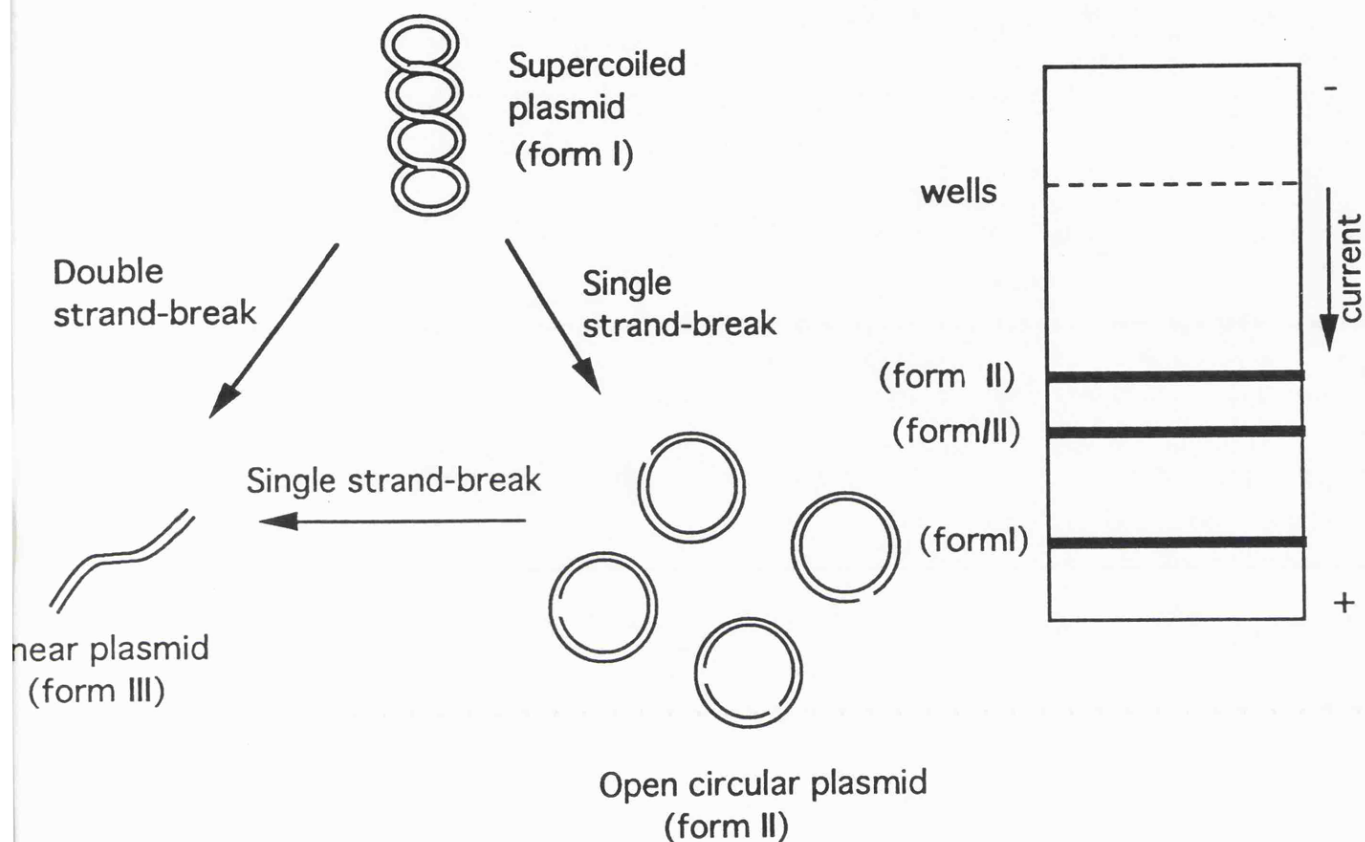
Figure 1–8. Schematic representation intact supercoiled, open circular and linear forms of pBR 322 plasmid DNA.

1.8. The significance of indirect and direct components of total DNA damage within the cell.

Experiments with dilute aqueous DNA demonstrate that the majority of initial energy deposition occurs within the solvent and that DNA damage a largely due to chemical attack by solvent radiolysis products. It has been shown that hydroxyl radical [OH˙] induced DNA damage dominates total DNA damage in dilute aqueous

26

systems irradiated at room temperature. However the DNA environment within the cell is radically different and direct DNA damage by ionizing radiation is of much greater significance.

Whilst the bulk of the cell does chiefly consist of water, most of this is confined to the cytoplasm. Highly reactive water radiolysis products formed within the cytoplasm cannot reasonably be considered to cause DNA damage.

Within the nucleus, DNA is densely compacted with histone proteins into chromatin with the exclusion of much water, thus the effective solvent target is greatly reduced compared with that of aqueous isolated DNA systems. Hydroxyl radicals react relatively unselectively and, given the high concentration of many other biomolecules such as ribonucleic acids [RNA's] and non–histone proteins within the nucleus, only limited OH radical damage to DNA may be expected. Consequently solvent radiolysis product derived DNA damage, predominantly due to OH radicals, is less likely.

Within the nuclear environment of DNA, the high abundance of polar macromolecules (such as DNA itself) results in perturbations in the water structure. The perturbed molecules form solvating regions in which the primary water radiolysis products, which are non–solvated or *dry* (H_2O ----> $H_2O^+_{dry}$ + e^-_{dry}), are transferred to the DNA by charge transfer before the more long–lived molecular water radiolysis products are formed. Radiation studies using hydroxyl radical scavengers in mammalian cells[1] have shown significant DNA damage despite the efficient scavenging of OH radicals, which must be due at least in part to direct damage.
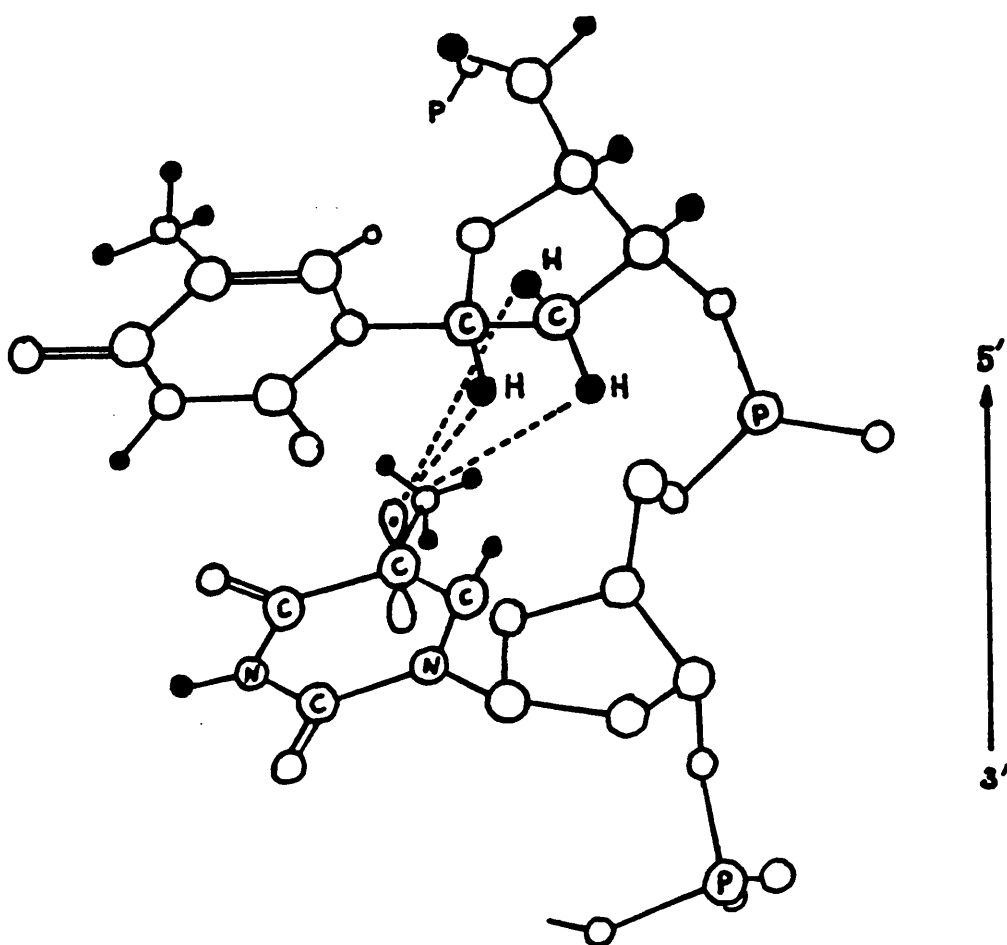
Figure 1-9. Local structure of a TH radical and surrounding DNA, showing how a

`poised' hydrogen atom may be transfered to form a sugar radical.

References for Chapter 1.

1. J. Kiefer, *Biological Radiation Effects*, Springer–Verlag, Berlin, 1990.

2. *Radiation Chemistry*, ed. Farhataziz and M.A. Rodgers, VCH Publisher, Inc. 1987.

3. D.E. Charlton, *Int. J. Radiat. Biol.*, 1989, **56 (1)**, 63–69.

4. J. Midander, P.J. Deschavanne, D. Debiey, E.P. Malaise and L. Revesz, *Int. J. Radiat. Biol.*, 1986, **49**, 403–413.

5. P.M. Cullis, G.D.D. Jones, J. Lea, M.C.R. Symons and M. Sweeny, *J. Chem. Soc., Perkin Trans. II*, 1987, 1907–1914.

6. S.B. Zimmerman, *Ann. Rev. Biochem.*, 1982, **51**, 395.

7. J.J. Champoux, *Ann. Rev. Biochem.*, 1978, **47**, 449.

8. P. Von Hippel, *Biol. Reul. Develop.*, 1979, **1**, 279.

9. R. Frey and U. Hagen, *Radiat. Env. Biophys.,* 1974, **11**, 125–133.

10. I.R. Radford., *Int. J. Radiat. Biol.*, 1985, **49**, 45–54.

11. K.M. Prise, S. Davies and B.D. Micheal., *Int. J. Radiat. Biol.*, 1989, **56** (6),

943–950.

12. Song–Mao Chiu, L.R. Friedman and N.L. Oleinick.,*Int. J. Radiat. Biol.*, 1990, **58**

(2), 943–950.

13. K.D. Held, J. Mirro, D.C. Melder, W.F. Blakely, N.L. Oleinick and Song–Mao

Chiu., *Radiation Research,* 1990, **123(3)**, 268–274.

14. K.F. Baverstock and R.B. Cundall., *Radiat. Phys. Chem.*, 1988, **32** (3), 553–556.

15. A. Gräslund, A. Ehrenberg, A. Rupprecht and G. Ström., *Biochim. Biophys. Acta.*,

1971, **254**, 172.

16. A. Gräslund, A. Ehrenberg and A. Rupprecht., *J. Radiat. Biol.*, 1977, **31**, 145.

17. J. Hüttermann, K. Voit, H. Oloff, W. Köhnlein, A. Gräslund and A. Rupprecht.,

Faraday Discuss. Chem. Soc., 1984, **78**, 135.

18. S. Gregoli, M. Olast and and A.J. Bertinchamps, *Radiat. Res.*, 1982, **89**, 238.

19. M.C.R. Symons, *J. Chem. Soc., Perkin Trans. I*, 1987, **83**, 1–11.

20. M.C.R. Symons, *J. Chem. Soc., Perkin Trans.*

21. M.D. Sevilla, *"Mechanisms for Radiation Damage in DNA Constituents and DNA"* in "Excited States in Organic Chemistry and Biochemistry," eds: B. Pullman and N. Goldblum, Reidel, Dordrecht, Holland, 1977, 15–26.

22. W.A. Bernhard, *J. Phys. Chem.*, 1989, **93**, 2187.

23. J. Hüttermann, *Free. Rad. Res. Commun.*, 1989, **6**, 103.

24. Proceeding of the International Conference of Free Radical and Radiation Induced Damage to DNA, *Free Radical Commun.*, 1989.

25. P.M. Cullis, I. Podmore, M. Lawson, M.C.R. Symons, B. Dalgarno and J. McClymont., *J. Chem. Soc., Chem. Commun.*, 1989, **15**, 1003–1005.

26. P.J. Boon, P.M. Cullis, M.C.R. Symons and B.W. Wren., *J. Chem. Soc., Perkin Trans. II*, 1984, 1393.

27. P.J. Boon, P.M. Cullis, M.C.R. Symons and B.W. Wren., *J. Chem. Soc., Perkin Trans. II*, 1985, 1057.

28. P.M. Cullis, S.R. Langman, I.D. Podmore and M.C.R. Symons, *J. Chem. Soc., Perkin Trans.*, 1990, **86**, 3267.

29. P.M. Cullis and M.C.R. Symons, in *Mechanisms of DNA Damage and Repair*, ed.

M.Simic, L. Grossman and A.C. Upton, Plenum, New York, 1985, 29.

30. J. Cadet, personal communication.

CHAPTER 2. EXPERIMENTAL TECHNIQUES AND PROCEDURES.

2.1. Introduction.

The aim of this chapter is to describe in detail the experimental techniques and

procedures employed in the studies of ionizing radiation damage to DNA presented in

this thesis.

Extensive use was made of electron spin resonance spectroscopy (esr) to study the

influence of several compounds upon the nature and mechanism of gamma–radiation

damage to DNA in frozen aqueous systems.

Neutral (pH 9.6) filter elution techniques based on those developed by *Kohn et al*[1]

were also used to monitor low linear energy transfer (LET) radiation induced DNA

double strand breaks in studies of the effects of novel polyammonium cation

nitroimidazole compounds.

2.2. Electron spin resonance spectroscopy.

2.2.a. Preparation of Samples.

Typically solutions of 25 or 50 mg ml^{-1} of calf thymus DNA sodium salt (BDH) in

water were prepared giving final DNA concentrations of 0.075 and 0.15M DNA base

pairs respectively (average molecular weight per base pair in calf thymus DNA being

660.4g). 0.15M samples were only used when low additive to DNA base pair ratios

were required. Additive compounds were included in the initial solutions prior to DNA being added.

In order to produce more clearly defined spectra of primary DNA and additive derived radicals, samples were also prepared in D_2O (BDH). However these samples give less information of the fate of DNA primary radicals on annealing. It must be stressed that the two solvents must be used in tandem to obtain the fullest understanding of radiation induced radical mechanisms; H_2O provided information on subsequent reactions of primary radicals and D_2O provided information on primary radical quantification.

These gel like solutions were the mixed thoroughly and then incubated at 4°C for 48 hours. After this period the solutions were again thoroughly mixed to ensure complete homogeneity.

The presence of molecular oxygen in samples results in the formation of the uncharacterised oxygen adduct radical ROO on annealing of the irradiated sample. (The effects of oxygen in these systems is discussed by *Symons et al*[2].) This obviously interferes with the study of DNA derived radicals and the influence of additives on their subsequent decay. To avoid RO_2 formation, each sample was degassed by passing nitrogen gas (which has been scrubbed free of even trace amounts of oxygen) through each sample solution whilst under a nitrogen atmosphere prior to freezing.

2.2.b. Oxygen removal from nitrogen.

Initially, nitrogen gas (`oxygen free' grade, BOC) was passed through alkali

pyrogallol solutions to remove trace amounts of oxygen prior to being passed through

the sample. For comparison two identical samples of aqueous DNA were degassed

using pyrogallol scrubbed nitrogen and argon respectively, these were then frozen,

gamma-irradiated and their esr spectra recorded as described below. Whilst neither

sample after annealing contained features assigned to RO_2, the TH yield in the

pyrogallol/nitrogen degassed sample was slightly diminished suggesting the presence

of trace amounts of oxygen, reducing TH yield.

Two more efficient methods of oxygen removal were adopted both of which were

based on transition metal redox cycling. In both cases the nitrogen gas was passed via

glass sinters through two sealed flasks in sequence containing solutions of aquated

Cr^{II} or V^{II} ions which were readily oxidized by any molecular oxygen present in the

gas. The gas was then passed through D_2O to remove any aerosols which might

otherwise contaminate the samples. This also had the effect of saturating the gas and

hence prevent sample dehydration. The redox reactions involved in each system are

described below.

2.2.c. Chromium II/III scrubber.

Blue aquated Chromium II ions, $[Cr(H_2O)_6]^{2+}$, were prepared by the reduction of

green hexa aquo Chromium III ions, $[Cr(H_2O)_6]^{3+}$, with zinc amalgamated with

mercury (Zn/Hg) in strongly acidic conditions[3,4]. The resulting blue solution is

producing a deep violet solution which again readily scavenged the trace amounts of oxygen present in the nitrogen gas[6] (Scheme 2-2). In this case the loss of the intense violet colour indicating solution exhaustion.

Scheme 2-2. A schematic representation of the oxidation of $[V(H_2O)_6]^{2+}$ ions by molecular oxygen and the subsequent reduction by Zn/Hg amalgam.

$$2[V(H_2O)_6]^{2+} + O_2 \longrightarrow 2[V(H_2O)_6]^{3+} \quad \text{Blue}$$

Violet

Zn^{2+} Zn
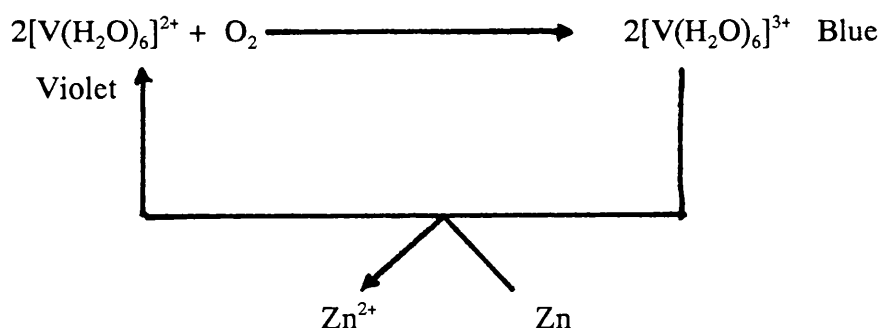
Once degassed with respect to oxygen, the homogeneous sample gels were carefully formed in liquid nitrogen into uniform cylindrical pellets, 30mm in length and 4mm in diameter.

All samples were gamma-irradiated in a Vickers ^{60}Co source for 4 hours. The dose rate of 20 Gy min^{-1} was measured using Fricke dosimetry[7].

2.2.e. esr measurements.

All spectra were recorded at 77K. Each sample pellet was placed in a quartz finger dewar filled with liquid nitrogen. The dewar was then inserted directly into the spectrometer cavity.

Great care was taken to ensure that the dewar was placed in the same position for each sample, that the sample completely filled the spectrometer cavity vertically and that the sample was always orientated in the same way (the `top' of each sample being marked). Since the samples are of identical uniform dimension, their distortion of the magnetic field in the cavity is close to identical. The response of the esr spectrometer cavity varies vertically and is at a maximum sensitivity in the centre. The samples were positioned so as to completely fill the `detected' cavity, ensuring the minimum error due to this non linearity.

The total error due to sample positioning was assessed by recording the esr spectrum of an irradiated 25mg ml^{-1} DNA sample at 77K after it had been annealed to 130K ten times. The sample being removed from and replaced into the dewar and cavity between each recording. The total variation in the peak height of the central feature proved to be less than 5 per cent total, significantly less than any augmented or diminished yield relative to controls reported in this thesis.

The first derivative X−band esr spectra were recorded using either a Varian E109 or a Jeol X−101 spectrometer, both spectrometers had 100 kHz magnetic field modulation and were interfaced to Acorn Archemeides A3000 microcomputers. Spectra were recorded by computer accumulation using software written and supported by Mr J.A. Brivati of this department. The software allowed rapid spectra storage, subtractions and the double integration of spectra. Multiple accumulation allowed great improvement in signal to noise ratios where sample radical populations were low, or when high amplifier gains were required. g−tensor values were measured relative to a retractable manganese g−marker fitted to the spectrometer.

Sample annealing was carried out by placing the sample pellets into pre-cooled

glass tubes under liquid nitrogen. The nitrogen was then decanted off and the tubes

placed in one of twelve accurately drilled 50mm deep holes in the top end of a solid

brass cylinder (60mm diameter and 300mm length) which was maintained at the

required temperature (±0.5K). The temperature of the block was monitored by a

platinum resistance thermometer positioned at the same depth as the samples. Brass

was used as the material to give high thermal conductance and hence minimal

temperature gradient between the thermometer position and the sample position. Up

to twelve samples could be simultaneously annealed in this way. After annealing for 8

minutes the samples were again placed under liquid nitrogen to quench any

proceeding reactions.

2.3. Quantification of radiation induced DNA double strand breaks (DSBs) by neutral (pH 9.6) filter elution.

2.3.a. Cell Culture.

A Chinese hamster V79-379a lung fibroblast cell line, a gift from Dr. Kevin Prise

of the Cancer Research Campaign Gray Laboratory (PO Box 100, Mount Vernon

Hospital, Northwood, Middlesex. HA6 2JR), was maintained in log phase growth

either on flat plates or in suspension. Eagle's minimal essential medium, MEM (ICN

Flow) was used in both cases supplemented with 7.5% (v/v) foetal calf serum for

suspension cultures and 10% (v/v) foetal calf serum for cultures where cells were

grown attached to flat plates. The medium in both cases was supplied supplemented

with penicillin and streptomycin. The cultures were maintained under an Air(95%)

$CO_2(5\%)$ (BOC) atmosphere.

2.3.b. Sample preparation and irradiation.

Exponentially growing cells were trypsinised and counted after re-suspension in

suspension modified MEM; this medium being used to prevent cell attachment to the

walls of the irradiation tubes. The cells were aliquoted out into sterile 2ml screw cap

cryotubes (Flow) in two main fractions, their density having been adjusted to give 2 x

10^6 cells per aliquot; the first fraction being the control, the second dosed with the

required concentration of drug compound.

Since the polyammonium cationic nitroimidazole compounds were supplied in the

hydrochloride form, care was taken to ensure the dosed fraction did not experience

any pH shock. This was done by careful pH measurement and adjustment of the dosed

media prior to the addition of the V79 cells.

These aliquots were then cooled on ice for 40 minutes. Hypoxic conditions were

generated by placing the cooled aliquots again on ice in a continuously purged

nitrogen(95%):$CO_2(5\%)$ (BOC) atmosphere for 90 minutes prior to irradiation.

Gamma-irradiation was carried out in a Vickers `Vickrad' ^{60}Co gamma source.

Each sample aliquot was enclosed in a pre-cooled lead sleeve to reduce the dose rate.

The temperature of the lead sleeve was maintained at 0°C for each irradiation to

minimise enzymic repair processes within the irradiated cells. The dose rate of 0.0998

$Gy \ s^{-1}$ was measured by Fricke dosimetry.

Once irradiated the sample aliquots were again placed on ice prior to lysis and

elution.

2.3.c. Filter Elution.

Filter elution was carried out using the *Swinnex funnel* column system based on

that described by *Kohn et al*[1]. Swinnex syringe barrels were connected to aluminium

foil covered 25mm swinnex filter holders (Millipore, UK) which contained 2.0 μm

polycarbonate filters (Millipore). Stop-cock valves (a gift from the Biophysics Group

CRC Gray Laboratory) were connected to the bottom of this assembly to control the

flow of fluids through the filter holder (Figure 2-1).

Ice cold phosphate buffered saline solution (PBS, Aldrich tablet form) was used to

charge the filter assembly prior to use; the solution being slowly injected from the

bottom of the assembly via the stopcock valves whilst the filter holders were

continually agitated to ensure no air bubbles were trapped in the filter holders. The

combination of trapped bubbles and fluid flow during elution has been shown to cause

DNA shearing during elution[1] and was thus avoided in this way. Once the filter

holders were full the syringe barrels were topped up with further ice cold PBS to

20ml, and the whole assemblies kept refrigerated until use.

Irradiated cells were added to the PBS in the syringe barrels and the sample tube

rinsed into this with a further 5ml of ice cold PBS. The solutions were then allowed to

drip through the assemblies until the solution meniscus reached the bottom waist of

the syringe barrel (as marked in Figure 2-1, the fluid levels were never allowed

below this point). The barrels were topped up again with a further 10ml of PBS and

the process repeated to ensure the cells were deposited on the filters.

SWINNEX FUNNEL

MINIMUM FLUID LEVEL

FILTER ASSEMBLY (enclosed in aluminium foil)

STOP COCK VALVE

TO PUMP
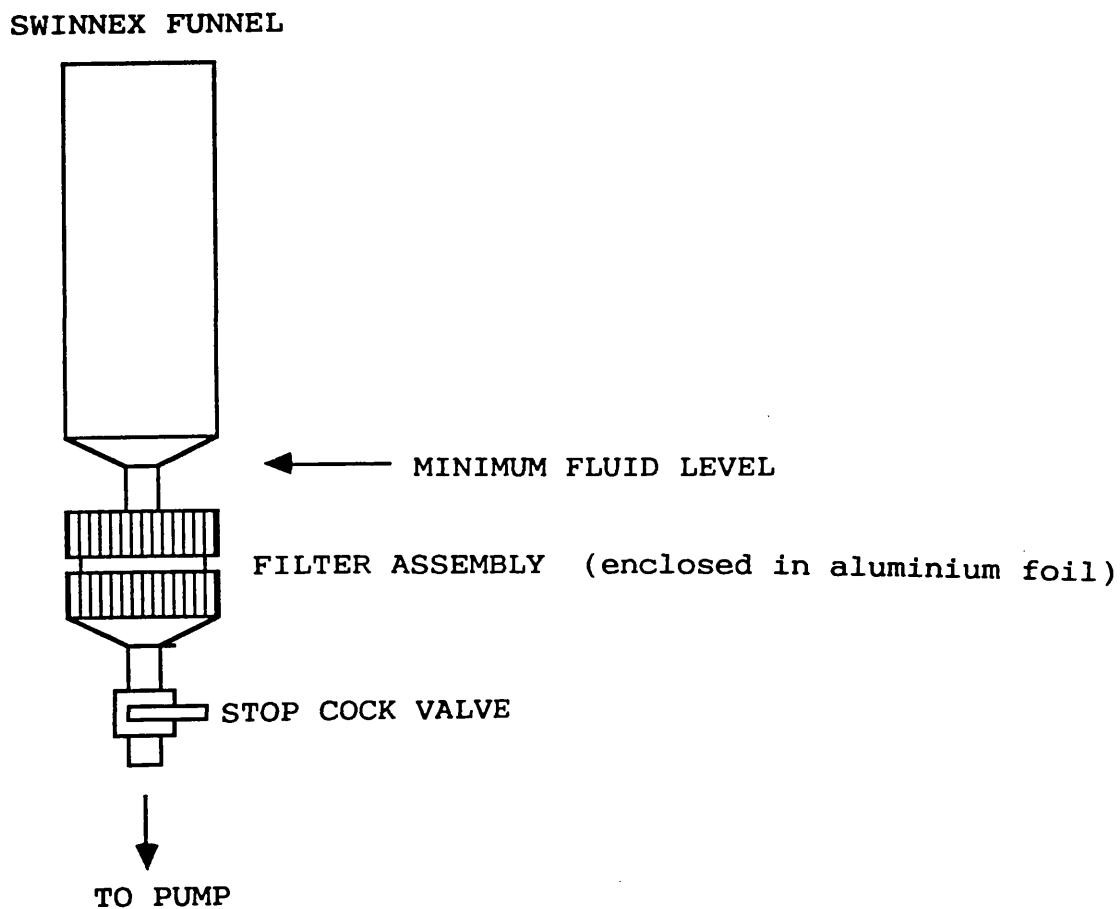
Figure 2-1. Diagram of the *Swinnex funnel* filter holder assembly. The minimum fluid

level is indicated.

1 ml of lysis solution (as supplied at 0.06% (v/v) Sarkosyl NL–30 in 0.04M

Na_4EDTA (tetrasodium salt) solution plus 1mgml^{-1} Proteinase K added immediately

prior to use) was then run onto each filter in the same way. Once the flow was stopped each column was incubated for 1 hour at room temperature.

40 ml of pH 9.6 eluting solution (1.2% (v/v) tetrapropylammonium hydroxide (Pr$_4$NOH) in 0.02M H$_4$EDTA (free acid) solution, pH 9.6) was then added to the syringe barrels and the stopcock taps connected to 0.89mm plastic peristaltic tubing via 19 gauge stainless steel hypodermic needles (Richardsons, Leicester). Stainless steel needles are required because aluminium needles were found to react with the caustic eluting solution. The tubing was then passed through a slaved reversible slow speed peristaltic pump (constructed in the workshops of this department) and connected to a 10 x 10 array automated fraction collector designed by Dr Yvette Goward (again constructed in the department workshops).

Once connected, the stopcock valves were opened and each column was pumped to waste for 30 minutes at 0.035ml min^{-1}. For each column, ten fractions were then collected each over a 90 minute period into 4ml sample cups (Richardsons) at the same pump rate. The fraction collector was timed to switch off the slaved pump after this was completed.

2.3.d. DNA quantification of the eluted fractions.

The quantitation of the DNA of each fraction was carried out by fluorimetric analysis using Hoechst 33258 dye, 2'-(4-hydroxyphenyl)-5-(4-methyl-1-piperazinyl)-2,5'-bi-1H-benzimidazole trhydrochloride pentahydrate.

The suitability of the dye for this type of quantitative determination has been demonstrated by *Cesarone et al*[7], and a discussion of the advantages this offers such as DNA specificity has also been published[8]. For these analyses, it was necessary to buffer the dye to neutralise the high pH of the eluting solution. It has been shown that the Hoechst 33258 fluorometric assay produces comparable results to those using [14C] thymidine-labelled cells, and a detailed comparison of the two techniques has been published by *Murray et al*[9]. The automated method described here was developed from that described by *Stout and Becker*[10].

The eluted volume of each fraction was recorded and the sample cups placed onto the carousel of a Chemlab CS 40-80 auto sampler, set to sample for 70s and wash for 90s. The sample aliquot of each fraction was then pumped using a Chemlab CPP 15 peristaltic pump through a glass mixing coil where it was thoroughly mixed with pre-buffered Hoechst 33258 dye solution (1mM sodium citrate in 0.04M KH_2PO_4 plus Hoechst 33258 dye immediately proir to use) and air, yielding a final dye concentration of 5 x 10^{-8} M, which was found to give the most linear response to DNA concentration[11,12].

Once mixed the buffered DNA-dye solution was passed through a de-bubbler and through the quartz flow cell of a Shimadzu RF-540 spectrofluorophotometer fitted with a Shimadzu DR-3 data recorder and a Shimadzu C-R6A Chromatopac integrator. A flow diagram of the analysis system is given below (Figure 2-2). The dye was excited at 350nm wavelength and the emission recorded at 90° to the excitation source at 475nm wavelength.

The Hoechst 33258 dye-Spectrofluorophotometer response was calibrated for each full analysis run by preceding and following complete fraction analysis with a series

of ten DNA standards, increasing in increments of 0.1 μg ml^{-1} from 0.1 to 1.0 μg ml^{-1}.

Each of the series of ten sample fractions for each column were separated by three

cups; the first and the third containing eluting solution the second containing a

standard 0.5 μg ml^{-1} DNA solution to allow any variation in Hoechst 33258
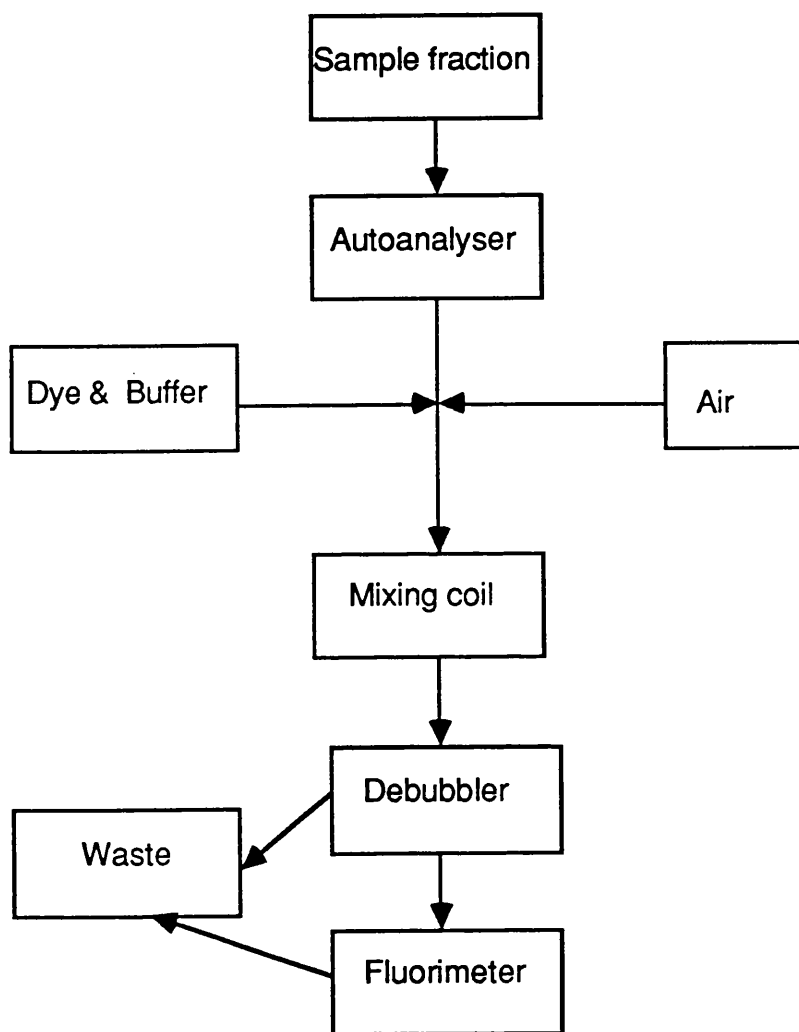
Figure 2-2. A flow diagram of the fraction analysis system.

dye–Spectrofluorophotometer response with time to be monitored and subsequently

corrected for.

The DNA retained on the filters and in the peristaltic pump tubing was collected

for quantitation by removing the syringe barrels, inverting the filter holder assemblies

and then back flushing each column with a further 4ml of eluting solution into 25ml

autoclavable screw cap bottles (Harris). The stopcock taps were then removed and the

filter holders carefully unscrewed. The filters were removed and added to the

backflushed volume using tweezers. Care was taken not to handle the filters or the

internal surfaces of the filter holders to prevent nuclease contamination. The filter

holders were then washed twice with two 5ml volumes of eluting solution, these

washes were also added to the backflushed volume.

To ensure dissolution of all the DNA from the filters these solutions were then

autoclaved for 20 minutes and then thoroughly shaken for 2 minutes. The volume of

each was then recorded and a 3ml sample taken for autoanalysis as described above.

2.3.e. Preparation of DNA standard solutions.

The 0.1 to 1.0μg ml^{-1} DNA standard solutions were prepared by dilution. A

standard solution of 10μg ml^{-1} Calf thymus DNA in eluting solution was prepared.

This was autoclaved for 20 minutes and, once cooled, diluted with eluting solution.

Since these studies use a mammalian cell line and given that Hoechst 33258 is

sensitive to the G and C base content of DNA[8] as is the case here a mammalian DNA

of very similar G and C content was used for this calibration.

2.3.f. Data Processing.

The integrated peak data for each eluted fraction was corrected for Hoechst 33258 dye-Spectrofluorophotometer response variation with time using the 0.5μg ml^{-1} response data.

The DNA standard solutions were used to generate a calibration curve of DNA concentration verses fluorescence. Linear regression was then carried out using *MINITAB* (Minitab Inc) data processing software on the university's DEC 8650 Vax mainframe computer.

The total amount of DNA in each eluted fraction and the total amount of DNA per filter prior to elution were calculated using a computer program written by Dr B.W. Taylor then of this department. The data was expressed as the proportion of DNA retained on the filter relative to the eluted volume.

References for Chapter 2.

1. M.O.Bradley and K.W.Kohn, *Nucl. Acids Res.*, 1979, **7**, 793.

2. Part 1. Boon, P.J., Cullis, P.M., Symons, M.C.R. and Wren, B.W., *J. Chem. Soc., Perkin Trans. 2*, 1984, 1393.

3. J. W. Mellor., *A comprehensive treatise of inorganic and theoretical chemistry IV*, 1943, 1038.

4. J. W. Mellor., *A comprehensive treatise of inorganic and theoretical chemistry XI*, 1946, 434.

5. F.A. Cotton. and G. Wilkinson., *Advanced Inorganic Chemistry, 4th Ed*, (Wiley, New York), 1980, p724.

6. L. Meites., *Polargraphic Techniques, 2nd Ed*, p89

7.

8. C.F. Cesarone, C. Bolognesis and L. Santi., *Anal. Biochem.*, 1979, **100**, 188–197.

9. B. Rowe., *Biotechnology*, 1982, 19–22.

10. D. Murray, S.C. Van Ankeren and R.E. Meyn., *Anal. Biochem.*, 1987, **160**, 149–159.

11. D.L. Stout and F.F. Becker., *Anal. Biochem.* 1982, **127**, 302–307.

12. Y. Goward, personal communication.

13. A. Harrison., *Ph.D thesis, Leicester*, in preparation.

CHAPTER 3. THE EFFECTS OF HYDROXYL RADICAL SCAVENGERS ON RADIATION DAMAGE TO DNA.

3.1. Introduction.

As discussed in Chapter 1, it is commonly thought that damage to DNA as a result of exposure to ionizing radiation leads to cell death. In vitro studies have shown there are two component mechanisms for primary damage to DNA; the direct ionization by interaction of radiation quanta or particles and DNA, and indirect damage caused by attack from water radiolysis products, principally hydroxide radicals (OH), solvated electrons (e_{aq}^-) and hydrogen atoms (H)[1-6]. It is OH radicals that are generally thought to be of major significance in indirect DNA damage.

The rate constants of DNA attack by OH radicals measured in pulse radiolysis studies of aqueous DNA suggest that *circa* 20% of attack is on the deoxyribose units[7-10]. This leads to a reasonable mechanism for strand breakage. These, and more recent studies involving model compounds have shown OH radical attack on the base residues is most significant[11-13]. OH adduct formation at a base residue and the subsequent elimination of H_2O followed by hydrogen atom transfer from a neighbouring deoxyribose unit gives a reasonable mechanism ultimately leading to strand breakage. This reaction, which is probably endothermic, is justified by the close location to the reaction centre of C–H hydrogen atoms, and that the resulting highly unstable deoxyribose centred radicals can react further to form stable breakdown products[14].

Whilst the indirect mechanism is thought to dominate in fluid aqueous DNA systems, the direct mechanism is believed to dominate in frozen aqueous DNA systems. The DNA environment in the cell nucleus is somewhere between these two extremes. The highly organised and tightly packed structure of cellular DNA restricts the volume of solvating water around the DNA. Nuclear water also contains a wide range of biomolecules in relatively high concentration which are highly reactive towards any hydrolysis products. Thus only solvent radicals generated in close proximity to `exposed' DNA may cause damage. Indirect damage is limited by these two factors and direct damage to DNA more significantly in the cell.

Using the plasmid DNA strand break assay technique, *Wren* observed no reduction in DNA strand breaks when tertiary butyl alcohol (TBA) was used as an OH radical scavenger at concentrations ranging from 1 to 100mM after gamma-irradiation at 77K. He concluded that within the DNA solvating region in frozen aqueous DNA samples, significant quantities of OH radicals are not produced and hence are not responsible for DNA damage in such systems[15].

The aim of the studies reported here was firstly to provide further evidence that OH radicals are not responsible for the observed radiation-induced DNA damage in frozen systems, and secondly to elucidate any influence OH radical scavengers may have upon direct radiation damage to DNA.

3.1.a. Dimethylsulphoxide, DMSO.

DMSO is an aprotic polar solvent. Its unique properties give many important and interesting chemical and biological effects. It is favoured with high diffusion rates

across cell membranes and is of great importance as an additive to cellular systems since it is commonly used as a cryoprotector.

DMSO also functions as a radioprotector. Ashwood–Smith demonstrated that DMSO, increased the surviving fraction of mice exposed to lethal dose X–rays[16]. In the same study both the oxidation product (dimethylsulfone) and the reduction product (dimethylsulfide) were found to have no appreciable action. This suggested strongly that the radioprotective effects were derived from DMSO and not its obvious metabolic products.

DMSO has also been shown to suppress radiation–induced transformation *in vitro*[17]. These suppressive effects were believed to be the consequence of both free radical scavenging by DMSO molecules and DMSO induced solvent structure alteration. The latter has also been proposed as a mechanism by which DMSO affords the cryoprotection of biomolecules[18].

Chapman and co–workers have demonstrated *in vitro* radioprotective effects of DMSO upon the surviving fraction of Chinese hamster fibroblasts after exposure to X–rays, both in the presence and less effectively in the absence of oxygen[19-21]. These protective effects were believed to be predominantly due to hydroxyl radical scavenging.

Radford using neutral filter elution, demonstrated radioprotection of frozen Mouse L cells from X–radiation induced DNA double strand breaks by DMSO and hence, since this was related linearly to cell survival, from lethal DNA lesions[22].

DMSO is an extremely efficient free radical scavenger, and thus is now commonly used as a probe molecule in studies of free radical reactions in biological systems. DMSO reacts with OH radicals at close to diffusion controlled rates to form the

sulphuranyl radical adduct (Figure 3-1). The sulphuranyl radical is highly unstable

and rapidly decomposes to yield a methyl radical[23,24] (Reaction 1). As a result DMSO

is widely used in radiation chemistry specifically to scavenge OH· radicals[25,26].

$$
\begin{array}{c}
\text{OH} \\
| \\
\cdot\text{S}\overset{\text{\tiny Me}}{\underset{\text{Me}}{\diagdown}} \\
| \\
\text{O}
\end{array}
$$
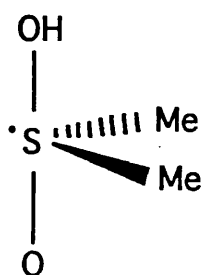
Figure 3-1. Structure of the sulphuranyl radical adduct formed by OH· radical

scavenging by DMSO[29].

$(Me)_2SO \; + \; OH· \; ----> \; (Me)_2S·(O)OH \; ----> \; MeS(O)OH \; + \; Me·$ (1)
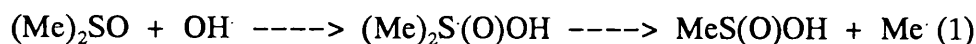
3.1.b. The radiation chemistry of DMSO.

The radiation chemistry of DMSO itself has not been extensively studied. Williams

and co-workers carried out the most significant solid state studies using dilute (circa.

1%) $(H_3C)_2SO$ in $(D_3C)_2SO$, showing that electron capture leads to the formation of

methyl radicals $(H_3C·)$ and the anion $MeSO^{-[27]}$. The expected radical anion is highly

unstable and remained undetected[28,29] (Reaction 2).

$(Me)_2SO \; + \; e^- \; ----> \; [\,(Me)_2S·O\,]^- \; ----> \; Me· \; + \; MeSO^-$ (2)
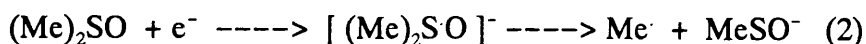
No methyl radicals were detected in pure solid DMSO irradiated at 77K, however a

carbon centred triplet feature was detected and assigned to $H_2C\text{-}S(Me)O$ radicals.

This is believed to be the product of rapid hydrogen atom abstraction by methyl

radicals from neighbouring molecules (Reaction 3).

$$Me\cdot + (Me)_2SO \longrightarrow CH_4 + H_2C\text{-}S(Me)O \qquad (3)$$

Deuterium abstraction at 77K is very slow when methyl radicals are generated in

$(D_3C)_2SO$ and thus methyl radicals remain trapped.

Optical pulse radiolysis studies with aqueous DMSO in contrast, have shown that

solvated electrons are the major product[24]. This was also found to be the case in the

pure liquid[30-32]. Reaction of solvated electrons and DMSO is relatively slow ($k = 1.7$

x 10^6 $lmol^{-1}s^{-1}$)[24] and yields a species of λ_{max} at 350nm, which is believed to be the

anion $(Me)_2SO^-$. In the pure liquid this is not the case where a transient species of λ_{max}

at 600nm was observed, this being either the parent radical cation, $(Me)_2SO^+$ or some

species derived therefrom[30].

The radical cation has since been unambiguously observed by esr spectroscopy in

dilute DMSO in $CFCl_3$ gamma-irradiated at 77K. The cation is characterised by a

septet feature of large g-tensor shift[33], due to spin localisation on the sulphur atom.

3.1.c. t-butyl alcohol, TBA.

t-butyl alcohol (TBA) is also commonly used as an OH radical scavenger in radiation chemistry[34,35]. Whilst reacting efficiently with OH radicals in aqueous solution, reaction with solvated electrons is unimportant. In the pure solid, TBA reacts with ejected electrons to form t-butyl radicals (reaction 4).

$$(CH_3)_3COH + e^- \; ----> \; (CH_3)_3C + OH^- \quad (4)$$
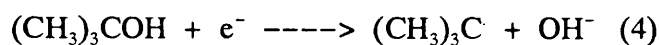
The radical cation may deprotonate and rearrange to form $H_2C-C(Me)_2OH$ radicals (Reaction 5), or release a methyl radical and acetone (Reaction 6)[36].

$$(Me)_3C\,OH^+ \; ----> \; (Me)_3CO \; ----> \; H_2C-C(Me)_2OH \quad (5)$$

$$(Me)_3C\,OH^+ \; ----> \; (Me)_3CO \; ----> \; Me + (Me)_2CO \quad (6)$$
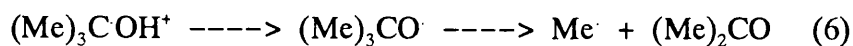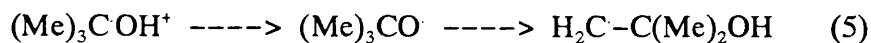
Reaction with OH radicals is extremely fast and results in hydrogen atom abstraction from the methyl groups to yield $H_2C-C(Me)_2OH$ radicals.
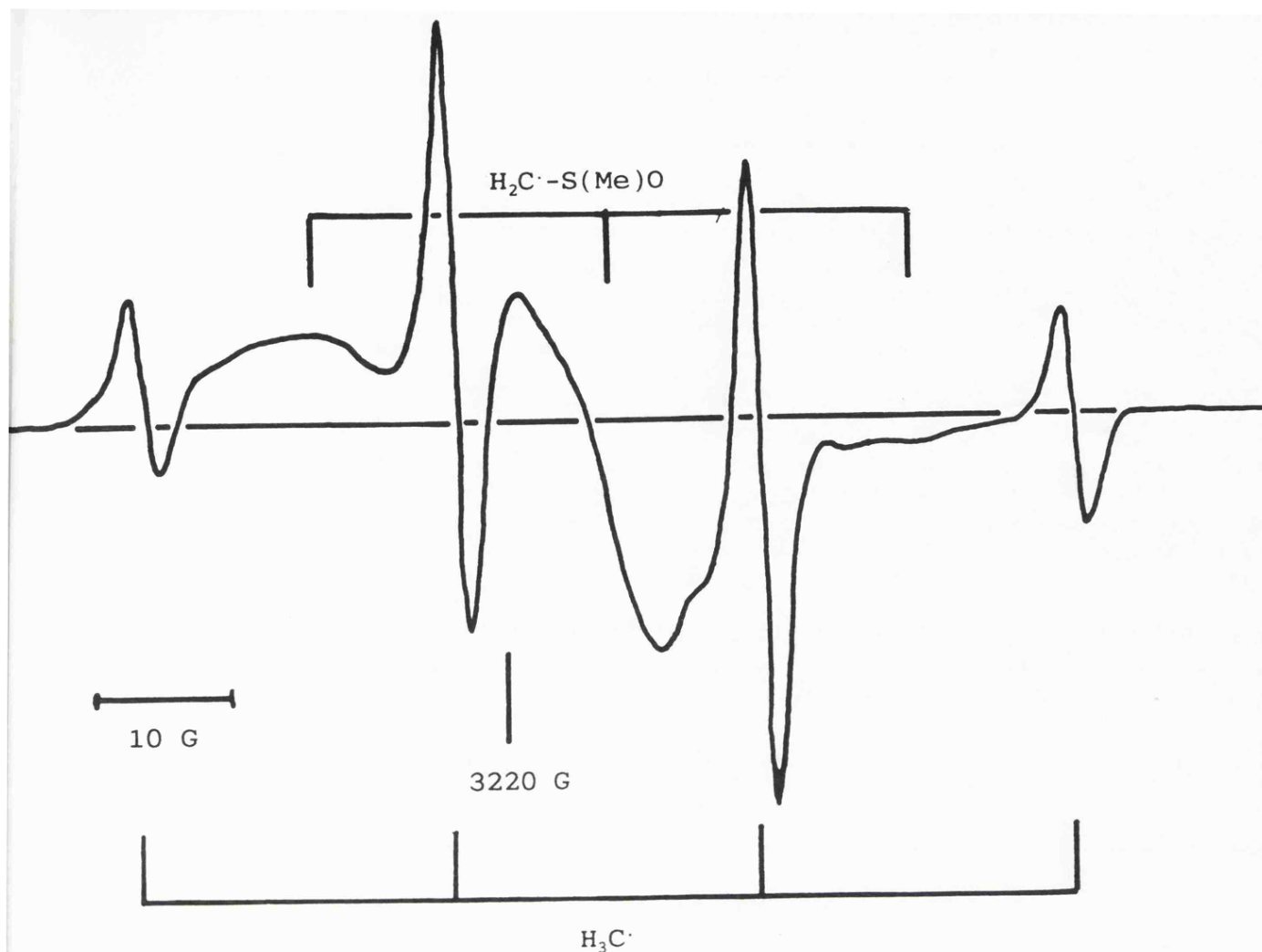
Figure 3–2. The first derivative X–band esr of DMSO irradiated at 77K in CD$_3$OD/D$_2$O glass, containing features assigned to Me and H$_2$C–S(Me)O radicals.

mM DMSO solutions giving DMSO to DNA base pair ratios of 1:20, 1:50 and 1:200 respectively. The samples were degassed with respect to oxygen, frozen, then gamma–irradiated at 77K simultaneously with an aqueous DNA control.

No reduction in DNA primary radical yield relative to that of the control was observed in the esr spectra of any of these samples. At 77K the spectra were almost identical to that of the control. This was also found to be the case after annealing to 130K. The measured yields of TH radicals formed on annealing were also found to be

very similar to that of the control sample. This is illustrated by a plot of total DNA

primary radical yield v. temperature (Figure 3-3).
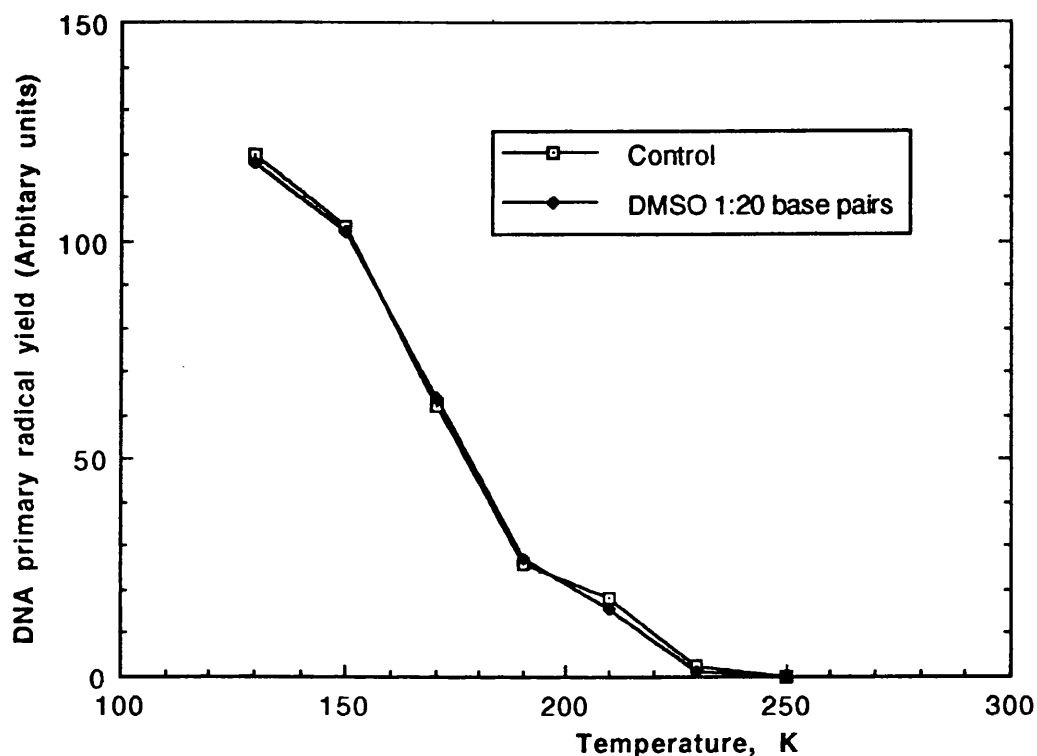
Figure 3-3. A plot of total DNA primary radical yield v. temperature for an aqueous

DNA control and a sample of DMSO to DNA base pair ratio of 1:20, demonstrating

no significant difference in DNA primary radical yield from the control.

For DMSO to DNA base pair ratios of as high as unity, the observed DNA primary

radical yields were found to be almost identical to the aqueous DNA control. However

for the 0.076M sample (1:1), a weak doublet feature of 23G splitting centred about

free spin was apparent in the esr spectrum superimposed over the DNA and OH·

radical features. This became more clearly defined after annealing to 130K. The

doublet features were irreversibly lost after annealing to 150K, and were thought to be

the central features of the quartet assigned to methyl radicals above.

DMSO concentrations producing DMSO to DNA base ratios of greater than one

however give rise to weak concentration–dependent radioprotective effects.

A series of 50mg ml^{-1} DNA samples were prepared and irradiated in DMSO

solutions giving DMSO to DNA base pair ratios of greater than one. When recorded at

77K, the esr spectrum of the 10:1 DMSO to DNA base pairs clearly demonstrated a

significant reduction in the intensity of the DNA primary radical features. This

reduction was quantified after annealing to 130K (to allow the OH· radical derived

features to be lost) by computer subtraction of the spectrum obtained from the

equivalent aqueous DMSO (0.758M) control at the same temperature. The reduced

yield was found to be 61 % that of the control, the loss of the central inflection from

the product spectrum suggesting that this was largely due to reduced yields of the

pyrimidine anion centres C$^-$/T$^-$ (Figure 3–4.ii).

This reduction in DNA primary radical yield was accompanied by the presence of a

sharp well defined 1:3:3:1 quartet (A$_{iso}$ = 23G), which was unambiguously assigned to

methyl radicals and a broad 1:2:1 triplet assigned to H$_2$C·–S(Me)O radicals (Figure

3–4.i). These features became more clearly resolved after the irreversible loss of OH·

radicals.

The more reactive methyl radicals are irreversibly lost after annealing to 150K.

However, the triplet features assigned to H$_2$C·–S(Me)O radicals are still present in the

esr spectrum after annealing to 170K, all be it at reduced intensity (Figure 3–5), but are lost after annealing further.

FIG 3-4.i.

3220 G

$H_2C\cdot-S(Me)O$

$H_3C\cdot$

10 G

FIG 3-4.ii.

3220 G
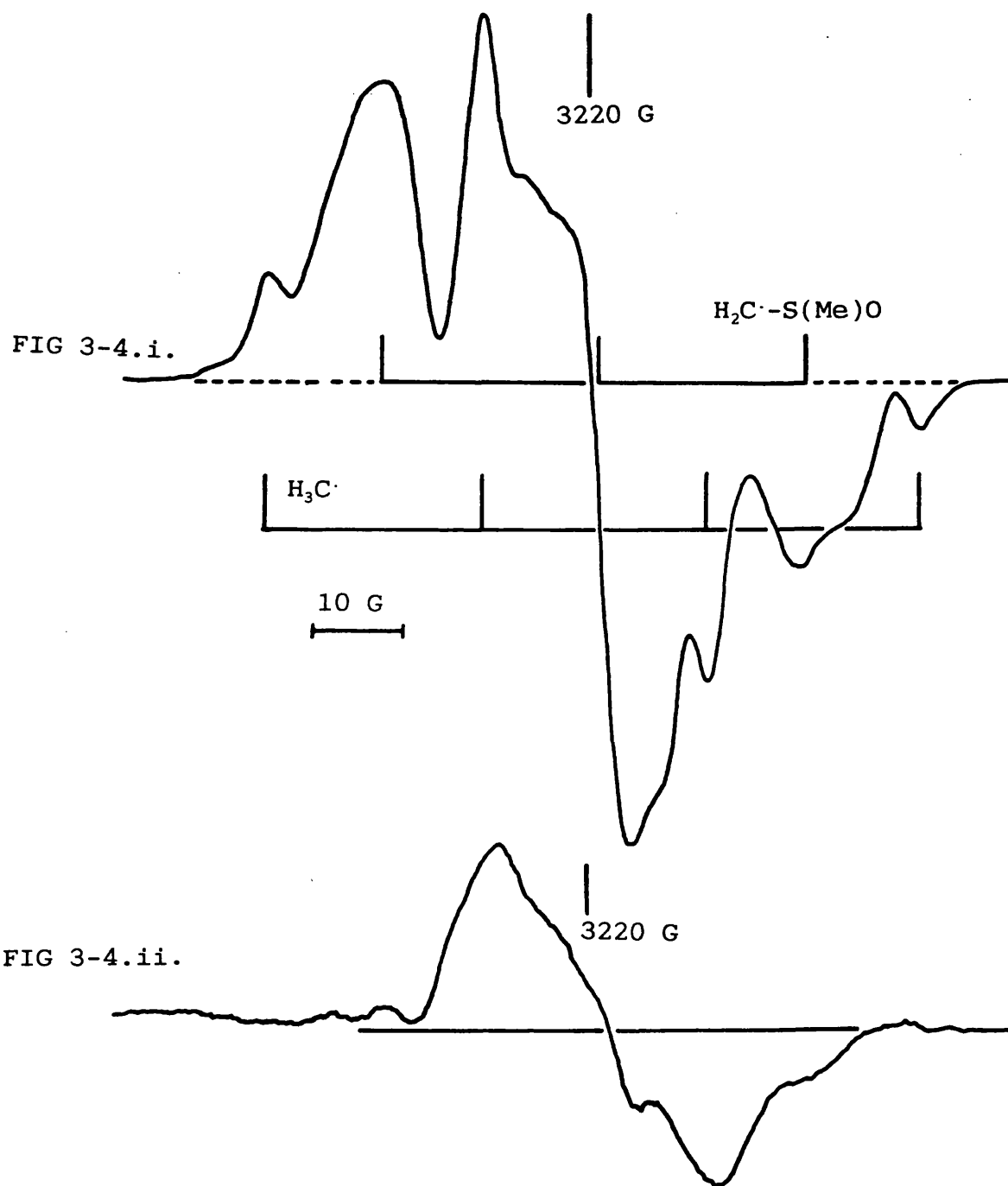
Figure 3–4.i) The first derivative X–band esr spectrum of 10:1 DMSO to DNA base pair sample after annealing to 130K, containing features assigned to Me and $H_2C\cdot-S(Me)O$ radicals.
ii)After computer subtraction of the spectrum of 0.758M DMSO again at 130K to reveal the composite central features assigned to DNA primary radicals, albeit with reduced contribution from the doublet features assigned to the pyrimidine anions.
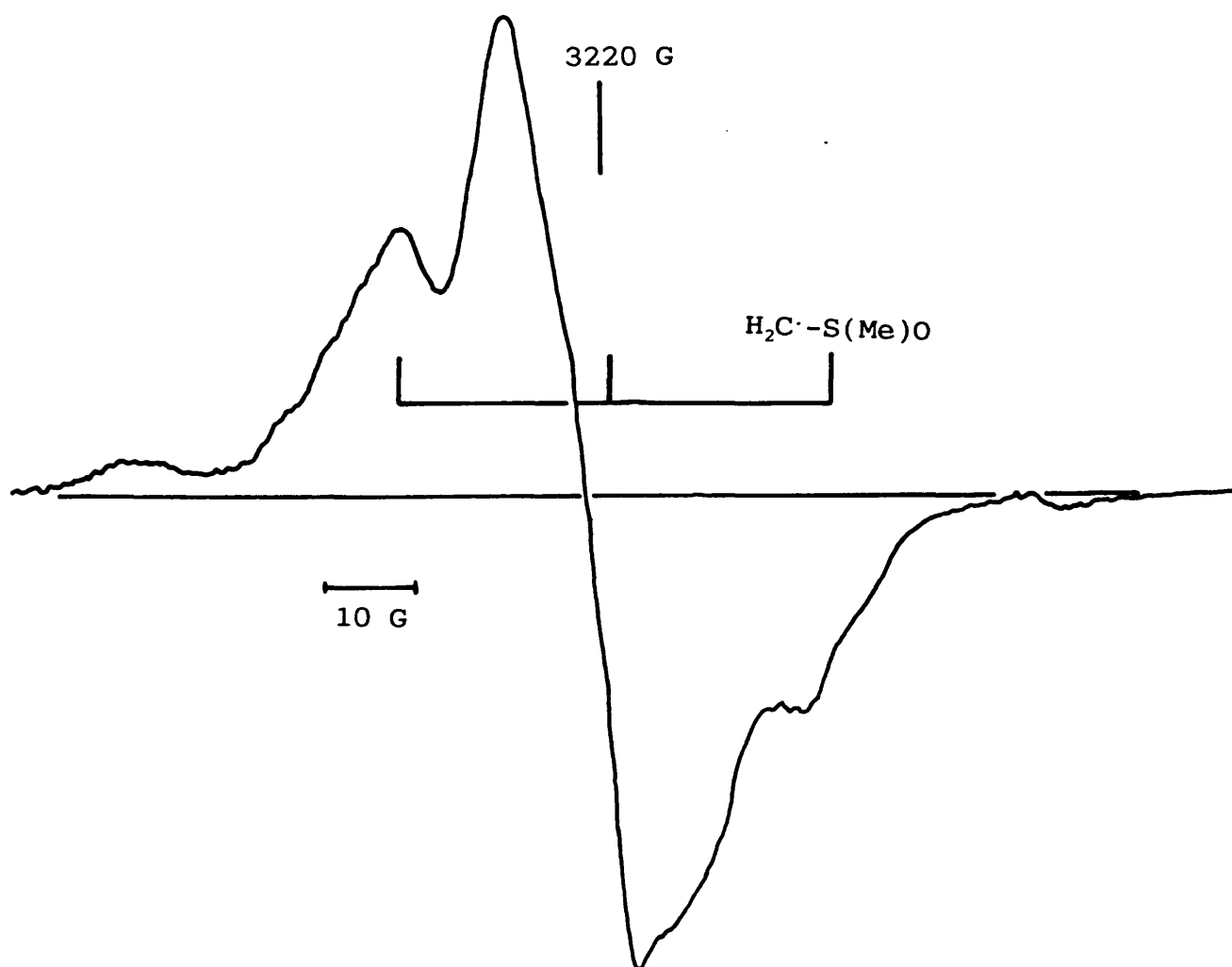
Figure 3-5. The first derivative X-band esr spectrum of 10:1 DMSO to DNA base pairs after annealing to 170K.

On annealing it is also clear that the reduced yield of the pyrimidine anion centres C^-/T^- is accompanied by a similarly reduced TH radical yield. At 190K, the TH radical yield was found to be 59% that of the aqueous DNA control.

The concentration dependence of this radioprotective effect is demonstrated in both; i) a plot of TH radical yield versus temperature for a range of DMSO to DNA base pair ratios (figure 3-6.i.), and ii)a plot of DNA primary radical yield at 130K versus DMSO concentration (Figure 3-6.ii).
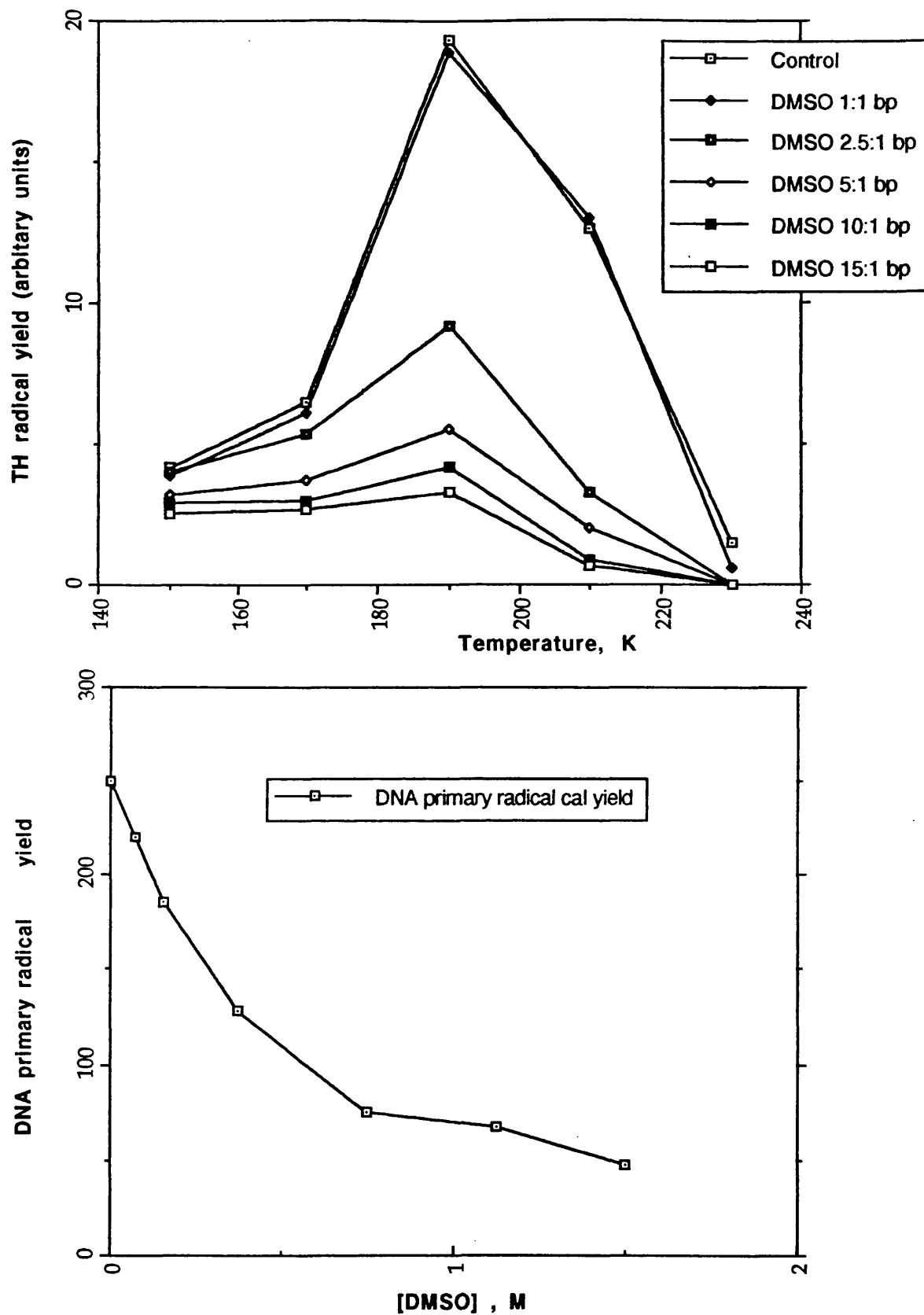
Figure 3–6.i) A plot of TH radical yield versus temperature for a range of DMSO to DNA base pair ratios.
ii) A plot of DNA primary radical yield at 130K versus DMSO concentration.

3.2.c. t–butyl alcohol–DNA systems.

Again based on additive to DNA base pair ratios used in previous studies, aqueous

50 mg ml^{-1} DNA samples were prepared in 1.52, 3.78, 7.58 and 75.75 mM t–butyl

alcohol (TBA) solutions, resulting in TBA to DNA base pair ratios of 1:50, 1:20, 1:10

and 1:1. These samples were then degassed with respect to oxygen and irradiated at

77K.

Similarly to the DMSO systems of comparable concentrations, no detectable

difference in the yield of DNA primary radicals was observed in the esr spectra of any

of these samples at 77K. On annealing to 130K, the observed spectra were effectively

identical to that of the control.

Though TBA derived radicals may have been expected, no such species were

detected. Even trace amounts of methyl($CH_3\cdot$) and tertiary butyl (($Me)_3C\cdot$) radicals,

whose narrow features may be detected at very low concentrations, were not detected.

However the effects of higher TBA concentrations are in marked contrast to those

observed with the equivalent DMSO concentrations. DNA samples containing 10:1

and 20:1 TBA to DNA base pair ratios demonstrated linear concentration dependent

radiosensitizing effects in that DNA primary radical yields are lineally increased with

increase in TBA to DNA base pair ratio.

Again no TBA derived features were detected in the esr spectra, despite the use of

high gain, narrow field modulation and multiple accumulations to optimise the

resolution of any narrow features. This was also found to be the case after annealing

to 130 K.

On further annealing it is clear that the increased DNA primary radical yield is also reflected in proportionally increased TH. radical yields (Figure 3–7).

FIG 3-7.i.

FIG 3-7.ii.
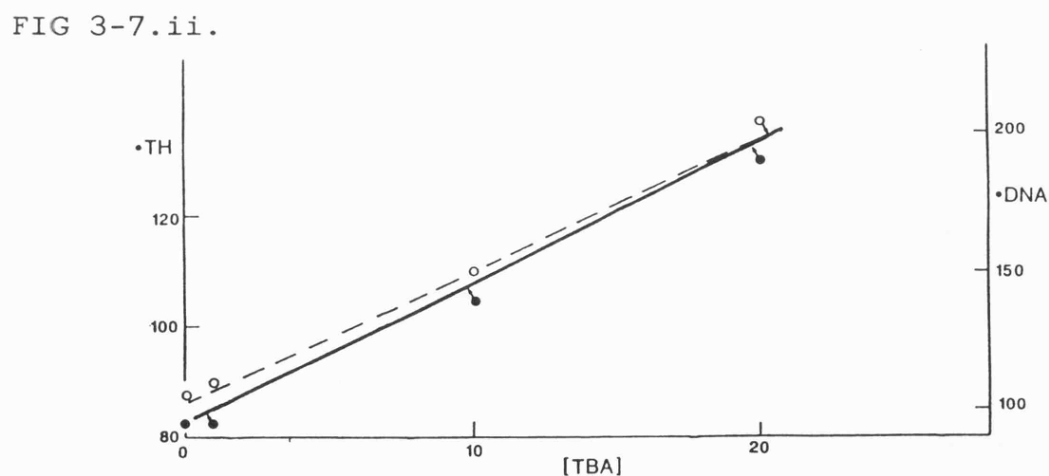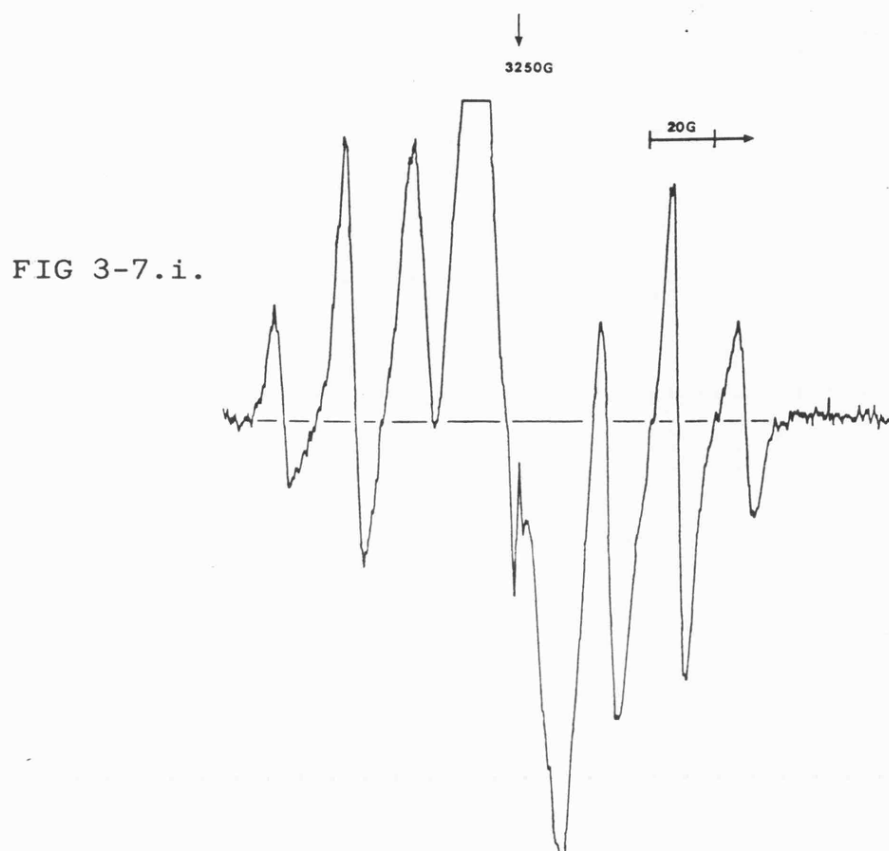
Figure 3–7. i) First derivative X–band esr spectrum for TBA–DNA (20:1) sample after exposure to gamma–radiation at 77K and annealing to 210K, showing features assigned to TH radicals. The intensity of of these features is *circa* twice that of the control.
ii) Effect of TBA concentration (TBA : DNA base pairs) on the intensities of DNA primary radical features at 150K and TH radicals at 170K (------ TH,——DNA).

64

3.3. Discussion.

At low concentrations, giving additive to DNA base pair ratios of less than 1:1 both DMSO and TBA gave no measurable reduction in DNA primary radical or TH radical yields. As stated above, electron- donor and acceptor systems have previously been shown to produce clear DNA radical yield reductions at concentrations giving additive to DNA base pair ratios of 1:50.

These results support the contention that OH radical reactions, in marked contrast to liquid aqueous systems, are not an important source of DNA damage in frozen aqueous conditions.

The esr spectra of samples containing high DMSO concentrations contain features assigned to Me and H_2C-S(Me)O radicals which were also observed in the equivalent aqueous DMSO samples. However, since their appearance is accompanied by significant reductions in both DNA primary radical and on annealing TH radical yields, these features are not simply derived from radicals formed in a separate $DMSO-H_2O$ phase.

The ionization potential of DMSO is 9.1 eV, which is greater than that of guanine (8.24 eV). Thus hole transfer from G^+ to DMSO should not be favoured and thus not contribute to the observed reduction in DNA primary radical yield. DMSO radicals are to be expected at high concentrations, however DMSO was shown to be ineffective at low concentrations.

Several factors probably contribute to the overall reduction in DNA radical yields. The reduction in water molecule concentration in the solvating region surrounding the DNA caused by the presence of DMSO molecules may facilitate charge

recombination or electron return, especially by the suppression of protonation from the solvent.

The reaction of H_2O^+ described in chapter 1, to give ultimately G^+ may be less favoured than reaction with DMSO to yield $DMSO^+$. DMSO molecules may also be expected to react with electrons thus preventing the formation of the pyrimidine anions T^-/C^-. They may potentially also scavenge electrons from the pyrimidine anion centres before protonation.

Electron transfer between DMSO molecules may also remove electrons from close vicinity to the DNA and thus reduce the yield of pyrimidine anion centres.

Whilst the effects of low TBA concentrations correlate closely to those observed with similar DMSO concentrations, the effects of high TBA concentrations are in marked contrast with those of high DMSO concentrations. This may be understood in the following way. In both cases, on freezing the co-solvent molecules are forced into close proximity to the DNA, thus increasing the DNA target volume (this effect is clearly defined for inert salt systems[37]). Both electron and hole capture by TBA are clearly inefficient, and insignificant here, so both the hole centres and the electrons formed in this increased target volume may reach the DNA, thus increasing the DNA radical yields.

The rates of both electron and hole capture with DMSO are sufficiently high that competition with the DNA can occur. Thus at high concentrations DMSO may dominate and act as an, albeit weak, radioprotector.

9. Farhataziz and A.B. Ross, *Natl. Stand. Ref. Data Ser., U.S. Natl. Bur. Stand.*, **1977**, 59.

10. G. Scholes, J.F. Ward and J. Weiss, *J. Mol. Biol.*, **1960**, 2, 210.

11. C. Von Sonntag, *The Chemical Basis of Radiation Biology*, Taylor and Francis, London, 1987.

12. L.R. Karam, M. Dizdaroglu and M.G. Simic, *Radiat. Res.*, 1988, **116**, 210.

13. M. Adinarayana, E. Bothe and D. Schulte-Frohlinde, *Int. J. Radiat. Biol.*, 1988, **54**, 723.

14. P.M. Cullis, S.R. Langman, I.D. Podmore and M.C.R. Symons, *J. Chem. Soc. Perkin Trans.*, 1990, **86**, 3267-3271.

15. B.J.W. Wren, *Ph.D. Thesis, Leicester*, 1985.

16. M.J. Ashwood-Smith, *Int. J. Radiat. Biol.*, 1961, **3**, 41.

17. A.R. Kennedy & M.C.R. Symons., *Carcinogenesis*, 1987, **8**(5), 683-688.

18. O. Vos, M.C.A. Kaalen and L. Budke, *Int. J. Radiat. Biol.*, 1965, **9**, 133.

19. J.D. Chapman, D.L. Dugle, A.P. Reuvers, C.J. Gillespie and J. Borsa, *Radiation Research – Biomedical Chemical and Physical Aspects*, eds. O.F. Nygaard, H.I. Alder and W.K. Sinclair, Accademic Press, New York, 1975.

20. J.D. Chapman, A.P. Reuvers, J. Borsa and C.L. greenstock, *Radiat. Res.*, 1973, **56**, 291–306.

21. J.D. Chapman, D.L. Dugle, A.P. Reuvers and C.J. Gillespie, *Radiat. Res.*, 1975, **64**, 365–375.

22. I.R. Radford, *Int. J. Radiat. Biol.*, 1985, **48**, 45–54.

23. B.C. Gibert, R.O.C. Norman and R.C. Sealy, *J. Chem. Soc. Perkin Trans. II*, 1975, 308.

24. G. Meissner, A. Henglein & G. Beck, *Z. Naturforsch.*, 1967, **22b**, 13.

25. L.G. Littlefield, E.E. Joiner, S.P. Colyer, A.M. Sayer & E.L. Frome, *Int. J. Radiat. Biol.*, 1988, **53**, 875.

26. J.D. Chapman, S.D. Doern, C.J. Gillespie, A. Chatterjee, E.A. Blakely, K.C. Smith and C.A. Tobias, *Radiat. Environ. Phys.*, 1979, **16**, 29.

27. Y.J. Chung, K. Nishikida and F. Williams, *J. Phys. Chem.*, 1974, **78**, 1882.

28. K. Nishikida and M.C.R. Symons, *J. Am. Chem. Soc.*, 1974, **96**, 4781.

29. M.C.R. Symons, *J. Chem. Soc. Perkin Trans. II*, 1976, 908–915.

30. A.M. Koulkes-Pujo, L. Gilles, B. Lesigne and J. Sutton, *Chem. Comm.*, 1971, 749.

31. D.C. Walker, N.N. Klassen and H.A. Gillis, *Chem. Phys. Letts.*, 1971, **10**, 636.

32. R. Bensasson and E.J. Land, *Chem. Phys. Letts.*, 1972, **15**, 195.

33. M.C.R. Symons and D.N.R. Rao, *Chem. Phys. Letts.*, 1982, **93**, 495.

34. *Radiation Chemistry*, ed. Farhataziz and M.A. Rogers, VCH Publisher, Inc. 1987.

35. H. Schuessler and E. Jung. *Int. J. Radiat. Biol.*, 1989, **56**, 423.

36. M.C.R. Symons and K.V.S. Rao, *Radiat. Phys. Chem.*, 1977, **10**, 35.

37. P.M. Cullis, A.S. Davis, M.E. Malone, I.D. Podmore and M.C.R. Symons, *J. Chem. Soc. Perkin Trans. II*, 1992, 1409–1412.

CHAPTER 4 – THE INFLUENCE OF BUFFER IONS ON RADIATION DAMAGE TO DEOXYRIBONUCLEIC ACID

4.1. Introduction.

The studies presented in this chapter are centred on the influence that buffering ions may have on direct damage to DNA by ionizing radiation. At pH values greater than pH 3, primary radical yields for water radiolysis at room temperature are essentially independent of pH[1]. But for such reasons as sample fragility, ease of sample preparation and ease of manipulation, aqueous DNA irradiation in several commonly used techniques is often carried out in solutions containing complex mixtures of buffering ions. The DNA concentrations are low relative to the concentration of buffering ions.

As described in Chapter 1, in aqueous DNA solutions the formation of ice crystallites on freezing, results in the formation of a 'glass' region as an extended solvation shell to the DNA. High relative buffer ion concentrations result in a much larger 'glass' region as many more buffer ions are forced into close proximity to the DNA. Since these frozen systems are used to study direct damage to DNA by ionizing radiation, it is important to understand any influence that buffer ions and similar additives may have upon:

i) the mechanisms of direct damage.

ii) the action of radiosensitizing and radioprotecting compounds.

The effects of two commonly used buffers are reported here; TRIS hydrochloride, $(HOH_2C)_3CNH_2.HCl$, and the hydrogen phosphate buffer system of potassium

dihydrogen orthophosphate (KH_2PO_4) and disodium hydrogen orthophosphate, (Na_2HPO_4) at pH 7.4. Also studied were the effects of sulphate ions in equivalent concentrations. The sulphate radical SO_4^-, generated by the radiolysis of persulphate ions, has been extensively used to probe the mechanisms of direct DNA damage, in recent studies with model systems[2-15]. Also given that the radiation chemistry of sulphate ions is well understood, sulphate ions were used to provide a comparison with phosphate ions.

In plasmid DNA strand break assay experiments, where sample irradiation is carried out at 77K, the buffer ion to DNA base pair ratio is commonly of the order of hundreds. Due to the experimental constraints of sample size and esr spectrometer sensitivity , buffer ion to DNA base pair ratios of this order are not reasonable. A ratio of 20:1 was felt to provide an increase in DNA solvation volume, whilst not reducing experimental sensitivity by reducing the DNA content of each sample.

Glasses are infinitely viscous liquids and hence retain liquid phase structure, for this reason glass systems are commonly used in esr spectroscopy. Buffered systems produce similar solvation conditions in the DNA solvation shell when frozen. For this reason and further comparison, sodium perchlorate a commonly used glass forming agent was also included in these studies.

4.2. Results.

4.2.a. TRIS hydrochloride Studies

Gamma-irradiation at 77K of the pure solid $(HOH_2C)_3CNH_2.HCl$ yielded a first

derivative esr spectrum, comprising of an 18G doublet centred about free spin (Figure

4-1.i.).

This doublet was also observed after irradiation of frozen aqueous TRIS.HCl

solution. This was further found to be the case when both protonated and amine forms

were irradiated in lithium chloride glass, although features for the electron loss centre

Cl_2-. were also observed (Figure 4-1.ii.).

In an attempt to gain further information, TRIS was also irradiated in DCl/D_2O at

77K. Whilst yielding features for Cl_2-, $ClOH^-$ and D radicals, the sample only

produced a more clearly resolved doublet again of 18G (Figure 4.1.iii.).

These uninformative spectra lead to the conclusion that in any TRIS derived

radical product, spin cannot be centred on the tertiary carbon (with NH_3 as a leaving

group) (Reaction 1), as might be expected from electron capture. Spin centred on

Nitrogen, as might be expected from electron loss, also clearly is not observed.

It therefore seems likely that a rapid rearrangement following both electron loss

and capture takes place even at 77K. There are two likely mechanisms of electron

capture after irradiation:

[R= -CH₂OH]

$$R_3C-NH^+_3 + e^- ----> R_3C + NH_3 \qquad (1)$$

$$(I)$$

$$R_3C-NH^+_3 + e^- ----> R_3CNH_2 + H \qquad (2)$$
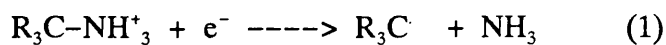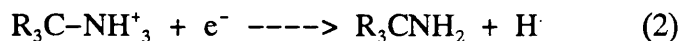
It might be expected that the rate constant for reaction 1 would be greater than that for reaction 2. However, in the 1,3,4 triol–tertiary butyl radical (I) the unpaired electron would experience hyperfine coupling to six beta–hydrogen nuclei and yield a complex multiplet in esr spectra. This clearly is not observed and suggests that reaction 2 may occur preferentially as the mechanism of electron capture. This is further supported by the possible subsequent reaction of the product hydrogen atom which may abstract a hydrogen atom from a neighbouring TRIS molecule:

$$H + (HOCH_2)_3C-NH^+_3 ----> (HOCH_2)_3C-N^+H_2 + H_2 \qquad (3)$$

$$H + (HOCH_2)_3C-NH^+_3 ----> (HOCH_2)_2(NH^+_3)C-CHOH + H_2 \qquad (4)$$
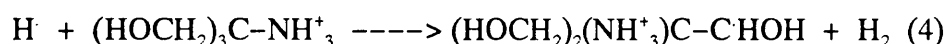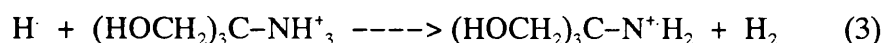
$$(II)$$

The highly labile hydrogen atom would be expected to favour reaction 4 thermodynamically because of steric effects. The observed 18G doublet is likely to be due to radical (II) where spin density is centred on the carbon atom with hyperfine coupling to a single –hydrogen atom.

Electron loss may proceed by the following mechanism (Reaction 5):

$$(HOCH_2)_3C-NH^+_3 \quad ----> \quad (HOCH_2)(NH^+_3)CCH_2O^{\cdot+}H \quad + \quad e^- \qquad (5)$$

<div align="center">(III)</div>

$$(HOCH_2)(NH^+_3)CCH_2O^{\cdot+}H \quad ----> \quad (HOCH_2)(N^+H_3)C\dot{C}HOH \quad + \quad H^+ \qquad (6)$$
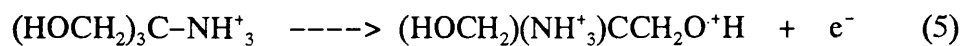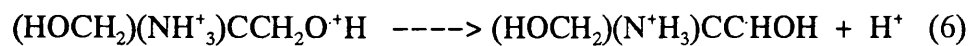
<div align="center">(II)</div>

the resulting radical (III) from reaction 5 is expected to rearrange whilst trapped in the

frozen liquid structure of the glass-like phase to again produce radical (II).

The unpaired electron of radical (II) would be expected to occupy a mainly

p-character orbital. However because of the high electronegativity of the oxygen

atom, the radical is slightly distorted from planarity to being pyramidal with the

introduction of more s-character into this orbital. Coupling to one -hydrogen atom

gives rise to the observed doublet A_{iso} of 18G.

FIG 4-1.i.

3215 G

20 G

FIG 4-1.ii.

20 G

FIG 4-1.iii.

$(HOCH_2)(N^+H_3)C-C \cdot HOH$

$Cl_2^{-\cdot}$

$D \cdot [+1]$

$ClOH^{-\cdot}$

$D \cdot [0]$

$D \cdot [-1]$

10 G
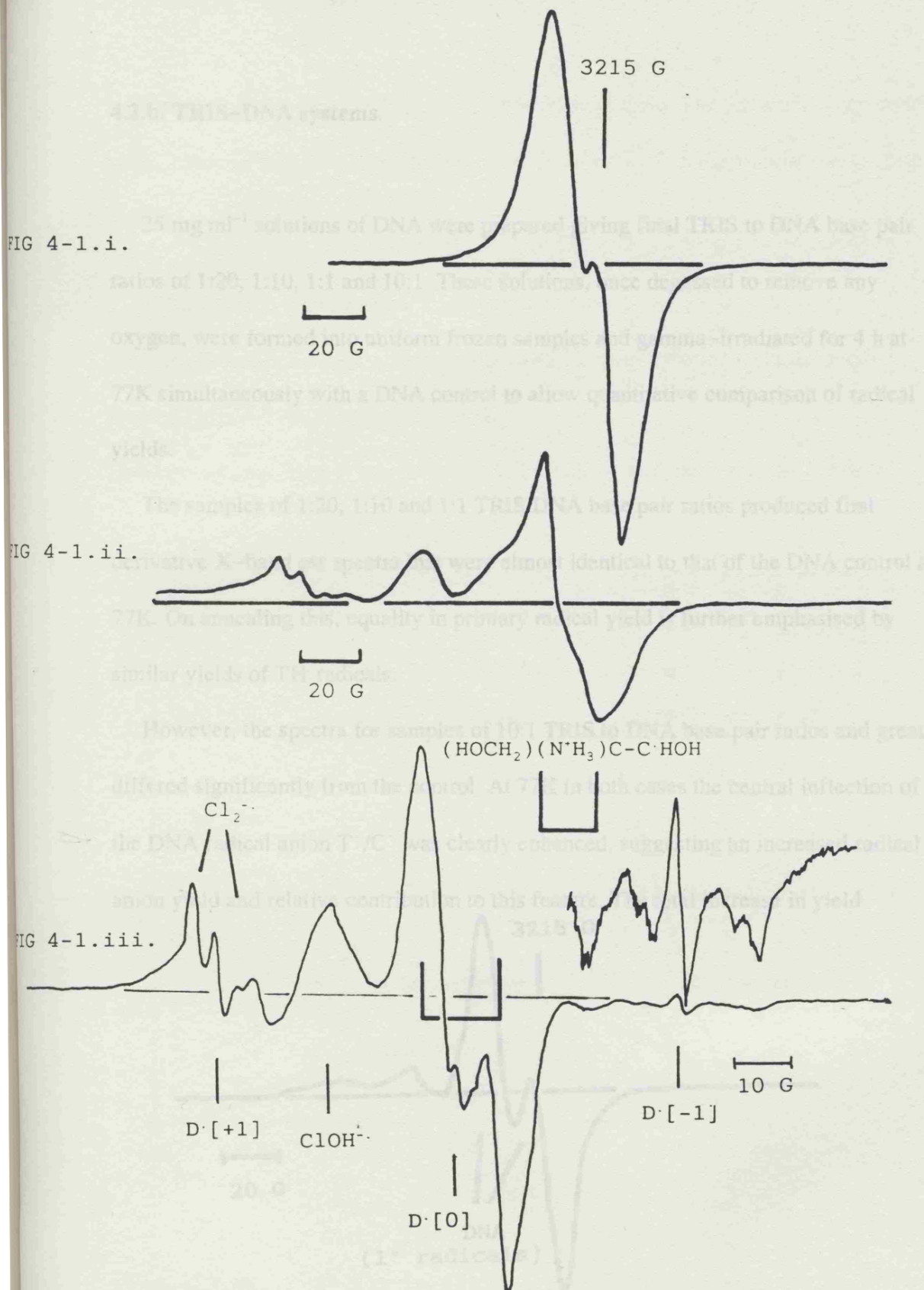
Figure 4-1. The first derivative X-band esr spectra of gamma-irradiated; i) TRIS hydrochloride solid at 77K. ii) TRIS in 10M LiCl solution at 77K and iii. TRIS in DCl/D_2O at 77K, all three spectra contain an 18G doublet feature assigned to $(HOCH_2)_2(NH_3^+)CC \cdot HOH$ radicals.

76

4.2.b. TRIS–DNA systems.

25 mg ml^{-1} solutions of DNA were prepared giving final TRIS to DNA base pair ratios of 1:20, 1:10, 1:1 and 10:1. These solutions, once degassed to remove any oxygen, were formed into uniform frozen samples and gamma–irradiated for 4 h at 77K simultaneously with a DNA control to allow quantitative comparison of radical yields.

The samples of 1:20, 1:10 and 1:1 TRIS DNA base pair ratios produced first derivative X–band esr spectra that were almost identical to that of the DNA control at 77K. On annealing this, equality in primary radical yield is further emphasised by similar yields of TH radicals.

However, the spectra for samples of 10:1 TRIS to DNA base pair ratios and greater differed significantly from the control. At 77K in both cases the central inflection of the DNA radical anion T$^-$/C$^-$ was clearly enhanced, suggesting an increased radical anion yield and relative contribution to this feature. The total increase in yield
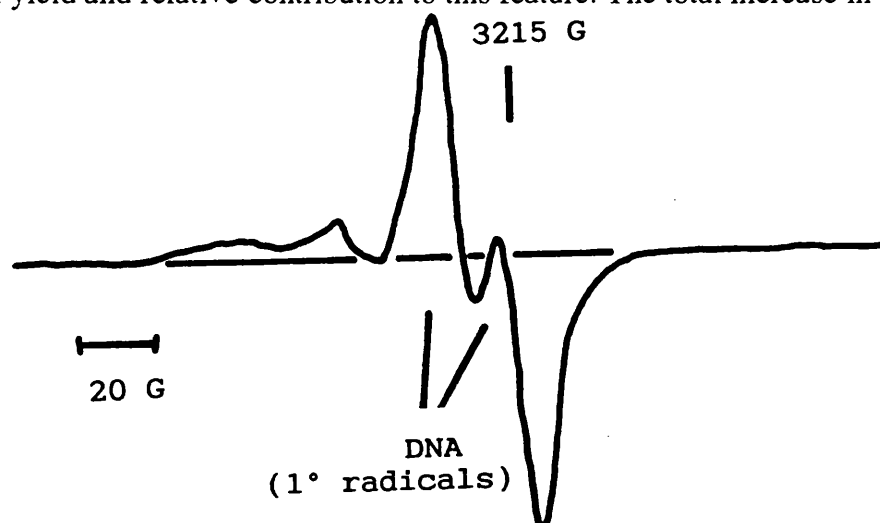
Figure 4–2. First derivative X–band esr spectrum of TRIS 10:1 DNA pairs at 77K, demonstrating a substantial enhancement in the doublet component of the DNA primary radical features, hence an enhancement in DNA radical anions.

77

appeared to be only from an increase in anion radical yield. The yield of G^+ appeared

to be unaltered; this was supported by comparison with computer simulations (Figure

4-2.).

Unfortunately, the magnitude of this enhancement could not be accurately

measured because the central feature also contains a contribution from the TRIS

derived radical $(HOCH_2)(NH^+_3)CCHOH$.

However on annealing, it was clear that TH yields in both cases are significantly
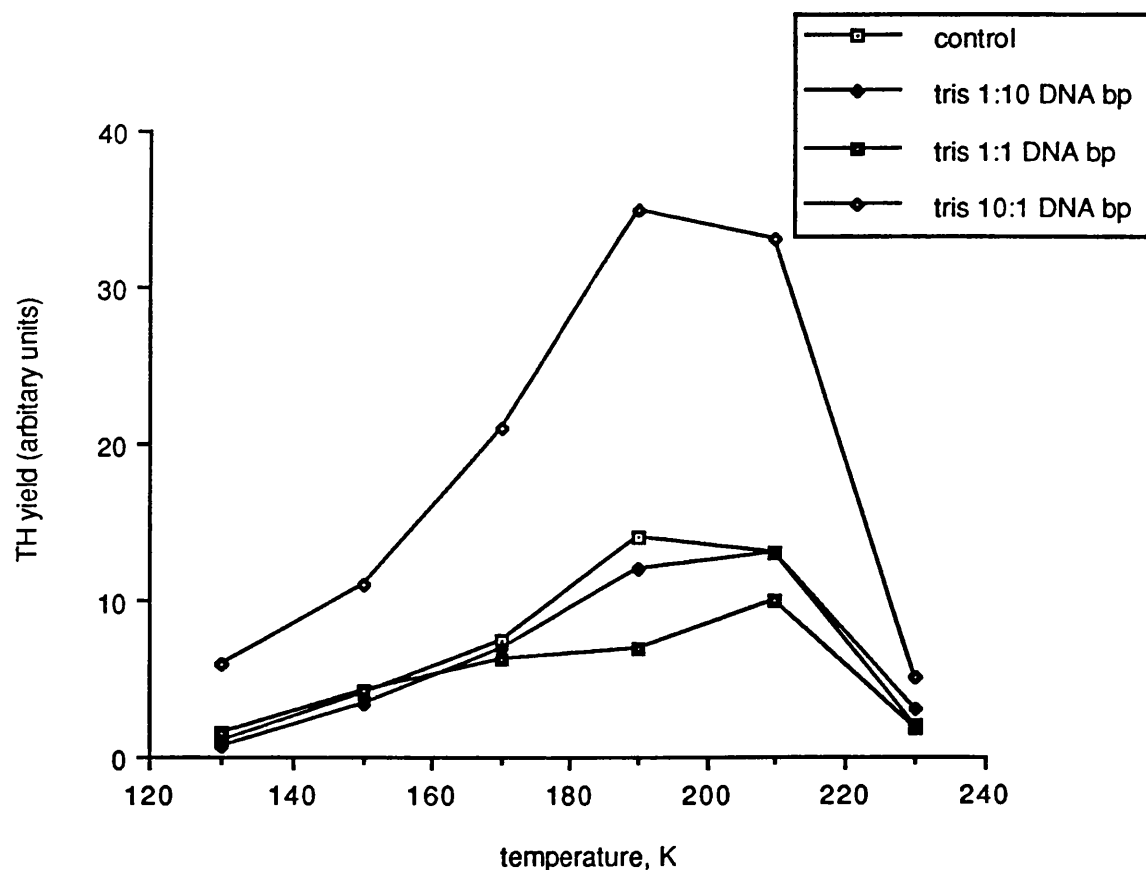
Figure 4-3. Plot of TH radical yield for Tris to DNA base pair ratios of 1:10, 1:1 and

10:1 versus temperature, demonstrating great enhancement of TH radical yield in the

10:1 sample.

larger than in the DNA control. Comparison of the spectra recorded after annealing to 190K demonstrates the enhancement in yield to be circa 260% . This is illustrated by a plot of TH yield versus temperature for these samples (Figure 4.3.).

The increase in DNA radical anion yield and consequently in TH yield, suggests that whilst electron capture by TRIS may occur, the rate constant for electron capture by the DNA is greater than that for electron capture by TRIS.

There appeared to be no enhancement in G^+ yield. Hole transfer to the DNA from the TRIS electron loss product radical (III) in reaction (5) is possible by electron transfer. However the formation of the $(HOCH_2)(NH^+_3)CC HOH$ radical is likely to be very fast and appears to prevent any enhancement in G^+ yield.

The increase in DNA primary radical anion yield observed at high TRIS concentration may be explained in the following way: The DNA target volume is increased relative to the control by the inclusion of a large number of buffer ions in the DNA solvation shell, the DNA competes favourably for electron capture resulting in the observe enhanced radical anion yield.

4.2.c. Phosphate in H_2O.

In order to obtain the buffered pH of 7.4, a ratio of 1:4.1 for potassium dihydrogen orthophosphate (KH_2PO_4) and disodium hydrogen orthophosphate (Na_2HPO_4) respectively was used to give a final total HPO_4^{2-} concentration in water of 0.75M.

The first derivative esr spectra recorded after gamma-irradiation at 77k contains a doublet feature assigned to hydrogen atoms, ^1H. A_{iso} for this doublet being 507.5G centred at free spin. The presence of hydrogen atoms in the esr spectrum is a clear

79

indication that glass regions are present, hydrogen atoms produced in the ice

crystallites react to form hydroxyl radicals even at 77K. Also apparent was a 34G

doublet assigned to the perpendicular features of the well characterised PO_4^{2-}

radical[16] superimposed over the expected perpendicular features of ·OH. It must be

stressed that these features may also be assigned to the protonated radical HPO_4^-.

Annealing to 130K resulted in the loss of hydroxyl radicals from the ice phase. The

parallel features of the PO_4^{2-} radical become apparent at this temperature, but these

3220 G

40 G

H· [+½]   507.5 G   H· [−½]
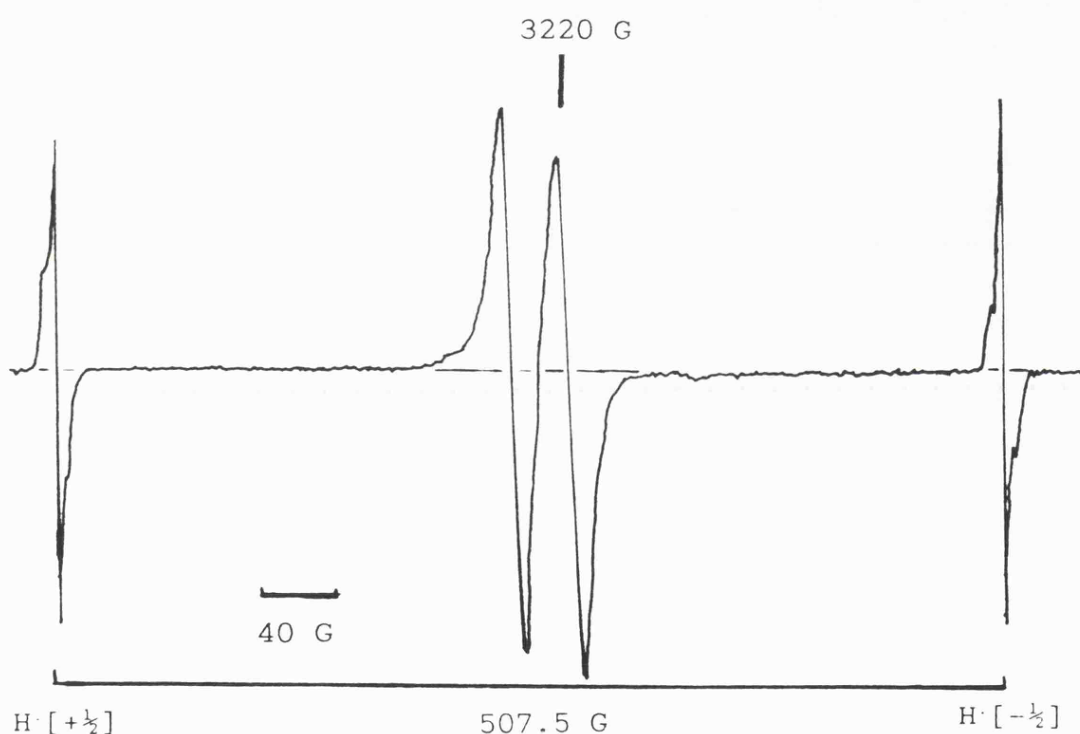
Figure 4–4. First derivative X–band esr spectrum of KH_2PO_4/Na_2HPO_4 (0.75M with

respect to HPO_4^{2-} ions and 1:4.1 ratio respectively) solution in H_2O after

gamma–irradiation at 77K and annealing to 130K, showing doublet features assigned

to H (A_{iso}= 507.5G) and the perpendicular features of PO_4^{2-} radicals.

were poorly defined and the perpendicular features dominated the spectrum. The recorded, A_{perp} 34G and g_{perp}–tensor = 2.008 agree well with values reported in the literature[17] (Figure 4-4).

The PO_4^{2-} radical has been studied extensively[18,19]. It is a 31–electron species with the unpaired electron confined to non–bonding orbitals on oxygen and has a distorted tetrahedral structure. The degree of distortion is dependent on the degree of delocalisation of the unpaired electron. The electron interacts with the phosphorous nucleus by spin polarisation of the P–O sigma bonds. This coupling is weak results in the small isotropic splitting.

g–Anisostropy arises as a result of confinement of the unpaired electron to less than all of the ligand oxygen atoms. The largest deviation from free spin would result from confinement to a single oxygen atom. The degree of deviation from free spin is a measure of the degree of confinement.

In the present case, g_{perp} was very close to free spin, whilst the parallel features were down field. This apparent axial symmetry suggests considerable localisation on a single oxygen ligand.

The PO_4^{2-} radical is thought to be the direct product of electron loss (Reaction 7):

$$HPO_4^{2-} \quad ----> \quad (H^+) + PO_4^{2-} + e^- \qquad (7)$$
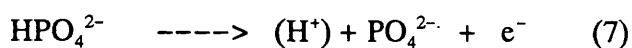
It may also be formed indirectly by electron capture (reaction 8):

$$HPO_4^{2-} + e^- \quad ----> \quad P(O)_3OH \qquad (8)$$
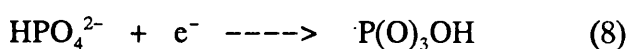
$$(I)$$

The resulting phosphoranyl radical (I) has spin centred on the phosphorous atom

and would yield a doublet of approximately 800G. This is clearly not observed

but it may react further to give hydrogen atoms (reaction 9):

$$HOPO_3^{3-} \; ----> \; PO_4^{3-} \; + \; H \cdot \qquad (9)$$
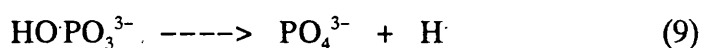
Hydrogen atoms were observed and may have reacted further to yield the observed

PO_4^{2-} radicals:

$$H \cdot \; + \; HPO_4^{2-} \; -----> \; H_2 \; + \; PO_4^{2-} \qquad (10)$$
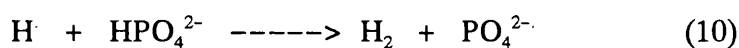
The interesting phenomenon of spin–flip satellites was observed in both features of

the 507.5G hydrogen atom doublet (Figure 4–5). Hydrogen atoms trapped in the glass

regions experience the 1/2 and –1/2 nuclear spin states of the neighbouring hydrogen

atoms of water molecules. Thus satellite lines were observed at high powers centred

about the esr resonance, with a splitting energetically equivalent to that of the nuclear

magnetic resonance of a proton at this field strength. The narrow lines of the hydrogen

atoms appeared as a doublet of triplets in the esr spectrum (Figure 4–5).

The intensity of these additional features is proportional to a number of factors:

i) the number of neighbouring atoms.

ii) the microwave power of recording.

iii) the inverse of the separation of spin and neighbouring nuclear spin.

At very high powers, further splitting may be observed and the hydrogen atom

resonance appearing as a doublet of quintets.
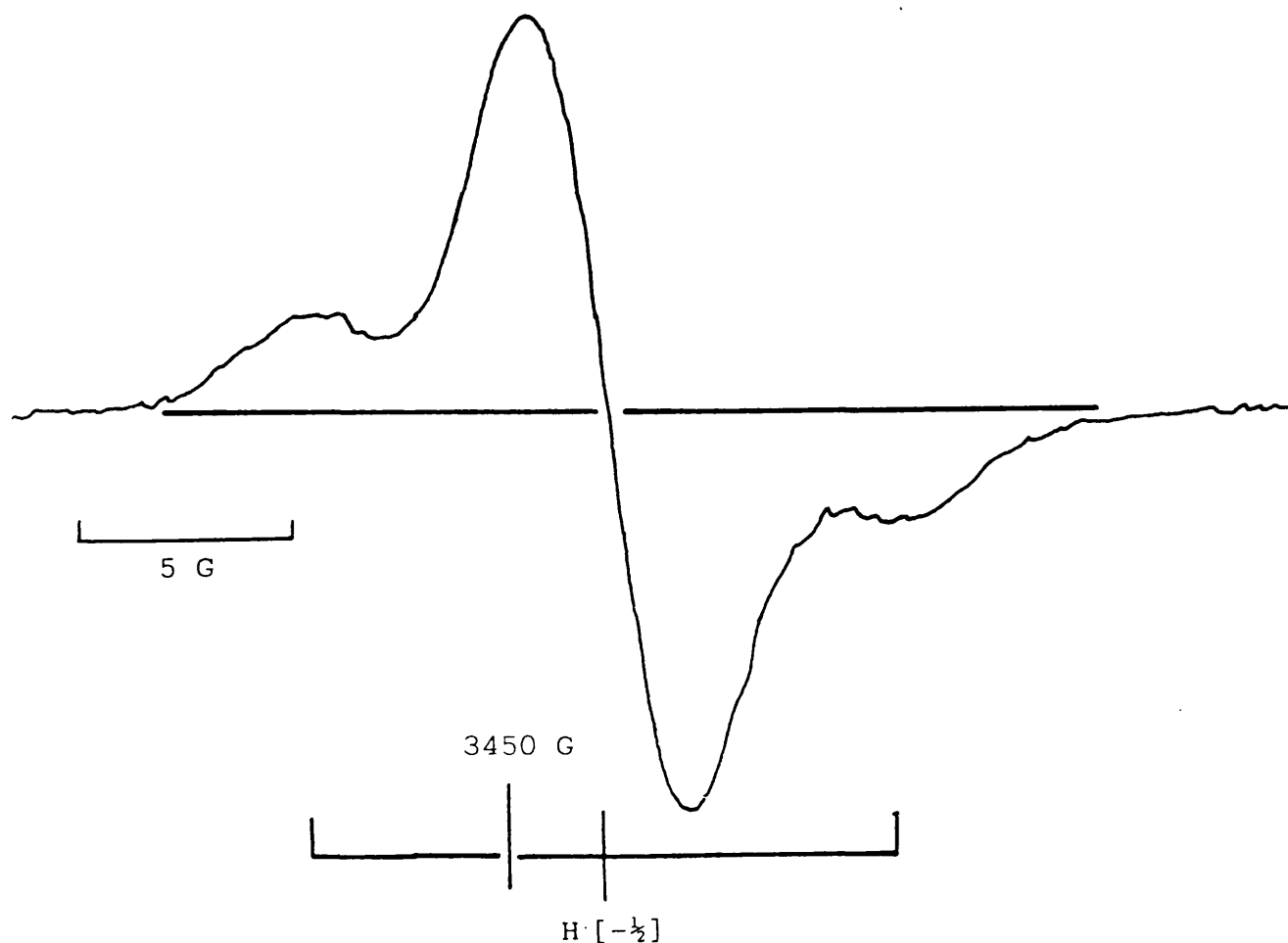
Figure 4-5. First derivative X-band esr spectrum of high field -1/2 hydrogen atom feature, demonstrating the phenomenon of spin-flip satellites.

4.2.d. Phosphate ions in D_2O.

The spectrum of the equivalent 0.75 M phosphate D_2O sample when recorded at

low power (0.01mW) yielded the expected first derivative esr spectra at 77K. The

spectrum contained a 1:1:1 triplet feature assigned to deuterium atoms, ˙D (A_{iso} =

55G), and features assigned to ˙OD and PO_4^{2-} radicals.

The PO_4^{2-} features were much better defined at 77K, and after annealing to 130K

(Figure 4–6.), in the deuterated solvent. The parallel features where more clearly

resolved and the g_{para}–tensor was measured. Whilst g_{perp} remains very close to free

spin, the shift in the g_{para}–tensor away from free spin again suggests that the unpaired
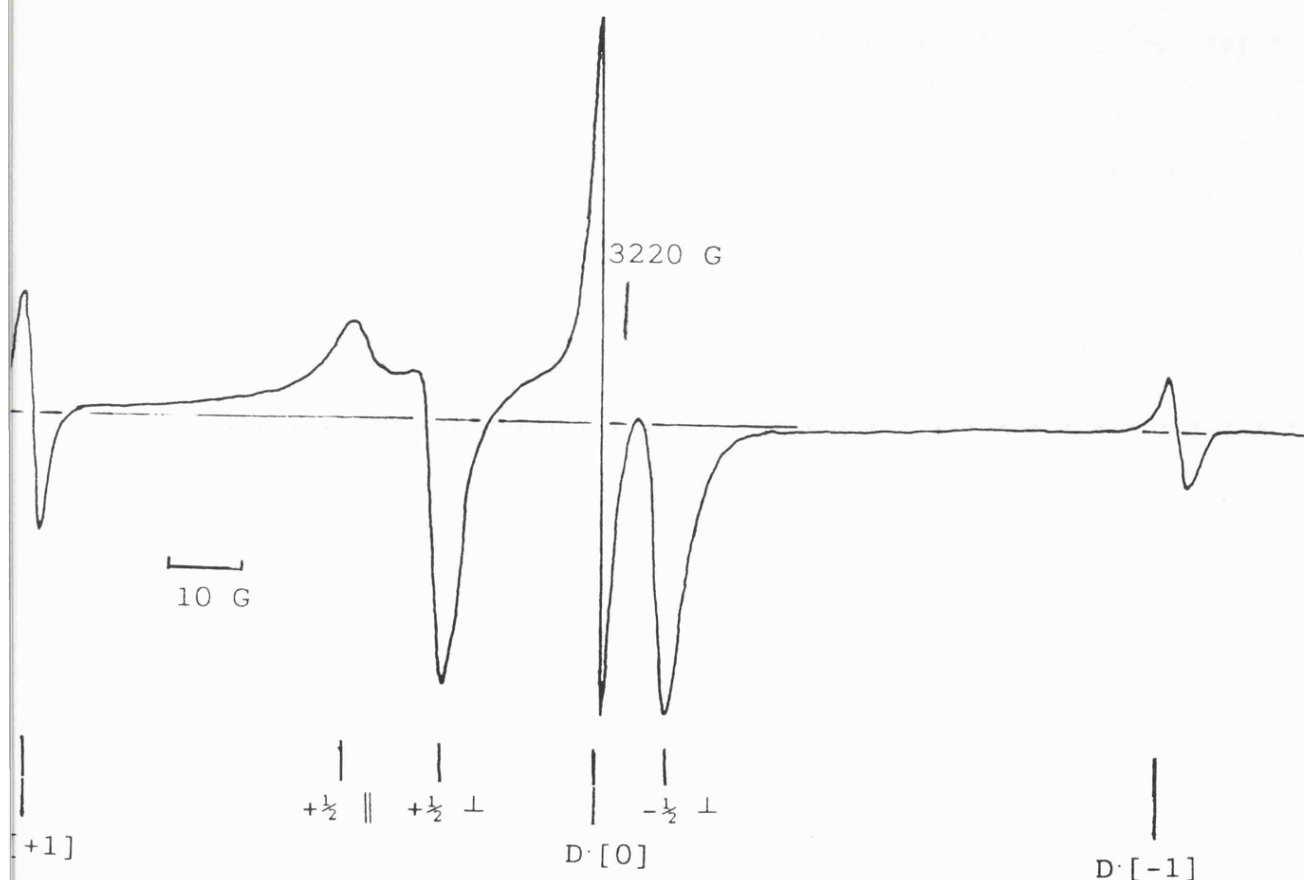
electron is confined to one oxygen atom, and that the PO_4^{2-} radical is distorted.

Figure 4–6. First derivative X–band esr spectrum of KH_2PO_4/Na_2HPO_4 (0.75M with respect to HPO_4^{2-} ions and 1:4.1 ratio respectively) solution in D_2O after gamma–irradiation at 77K and annealing to 130K, containing well defined perpendicular and parallel doublet features assigned to PO_4^{2-} radicals and a triplet feature assigned to ˙D (A_{iso}= 55G). The shift in g_{para}–tensor down field of free spin suggesting axial–symmetry and hence spin localisation predominantly on a single oxygen atom. The central feature (D [0]) of the triplet feature assigned to deuterium atoms demonstrating relaxation transfer effects.

Higher power (0.2mW) revealed inequalities in the intensities of the D triplet.

This was due to spin relaxation transfer effects. Single resonances may become power

saturated at high microwave powers. In this case the D±1 features became partially

saturated. Complex resonances however, may exchange some spin state relaxation;

the central resonances here, which saturate at relatively high powers, induced spin

relaxation in the central D feature and its intensity was thus less diminished by the

increased microwave power.

4.2.e. Phosphate DNA Systems.

As described above and in Chapter 2, DNA (25mg ml^{-1}), samples were prepared

with an $HPO_4 2-$ ion to DNA base pair ratio of 20:1 buffered at pH 7.4 in both H_2O

and D_2O solvents. Samples of uniform size were simultaneously gamma–irradiated,

positioned accurately in the spectrometer cavity and recorded along with the

equivalent phosphate and DNA controls to enable accurate computer subtractions and

measurement of DNA radical yields.

At 77K, the uninformative first derivative esr spectrum contained the expected

features of hydroxyl (OH) radicals; their yield was diminished in comparison with that

of the DNA control. This was probably due to the increased volume of the

DNA–solute glass region relative to that of the ice crystallite phase. The $-1/2$

perpendicular OH feature was also altered in shape when compared with the DNA

control due to a contribution from the parallel features of PO_4^{2-} radicals. The central

broad feature was a composite of the DNA primary radicals G^+ and T^-/C^- and the

perpendicular features of the PO_4^{2-} radical. Computer subtraction of the spectra

obtained from 0.75M HPO_4^{2-} control (equivalent phosphate concentration) revealed a 60% decrease in DNA primary radical yield when compared with the DNA control.

After annealing to 130K, the poorly resolved parallel features assigned to the $PO_4^{2-\cdot}$ radical were apparent (Figure 4–7.i.). For the deuterated solvent computer subtraction of the DNA control confirmed that the central complex resonance was indeed composed of DNA primary radical features and the perpendicular features of the $PO_4^{2-\cdot}$ radical (Figure 4–7.ii.).

FIG 4-7.i.

10 G

∥

⊥

3220 G

$PO_4{}^{2-}$

$+\frac{1}{2}$ ∥ $-\frac{1}{2}$ ∥

$g_\parallel$

FIG 4-7.ii.

$+\frac{1}{2}$ ⊥ $-\frac{1}{2}$ ⊥

$PO_4{}^{2-}$

Figure 4–7.i. First derivative X–band esr spectrum of 20:1 phosphate to DNA base pair ratio sample in H_2O after gamma–irradiation at 77K and annealing to 130K, containing poorly defined parallel features of $PO_4{}^{2-}$ radicals down field of free spin. ii. The resulting spectrum obtained by subtracting the spectrum of the DNA control from that of the phosphate–DNA sample after annealing to 130K. Clearly defined are both the perpendicular and parallel features assigned to $PO_4{}^{2-}$ radicals (g_{perp}= 2.014 and g_{para}= 2.032).

87

There was no measurable increase in the yield of PO_4^{2-} radicals with the loss of OH radicals after annealing. OH radicals might be expected to react with PO_4^{3-} ions to give further PO_4^{2-} radicals and OH^- ions. This supports the premise that all the observed OH radicals are present only in the ice phase and that the vast majority of the solute ions are confined to the DNA–glass and possibly other glass regions.

On further annealing, it was apparent that the reduced yield in DNA primary radicals resulted in reduced yield of TH radicals relative to that of the control. This reduction is best illustrated by a plot of TH yield verses temperature (Figure 4–8).
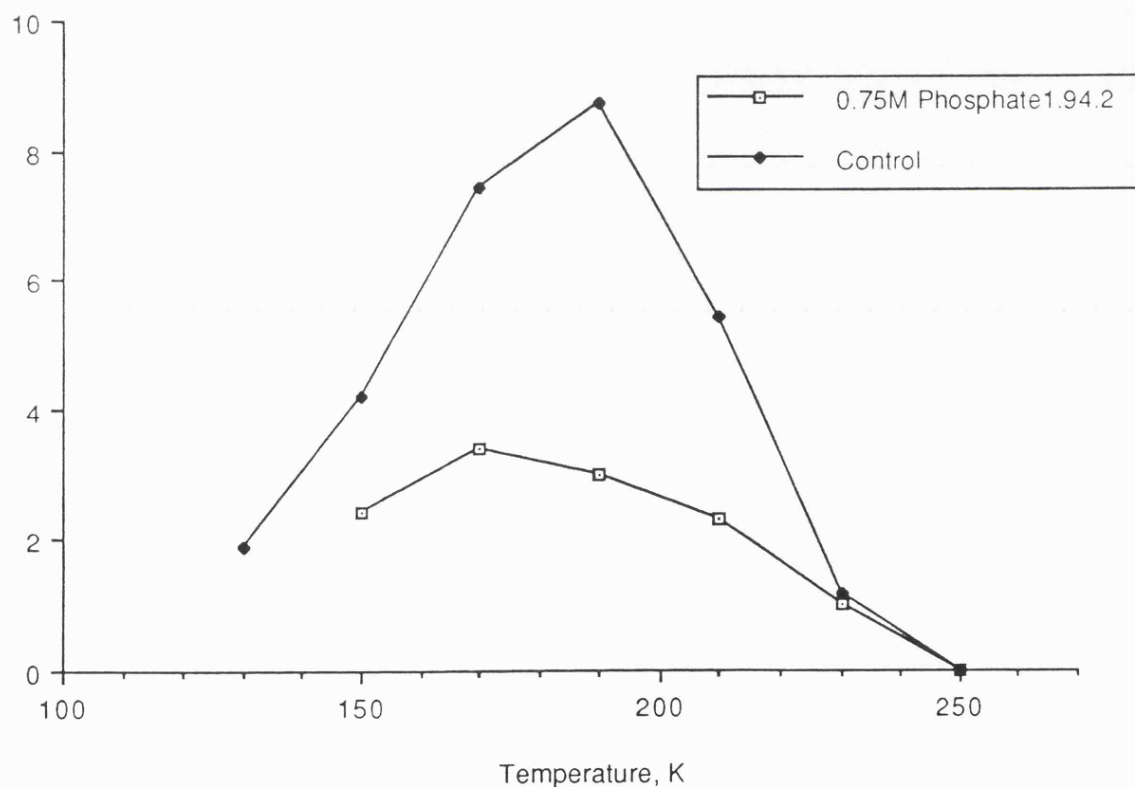
Figure 4–8. Plot of TH radical yield versus temperature for phosphate–DNA and DNA control samples in H_2O, illustrating the reduction in TH radical yield in the phosphate–DNA sample.

At 190K, the poorly defined parallel and well defined 31G splitting perpendicular features of PO_4^{2-} were apparent in the esr spectrum, g_{perp}-tensor being 2.014. Due to poor definition, the g_{para}-tensor could not be accurately measured (Figure 4–9).

All DNA derived features were lost after annealing to 230K, leaving only the features of the PO_4^{2-} radical, from which g_{para}-tensor was estimated to be 2.03. Continued annealing to 270K did not result in the rapid decay of these signals.

After decanting off the liquid nitrogen, the sample was allowed to continue annealing in the spectrometer cavity whilst the spectra was continuously recorded in 30s cycles. This demonstrated the PO_4^{2-} radical only decayed rapidly at the melting point of the system.
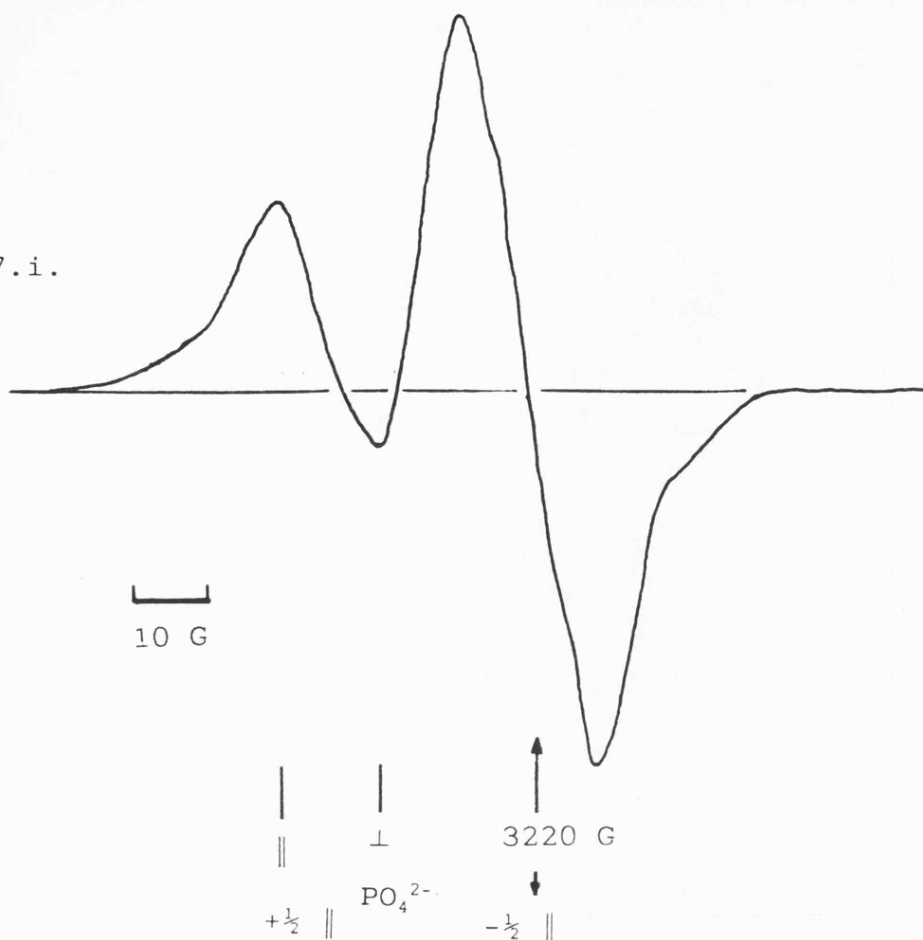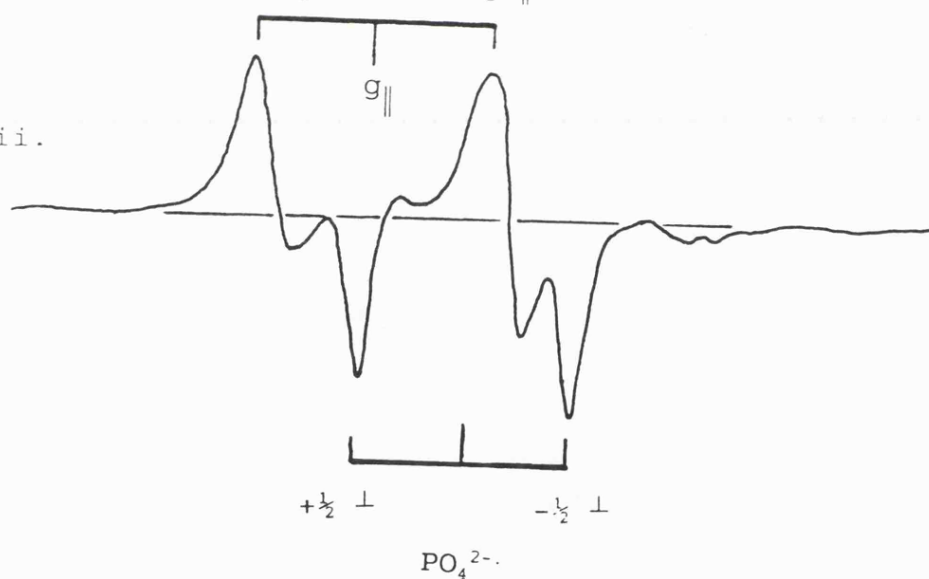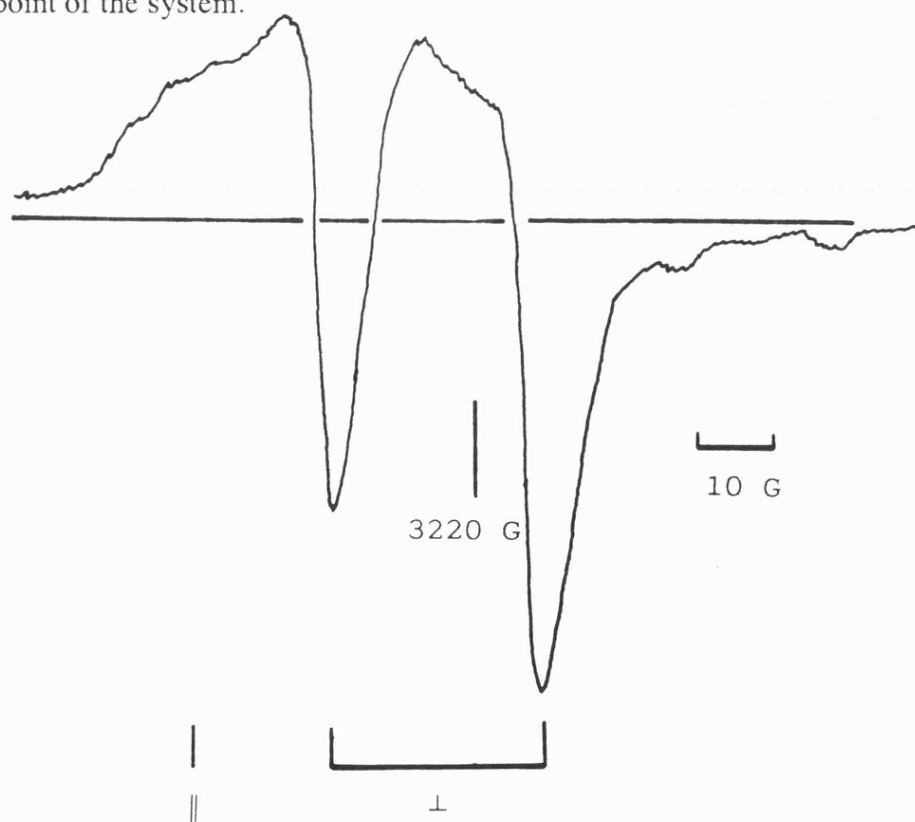

Figure 4–9. First derivative X–band esr spectrum of 20:1 phosphate to DNA base pair ratio sample in H_2O after gamma–irradiation at 77K and annealing to 190K. Containing the poorly resolved parallel feature and well resolved doublet parallel feature of PO_4^{2-} radicals.

89

4.2.f. Sulphate ions in H_2O and D_2O.

After irradiation at 77K the first derivative esr spectrum for 0.75M sodium sulphate

in H_2O contained features assigned to OH radicals. The existence of a sodium and

sulphate ion containing glass region is demonstrated by the presence of a 508G

doublet assigned to hydrogen atoms in the esr spectrum. The central feature is also

enhanced by an unknown resonance centred very close to free spin. After annealing to

130K, the loss of ice phase derived OH radical features allowed this sharp central

feature to be characterised as SO_3^- radical anions, the recorded g–tensor g = 2.0036,

being in good agreement with the published value[18].

SO_3^- radicals are believed to be the product of electron capture by sulphate ions

(Reaction 11):

$$HSO_4^- + e^- ----> HSO_4^{2-} ----> SO_3^- + OH^- \quad (11)$$
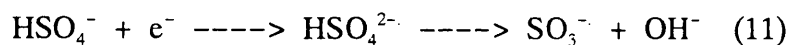
Features down field of free spin were assigned to the electron loss product SO_4^-

radical anions (Reaction 12):

$$SO_4^{2-} ----> SO_4^- + e^- \quad (12)$$
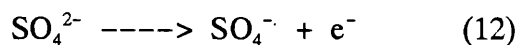
the resulting 'hole' may be centred on one, two or three oxygen atoms and hence gives

rise to three g tensors; g_x, g_y and g_z, the g_x tensor giving the greatest chemical shift

from free spin, the g_z tensor being very close to free spin and obscured by the intense

central feature of SO_3^- radicals. These features were more clearly resolved in the

spectrum of the deuterated solvent sample (Figure 4–10), where $g_x = 2.034$ and $g_y = 2.02$.

An unassigned feature at $g = 1.996$ was also observed at 130K having been gained on annealing, this was also observed in both solvents and remains uncharacterised.
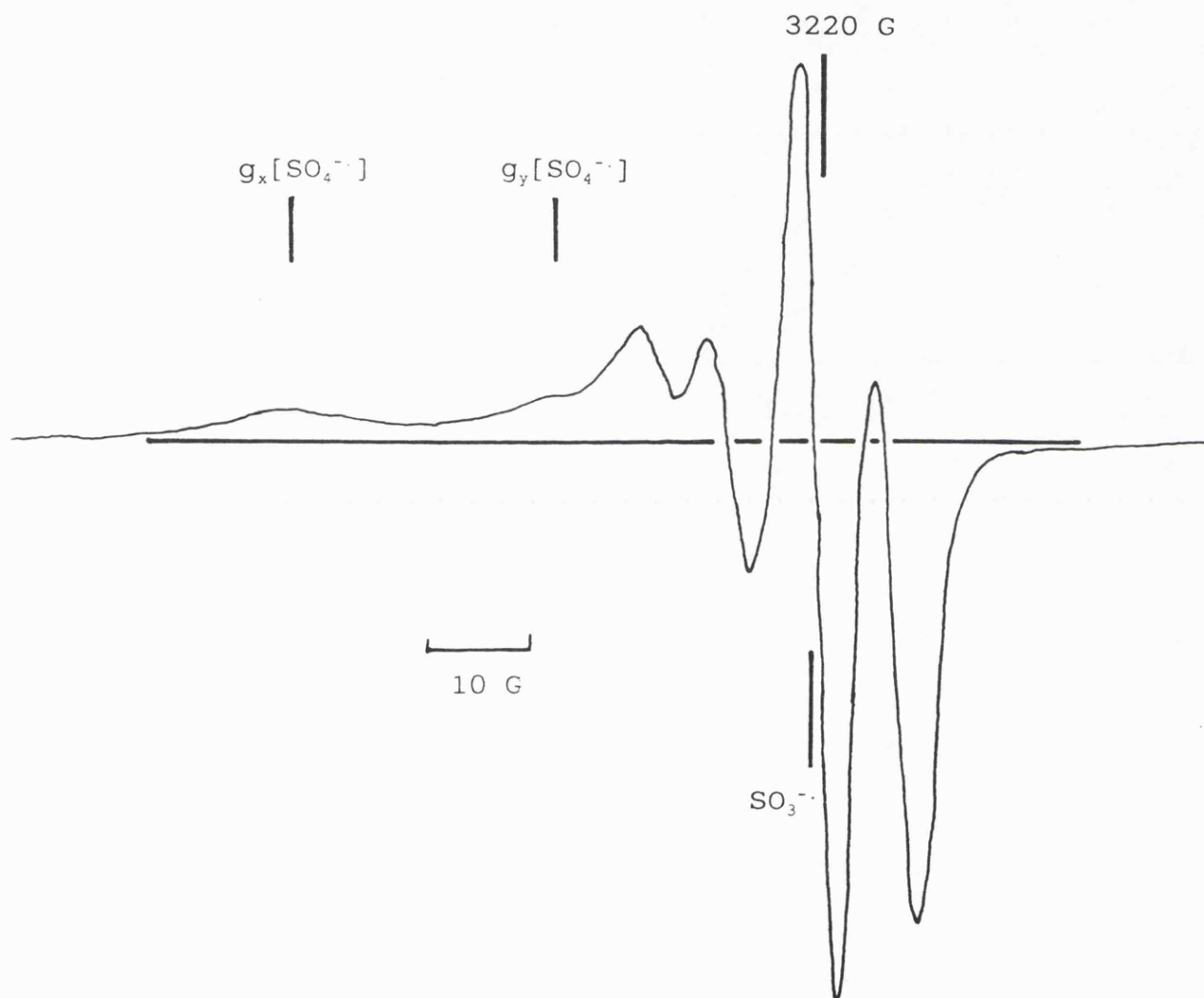
Figure 4–10. First derivative X–band esr spectrum of 0.75M Na_2SO_4 solution in D_2O after gamma–irradiation at 77K and annealing to 130K, containing features assigned to SO_3^- (g=2.0036) and SO_4^- ($g_x= 2.034$, $g_y= 2.02$) radicals.

4.2.g. DNA–Sulphate systems.

25mg ml^{-1} DNA samples were prepared in 0.75M sodium sulphate solutions in both H_2O and D_2O, these were degassed, frozen and irradiated as described above.

At 77K, the first derivative esr spectrum of the H_2O sample contained the expected features assigned to DNA primary radicals and OH radicals. In addition a sharp singlet feature was also apparent at g = 2.0036, this was again assigned to SO_3^- radicals as above. The same spectrum recorded at 800G contained a 507G doublet assigned to hydrogen atoms, demonstrating the existence of glass–like regions.

$g_x[SO_4^{-\cdot}]$ $g_y[SO_4^{-\cdot}]$ $SO_3^{-\cdot}(g=2.0036)$ 3236 G
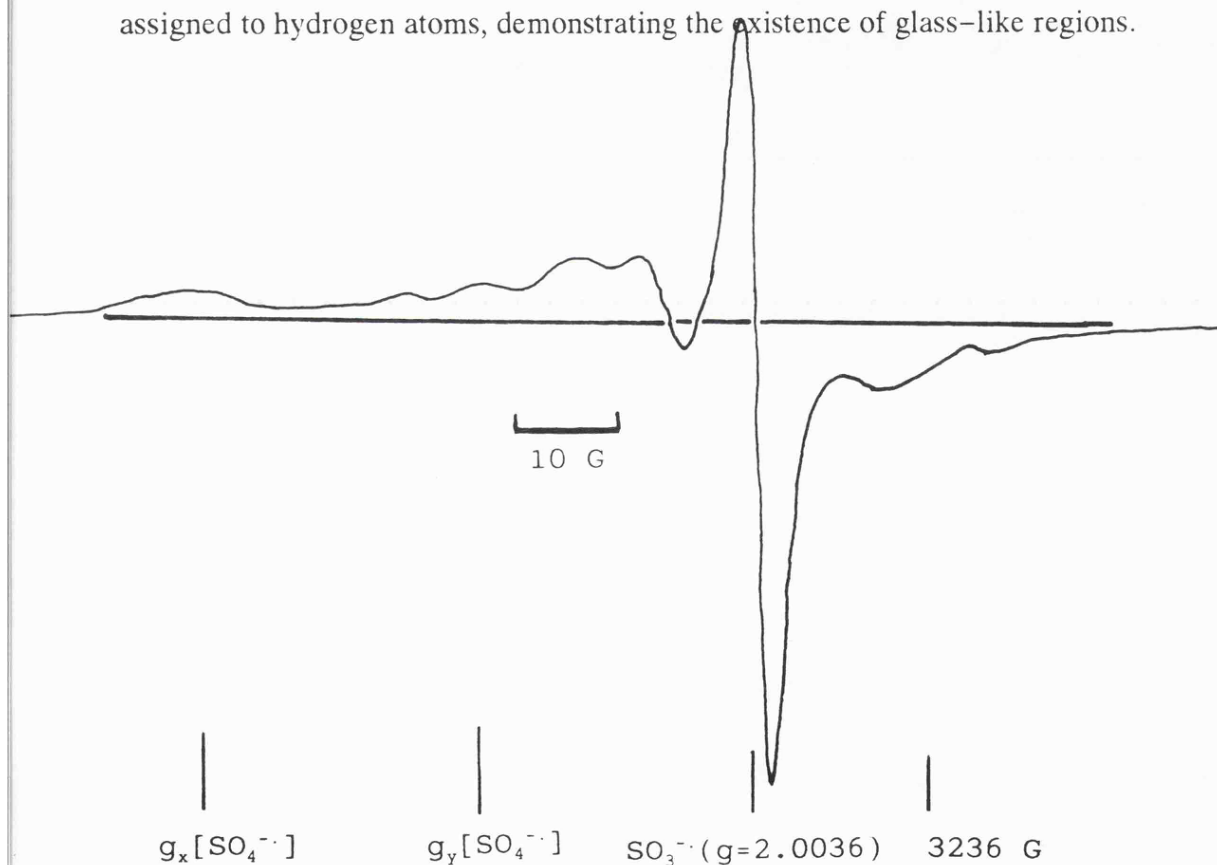
Figure 4–11. The resulting spectrum obtained by subtracting the spectrum of the DNA control from that of the sulphate–DNA sample(both samples in D_2O) after annealing to 130K. The spectrum contains features assigned to SO_3^- and SO_4^- radicals.

Annealing to 130K resulted in the loss of OH and H features, and OD and D features from the spectra of the H_2O and D_2O samples respectively. In the spectra of

both samples, the feature assigned to SO_3^- radicals was more clearly resolved than at 77K. Computer subtraction of the spectrum of the DNA control(D_2O) from that of the sulphate-DNA(D_2O) sample revealed features assigned to SO_4^- radicals (Figure 4-11).

On further annealing of the H_2O sample it became clear that whilst TH features were observed, with the corresponding loss of intensity in the DNA primary radical features, the TH yield was significantly reduced in comparison with that of the DNA control. Presumably this was due to the competition for electron capture by sulphate ions, resulting in the observed SO_3^- radicals.

At 210K the yield of TH was found to be significantly less than that of the DNA control, this is illustrated by a plot of TH yield versus temperature (Figure 4-12). The features assigned to SO_3^- and SO_4^- radicals were still detected in spectra recorded at 270K (although the total number of spins was only *ca.* 30% that of the equivalent phosphate sample at 270K) and were only lost after thawing.
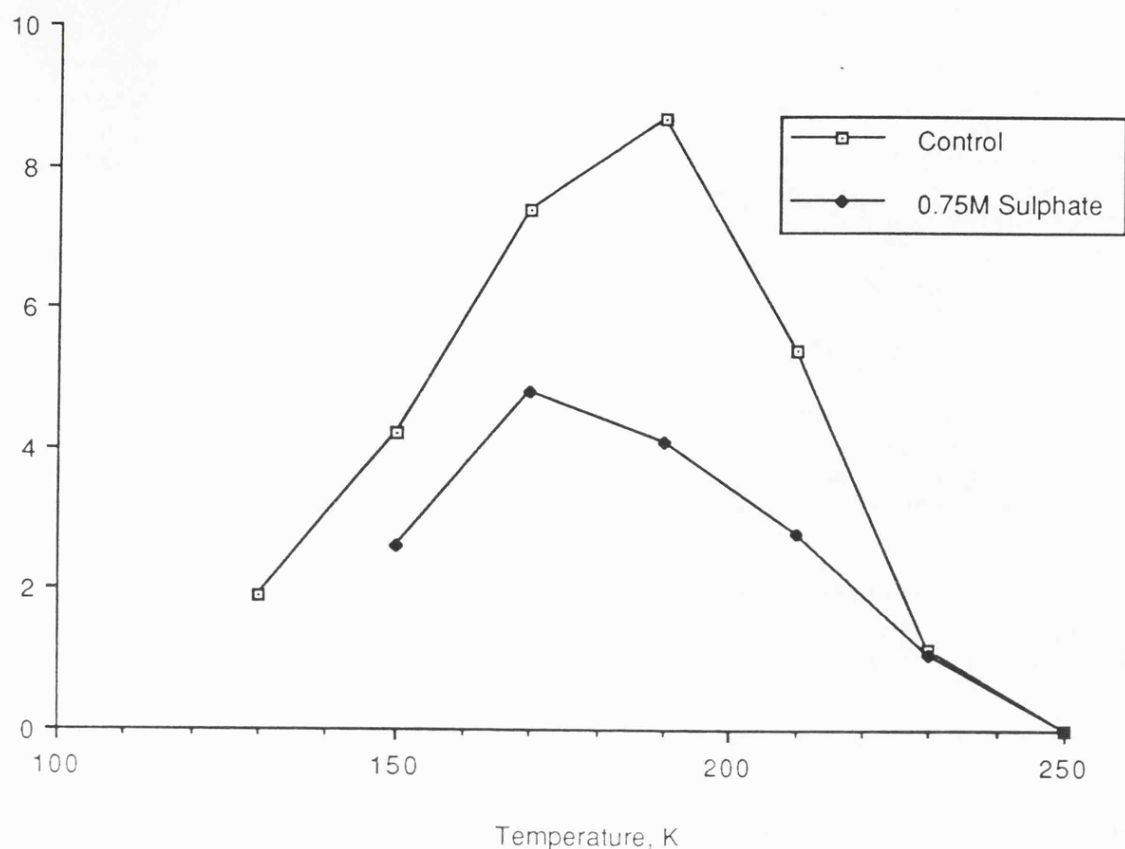
Figure 4–12. Plot of TH radical yield versus temperature for sulphate–DNA and DNA control samples in H_2O, illustrating the reduction in TH radical yield in the sulphate–DNA sample.

4.2.h. Perchlorate ions in H_2O and D_2O.

The radiation chemistry of perchlorate ions in frozen aqueous systems has been extensively studied, since these ions are commonly used as glass forming agents in esr studies of frozen aqueous systems. 0.75M sodium perchlorate solutions were prepared with H_2O and D_2O solvents and irradiated at 77K as described above. Both samples produced the expected first derivative esr spectra at 77K.

The spectrum of the perchlorate–H_2O sample contained a 507 G doublet assigned to hydrogen atoms (demonstrating the formation of glass–like regions within each sample even at this relatively low concentration), as well as the parallel features of OH radicals. Also present down field of free spin was a broad singlet feature assigned to the perpendicular feature of O^- radical anions. The g_{perp}–tensor being 2.08 which corresponds well with literature values[19,20]. The parallel feature of the O^- ions (g_{para} free spin) was obscured by the large parallel features of the OH radicals.

The O^- radical features were more clearly resolved in the 77K spectrum of the sample prepared in D_2O, along with with features assigned to deuterium atoms and OD radicals (Figure 4-13).

O^- radicals are believed to be the product of electron capture by perchlorate ions:

$$ClO_4^- + e^- \longrightarrow ClO_4^{2-}$$
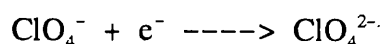
The resulting ClO_4^{2-} radicals is extremely unstable in aqueous solution and decay rapidly to yield ClO_3^- ions and the observed O^- radicals[19]:

$$ClO_4^{2-} \longrightarrow ClO_3^- + O^-$$
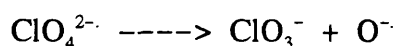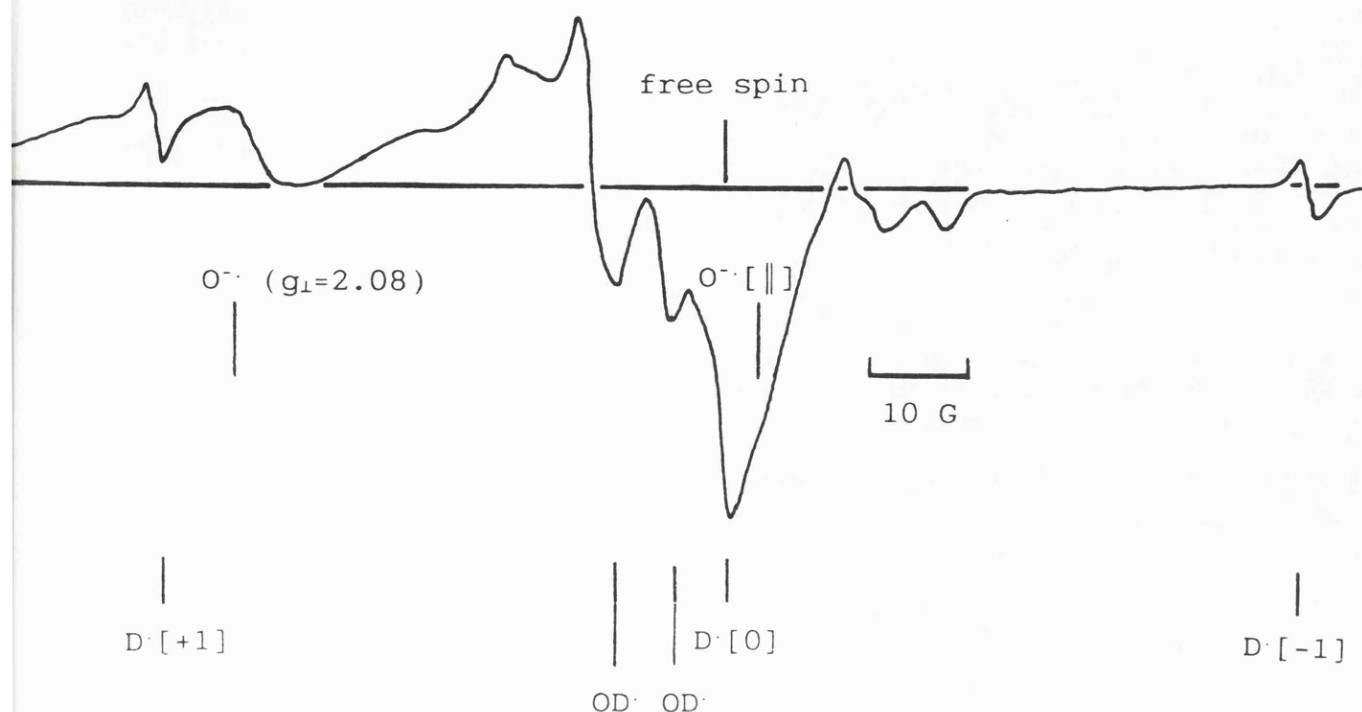
Figure 4–13. First derivative X–band esr spectrum of 0.75M NaClO$_4$ solution in D$_2$O after gamma–irradiation at 77K. The spectrum contains features assigned to O$^-$, D and OD radicals.

4.2.i. DNA–Perchlorate systems.

25 mg ml^{-1} DNA samples were prepared in 0.75M sodium perchlorate solutions in both H$_2$O and D$_2$O, these were degassed and gamma–irradiated at 77K as described above to allow direct comparison with a DNA control.

At 77K, the first derivative esr spectrum of the H$_2$O sample contained features assigned to ice phase OH radicals, the DNA primary radical features of G$^+$ and T$^-$/C$^-$. The G$^+$ yield was found to be slightly enhanced relative to the DNA control. This enhancement was probably due to 'hole' transfer from the perchlorate glass. Hole

centres are not extensively trapped in perchlorate glasses and may be transferred to the DNA by the following charge transfer processes:

$$ClO_4 + ClO_4^- ---- ClO_4^- + ClO_4$$

$$ClO_4 + G ----> ClO_4^- + G^+$$
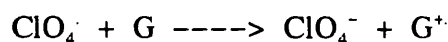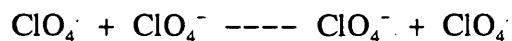
Also present in the spectrum was the low field perpendicular feature assigned to O^- radicals, $g_{perp} = 2.08$. These again being the product of electron capture by perchlorate ions as described above. A singlet feature positioned very close to free spin was also detected, the intensity of which was found to increase on annealing to 130K. This feature was not due to trapped electrons, since the sample did not appear to be coloured as might be expected as the result of such trapped centres. Also 'Photobleaching' by exposure of the sample to visible light did not result in any reduction of the feature's intensity. Thus the feature remained unassigned since the singlet feature gave little information of the nature of the species responsible. The unknown radical is termed radical γ.

Annealing to 130K resulted in the irreversible loss of the ice phase OH radicals and the loss of features assigned to O^- radicals from the spectrum. Features assigned to DNA primary radicals were present, and as stated above the intensity of the central singlet feature due to the unknown radical was increased. Also apparent was an intense, well resolved unassigned 40G doublet centred on free spin, and a poorly resolved 89G doublet also centred about free spin. These features were more clearly

resolved in the spectrum of the sample prepared in D_2O (Figure 4-14), and were termed radicals α and β respectively.

The three unassigned radicals α, β and γ were gained within the spectra, with the corresponding loss of the features assigned to O^- radicals. These radicals have g tensor values very close to free spin, and radicals α and β have hyperfine splitting suggestive of coupling to hydrogen nuclei. Such esr parameters suggest that these radicals have spin density centred on C-H units (22G), this strongly suggests that these features may have been due to trapped sugar centred radicals formed as a result of attack on the DNA by O^- radicals. O^- radicals are expected to react like OH radicals given their chemical similarity, thus they might be expected to react with DNA by hydrogen atom abstraction to give sugar radicals and hydroxide ions.
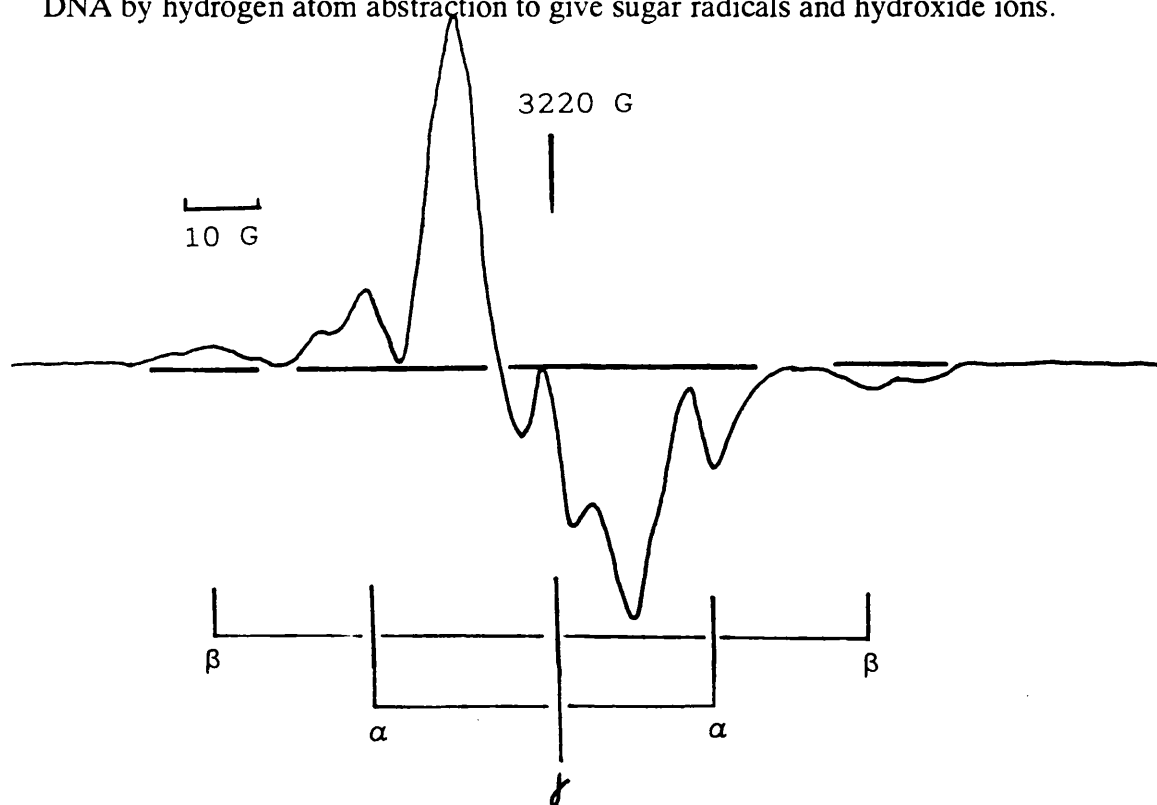
Figure 4-14. First derivative X-band esr spectrum of 20:1 perchlorate to DNA base pair ratio sample in D_2O after gamma-irradiation at 77K and annealing to 130K, containing a singlet feature and two doublet features of the unassigned `sugar' radicals γ, $\alpha(A_{iso}=$ 40G) and $\beta(A_{iso}=$ 86G) respectively.

On annealing to 150K the intensity of these radicals remained constant, the fact that their intensity did not increase again suggests that they were the result of DNA attack by O⁻ radicals.

Further annealing to 170K results in the loss the features of β and γ in the spectra in both solvents, whilst the doublet feature of α was lost after annealing to 190K. After annealing to this temperature, the yield of TH radicals was found to be reduced in comparison with that of the DNA control. This is illustrated by a plot of TH intensity versus temperature (Figure 4-15) and is thought to be the result of competition for electron capture at the pyrimidine bases by perchlorate ions. Electron capture by the perchlorate ions giving rise to the observed O⁻ radicals.
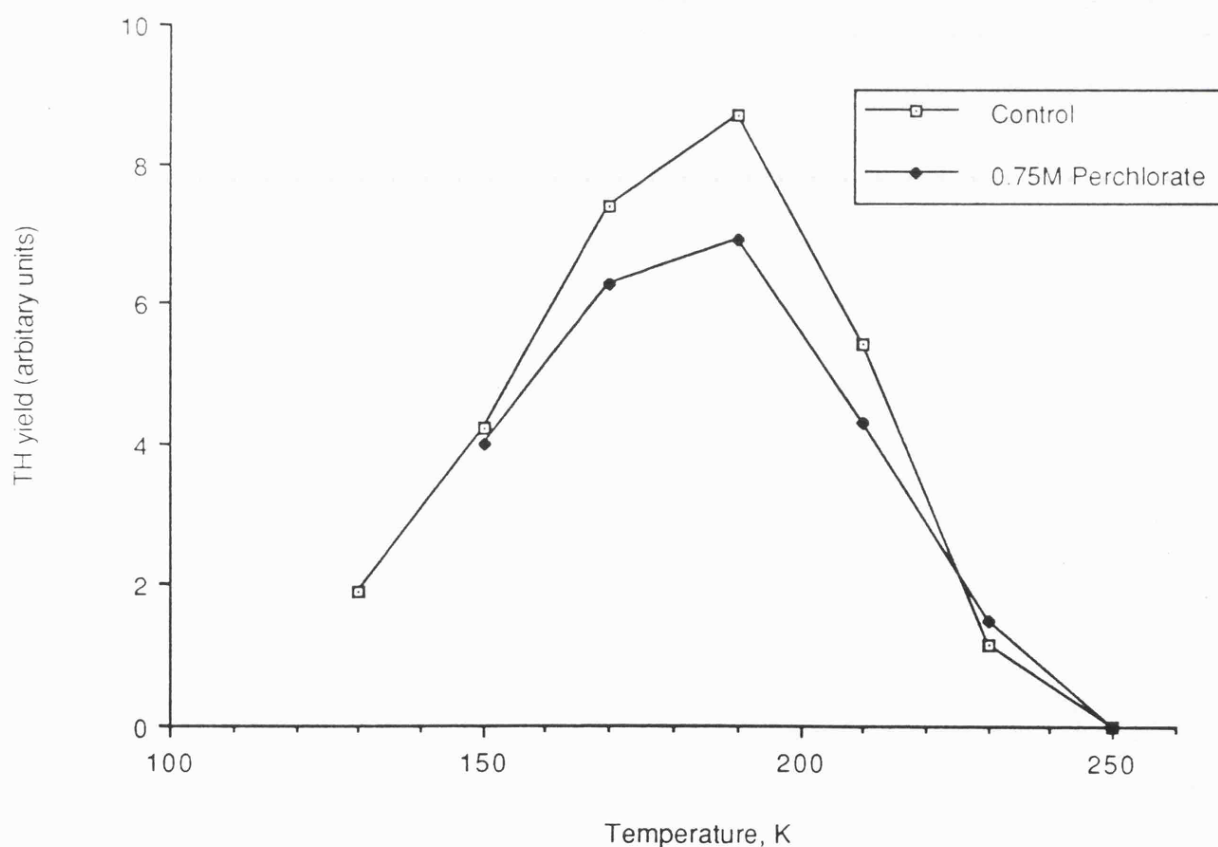
Figure 4-15. Plot of TH radical yield versus temperature for perchlorate-DNA and DNA control samples in H_2O, illustrating the reduction in TH radical yield in the perchlorate-DNA sample.

99

4.3. Discussion.

Fan using the plasmid DNA strand break assay technique with irradiation at 77K demonstrated that, for both single and double strand breaks (in order of effectiveness, greatest to least), phosphate, sulphate and perchlorate ions all give significant radiosensitization relative to plasmid DNA irradiated in the absence of buffering ions[21].

However in the esr results reported here, the DNA primary radical yields are significantly reduced by these ions compared with their yield in the DNA control. After annealing, TH· yields were also found to be similarly reduced. A plot of TH· yield versus temperature (Figure 4–16.i) demonstrates this apparent radioprotective effect.

This paradox may be resolved by considering the fate of the observed inorganic radicals produced by radiolysis in the DNA solvating phase. As described in Chapter 2 relative radical yields throughout the annealing process may be compared by double integration of the recorded first derivative esr spectra (Figure 4–16.ii).

After annealing to 130K, all ice crystallite phase radiolysis products decay and the remaining radical concentrations were due to the DNA and its associated solvation shell. At this temperature there was a significant increase of the order of 160% in the number of radicals present in this solvating glass like phase in the phosphate, sulphate and perchlorate samples compared with that of the DNA control.

TH yield (arbitary units)

10

8

6

4

2

0

100   150   200   250   300

Temperature, K

Control
0.75M Perchlorate
0.75M Sulphate
0.75M Phosphate

20e+15

00e+15

00e+14

00e+14

00e+14

00e+14

00e+14

.00e+0

130   180   230   280

Temperature, K

0.75M Phosphate
0.75M Sulphate
0.75M Perchlorate
Control
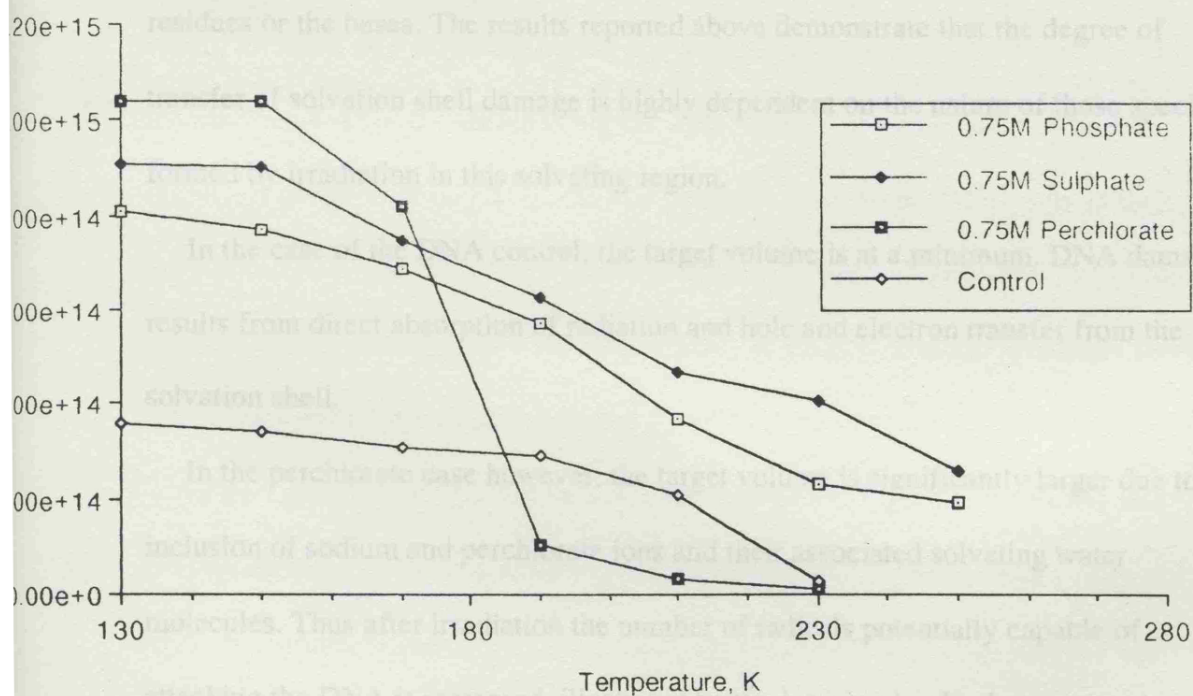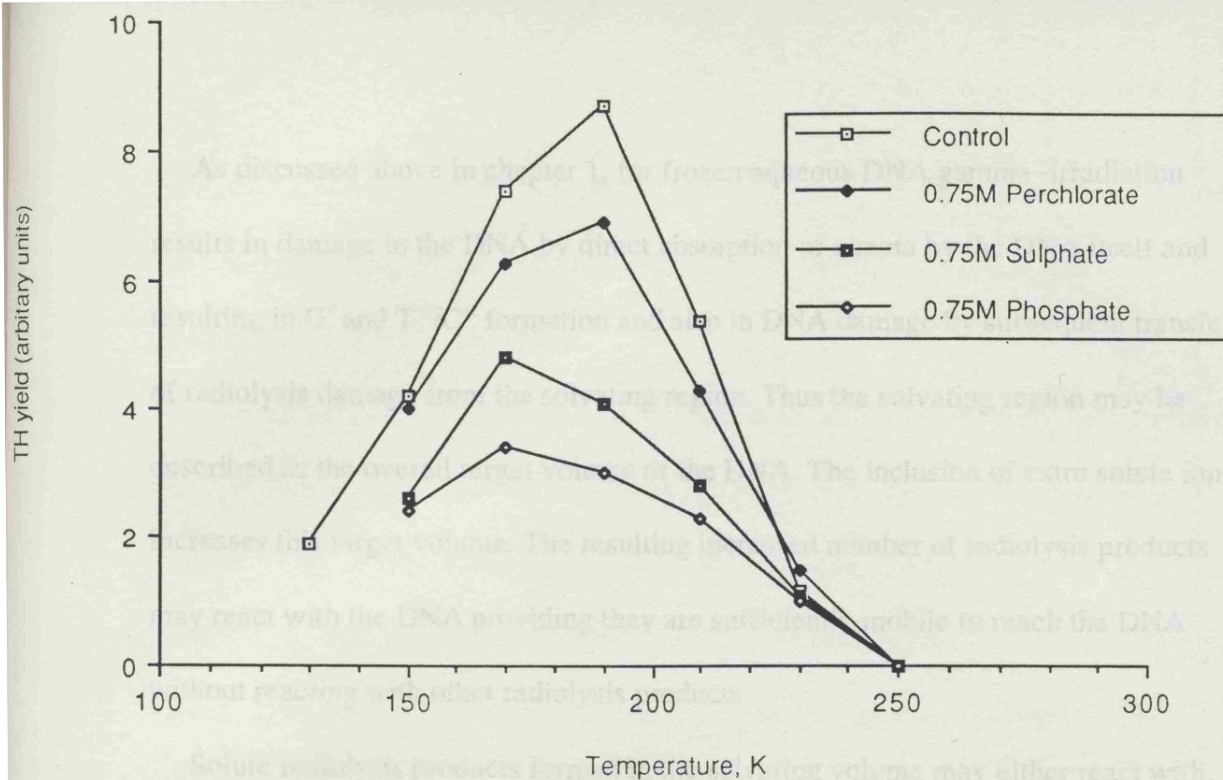
Figure 4–16.i. Plot of TH radical yield versus temperature for phosphate–DNA, sulphate–DNA and perchlorate–DNA and DNA control samples in H_2O. ii. Total radical yield versus temperature for phosphate–DNA, sulphate–DNA and perchlorate–DNA and DNA control samples in H_2O.

As discussed above in chapter 1, for frozen aqueous DNA gamma–irradiation

results in damage to the DNA by direct absorption of quanta by the DNA itself and

resulting in G^+ and T^-/C^- formation and also in DNA damage by subsequent transfer

of radiolysis damage from the solvating region. Thus the solvating region may be

described as the overall target volume of the DNA. The inclusion of extra solute ions

increases this target volume. The resulting increased number of radiolysis products

may react with the DNA providing they are sufficiently mobile to reach the DNA

without reacting with other radiolysis products.

Solute radiolysis products formed in the solvating volume may either react with

each other by, for example dimerisation, or react with the DNA at either the sugar

residues or the bases. The results reported above demonstrate that the degree of

transfer of solvation shell damage is highly dependent on the nature of those species

formed by irradiation in this solvating region.

In the case of the DNA control, the target volume is at a minimum. DNA damage

results from direct absorption of radiation and hole and electron transfer from the

solvation shell.

In the perchlorate case however, the target volume is significantly larger due to the

inclusion of sodium and perchlorate ions and their associated solvating water

molecules. Thus after irradiation the number of radicals potentially capable of

attacking the DNA is increased, illustrated by the increased radical concentration at

130K (Figure 4–16.ii) in the perchlorate sample. As described above, electron capture

after irradiation produces O^- radicals, which may eventually dimerise or, because of

their chemical similarity with OH radicals, may be sufficiently mobile to react with

the DNA. O^- radicals would be expected to attack the sugar residues by hydrogen

atom abstraction to yield the observed sugar radicals α, β and γ. Thus the increase in

DNA target volume results in increased damage to the DNA which is reflected in the

plasmid strand break assay results.

It seems likely that similar processes occur in the sulphate and phosphate cases.

The reactions of SO_4^- radicals with DNA model systems have been extensively

studied [12], and it is probable that PO_4^{2-} radicals behave in a similar way.

However, both sulphate and phosphate are more heavily solvated than perchlorate

ions in water, with solvation numbers of *circa* 8 and 12 (plus secondary solvation)

respectively. Their electron loss and gain products described above are likely to be

similarly solvated. This would be expected to substantially reduce their mobility

within the glass like solvating region and hence their reactivity at these temperatures,

the phosphate derived radicals being the least mobile. As described above, the

radiolysis products of both sulphate and phosphate ions were still present in the esr

spectra at 270K, the DNA derived radicals decaying below 230K. Any DNA radicals

produced at by attack by the observed sulphate or phosphate derived radicals decay

too quickly to be trapped and observed by esr spectroscopy at these temperatures.

In the radical concentration versus temperature plot (Figure 4–16.ii), the less

heavily solvated and hence more mobile sulphate derived radicals decay at slightly

lower temperatures than the PO_4^{2-} radical, supporting the argument that the degree of

solvation at least partially governs reactivity in these systems.

The sulphate radicals may also dimerise to form persulphate:

$$2 \, SO_4^- \, \text{----}> [\, O_3S\text{-}O\text{-}O\text{-}SO_3 \,]^{2-}$$
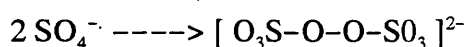
However PO_4^{2-} radicals dimerise less readily and are more likely to attack the DNA, ultimately leading to the observed yield strand breaks.

In conclusion, the major increase in DNA strand breaks induced by phosphate buffers must be largely due to the major increase in target volume induced by these glass-forming ions. The contrast between the esr results and the plasmid strand break assay results is largely explicable in terms of the lack of mobility of the phosphate radicals, ascribed to their high degree of solvation, such that esr spectroscopy is unable to detect their ultimate reactions with DNA because the resulting DNA radicals are not trapped at these temperatures.

References for Chapter 4.

1. J. Keifer., "*Biological Effects in Radiation Chemistry*", Springer – Verlag, New York, 1991.

2. K.M. Bansal and R.W. Fessenden., *Radiation Research,* 1978, **75**, 497–507.

3. S.N. Rustgi and P. Riesz., *International Journal of Radiation Biology*, 1978, **34**, 301–316.

4. M.D. Sevilla, D. Suyanarayana and K.M. Morehouse., *Journal of Physical Chemistry*, 1981, **85**, 1027–1031.

5. H. Riederer and J. Hüttermann., *Journal of Physical Chemistry*, 1982, **86**, 3454–3463.

6. A.J.S.C. Viera and S. Steenken., *Journal of the American Chemical Society*, 1987, **109**, 7441–7448.

7. S.I. Fujita and Y. Nagata., *Radiation Research*, 1987, **114**, 207–214.

8. P. O'Neill and S.E. Davies., *International Journal of Radiation Biology*, 1987, **52**, 577–587.

9. G. Behrens,K. Hilderbrand, D. Schulte-Frohlinde, D. and J.N. Herak., *Journal of the Chemical Society, Perkin Trans II*, 1988, 305–317.

10. K. Hildenbraud, G. Behrens, D. Schulte–Frohlinde and J.N. Herak., *Journal of the Chemical Society, Perkin Trans II*, 1989, 283–289.

11. L.P. Candeias and S. Steenken., *Journal of the American Chemical Society*, 1989, **111**, 1094–1099.

12. C. Von Sonntag, R. Rashid., H.P. Schuchmann and F. Mark., *Free Radical Research Communications*, 1989, **6**, 111–112.

13. K. Hildenbrand., *Zeitschrift für Naturforschung*, 1990, **45c**, 47–58.

14. D.J. Deeble, M.N. Schuchmann, S. Steenken, C. Von Sonntag., *Journal of Physical Chemistry*, 1990, **94**, 8186–8192.

15. E. Bothe, D.J. Deeble, D.G.E. Lemaire, R. Rashid, H.P. Schuchmann, D. Schulte–Frohlinde, S. Steenken, and C. Von Sonntag, *Radiation Physics and Chemistry*, 1990a, **36**, 149–154.

16. S. Subramanian, M.C.R. Symons and H.W. Wardale., *J. Chem. Soc.(A) Inorg. Phys. Theor.*, 1970, 1239–1242.

17. R.A. Serway and S.A. Marshall, *J. Phys. Chem.*, 1966, **45**, 4098.

18. Atkins, Brivati, Horsfield, Symons and Travalion, *6th International Symposium on Free Radicals*, Cambridge, 1963.

19. M.D. Sevilla, J.B. D'Arcy, K.M. Morehouse and M.L. Engelhardt, *Photchem. Photobiol.*, 1979, **29**, 37.

20. M.J. Blandamer, L. Shields and M.C.R. Symons, *J. Chem. Soc.*, 1964, 4352.

21. S. Fan, *Ph.D. Thesis, Leicester.* 1993.

CHAPTER 5– The effects of polyammonium cationic derivatives of

2–nitroimidazole compounds on direct damage to DNA.

5.1. Introduction.

The potent radiosensitizing effects of molecular oxygen are well documented, in that the effects of X–irradiation in the absence of molecular oxygen are much reduced. In fact oxygen is the most powerful radiosensitizer yet discovered. However this is an undesirable phenomenon in the context of cancer radiotherapy, where a tumour must be considered as part of the body and not as an isolated system. Whilst with sufficiently high doses all tumour cells can be killed, the most important consideration is to minimise damage to the surrounding normal tissue, the 'tumour bed', and so ensure its future function.

Reduced blood supply in tumours and high metabolic rates within tumour cells themselves, results in layers of cells within the tumour that are hypoxic. These cells are thus less sensitive to radiation treatment than the surrounding oxic tissues.

Compounds which specifically sensitise hypoxic cells to radiation, whilst not being metabolised themselves, have potentially great value in the clinical treatment of cancer by radiotherapy. Such compounds might allow more efficient tumour cell killing with lower doses of radiation, thus reducing radiation damage to the surrounding normal tissue. For this reason, a great volume of work has been devoted to the phenomenon of radiosensitization and to the development of effective radiosensitizers both *in vitro* and *in vivo*.

Radiosensitization of the cell may be brought about in a number of ways; the mimicry of the effects of molecular oxygen, the inhibition of repair processes and the depletion of natural intracellular radioprotectors. For example the drugs N-acetyl-maleimide (NEM) and diamide inhibit and deplete the non-protein sulfhydryl compounds such as glutathione within the cell. Thus both compounds demonstrate radiosensitizing effects in both oxic and hypoxic conditions[1].

A great deal of radiosensitization research has been devoted to the development of drugs which give sensitization by mimicking the effects of oxygen. Initially studies were confined to bacterial systems[2,3]. The electron affinic compound p-nitroacetophenone was found to sensitize mammalian cell cultures to the effects of radiation in hypoxic conditions[4,5]. These findings led to interest in other electron affinic nitro-substituted aromatic compounds particularly heterocycles, for example nitro substituted furans, as potential clinical radiosensitizers[6]. However, whilst proving to be effective radiosensitizers *in vitro*, these compounds were found to be cytotoxic and therefore were unsuitable for clinical applications.

The 5-nitroimidazole, metronidazole (Figure 5-1.i.) was similarly found to sensitize hypoxic mammalian cells to the effects of radiation *in vitro*[7]. Metronidazole had previously been in use clinically for several years as an anti-microbial agent and had proved effective in the treatment of anaerobic microbial infections in wounds and burns, therefore demonstrating a relatively low cytotoxicity. This report led to studies based on a wider range of electron affinic nitroimidazole compounds, leading to the development of more efficient radiosensitizing compounds such as the 2-nitroimidazole, misonidazole (Figure 5-1.ii.)

109

Metronidazole is believed to exert its anti-microbial effect via reduction of the nitro- group, this is believed to form a reactive intermediate which is thought to disrupt DNA transcription and replication[8]. The ability of nitroimidazoles to sensitize mammalian cells to the effects of radiation in hypoxic conditions has been related to their reduction potential (and hence electron affinity)[9]. In studies using radical scavengers such as cysteamine, the radiosensitizing mechanism of misonidazole has been shown to be a fast process occurring via free radical reactions, and leading to DNA strand breakage[10]. These studies demonstrated that reduced misonidazole yielded DNA strand breaks in alkaline sucrose gradients, although the specific nature of the reduction product was not determined. The radical anions of nitroimidazoles are believed to be a key reduction product produced during radiolysis, these have been extensively studied and characterised by esr and pulse radiolysis techniques[11-13].

A number of mechanisms have been proposed for the radiosensitizing action of nitroimidazoles. Adams[3,14] proposed that following direct ionization of DNA a high degree of charge recombination occurs, and that electron capture by electron affinic drugs, such as nitroimidazoles, may prevent this recombination. This would result in excess DNA electron loss centres and would he proposed, favour the decay of the positive centre to form a neutral free radicals which might decay further to give strand breakage.

Studies have indeed demonstrated that electron capture by metronidazole and misonidazole competes with the formation of DNA radical anions, py^-. The metronidazole and misonidazole electron capture products were both found to have spin centred on the nitrogen atom of the nitro- group[13,15]. However in this and previous studies[16], little evidence of charge recombination was found, and plasmid

strand break assays under conditions of direct damage demonstrated radioprotection

by both metronidazole and misonidazole, suggesting the reduction in strand breakage

was the result of reduction in total DNA radical yield due to nitroimidazole

competition for electron capture.

The resulting radical anions MET⁻ and MISO⁻ were found to relatively stable, it

has been suggested that these may attack the DNA to give sugar centred radicals

which may yield strand breaks[17]. It has also been suggested that further reduction of

these radical anions takes place and that the product nitroxide radicals or

hydroxylamines may be responsible for DNA damage. However, the mechanism by

which electron affinic compounds radiosensitize hypoxic cells still remains

unresolved.
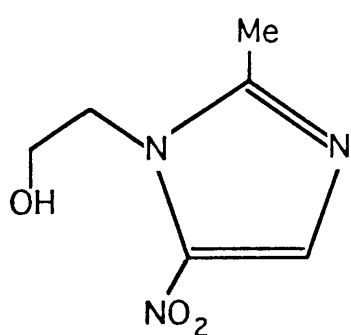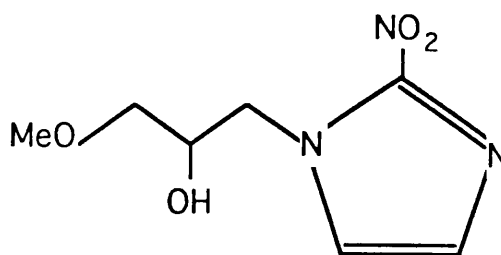
Metronidazole   Misonidazole.

Figure 5-1.i. Metronidazole   ii. Misonidazole

The aim of the studies presented in this chapter, was to elucidate the effect of condensing 2-nitroimidazole compounds into close proximity to the DNA upon radiation induced DNA damage under conditions of direct damage.

As noted above, the site of action within the cell of nitroimidazole radiosensitizers, is believed to be the DNA. Thus the ability to target such radiosensitizers to their site of potential action, offers great advantages in clinical applications.

Polyamines are ubiquitous in living cells and have been implicated in a variety of regulatory processes within the cell[18,19]. At physiological pH, polyamines are fully protonated polycationic species[20]. Polyamines have been shown to bind to the negatively charged phosphate backbone of DNA because of electrostatic forces. This however is not site specific, in fact ^{23}Na and ^{1}H nmr studies of DNA interactions with spermine and spermidine, have shown that such binding is dynamic and that the bound polyammonium cation may migrate laterally along the DNA at close to diffusion controlled rates[21].

The effects of polyammonium cationic derivatives of two 2-nitroimidazole compounds upon radiation damage to DNA under conditions of direct damage were studied using esr spectroscopy and are reported here. The two 2-nitroimidazole compounds, AM-1229 and AM-1254 (Figures 5-2.i. and ii.), have both previously been shown to bind to DNA[21], thus the electron affinic nitroimidazole is condensed into close interaction with the DNA. The polyamine substituents were believed not to reduce the electron affinity of these compounds significantly, this has not been quantified however, since their one electron redox potentials have not been measured.

Fig 5-2. i.
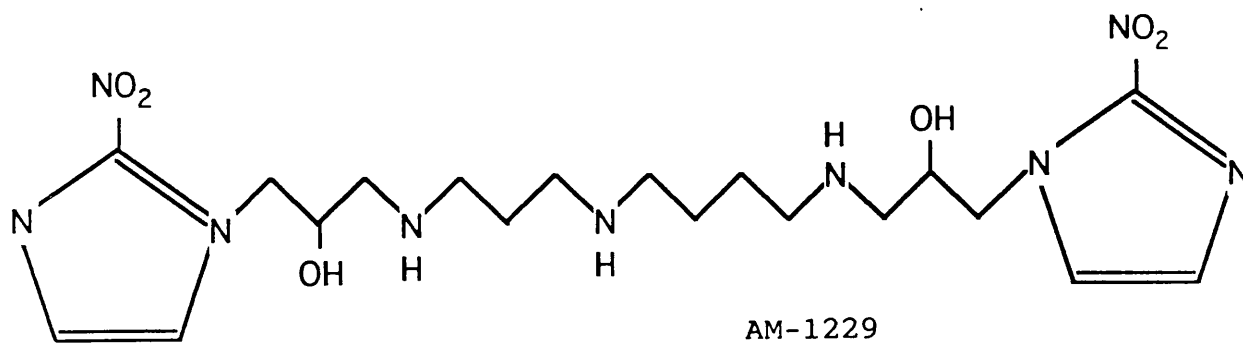
AM-1229
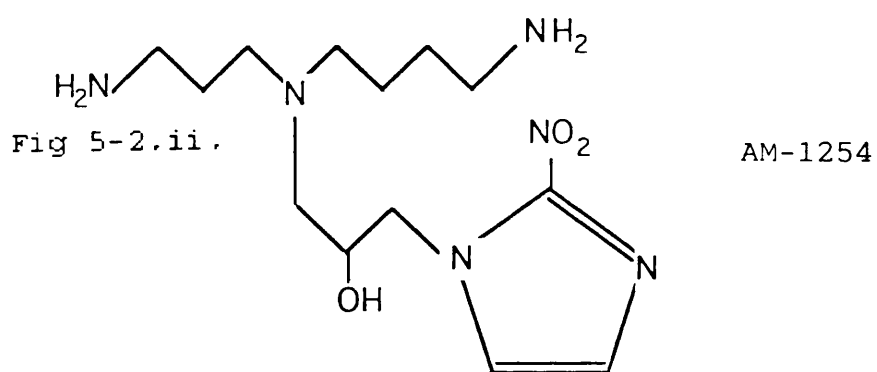
Fig 5-2.ii.

AM-1254

Fig 5-2.iii.
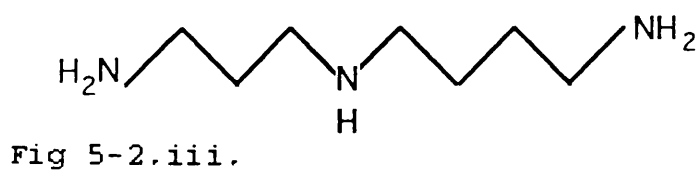
Figure 5-2.i. AM-1229, ii. AM-1254 and iii. spermine.

5.2. Results.

For the initial studies, 50 mg ml^{-1} DNA samples were prepared with AM 1229 and AM 1254 concentrations of 1.9mM and 3.8mM respectively, giving a final nitroimidazole group to DNA base pair ratio of 1:20 for each sample. The compounds AM 1229 and AM 1254 were prepared and purified by Dr. Andy Mather of this department. For direct comparison, a sample containing the commonly studied 2-nitroimidazole, misonidazole (3.8mM) was also prepared along with a DNA control. These samples were then thoroughly degassed with respect to oxygen and irradiated at 77K as described in Chapter 2.

When recorded at 77K the first derivative esr spectra of all three samples containing nitroimidazole compounds were very similar. The spectra comprised of the expected features assigned to the DNA primary radicals G^+ and C^-/T^- together with features assigned to OH radicals, confined within the phase separated ice crystallites. Also apparent up field of the central DNA features in each sample was the high field $M_I = -1$ (^{14}N) parallel feature of a triplet assigned in all three samples to nitroimidazole radical anions (Figure 5-3.i). These radical anions are believed to be the product of electron capture by the nitroimidazole groups, electron density being largely centred on the nitrogen atom of the nitro-substituent, the resulting radical anions being stabilised by delocalisation on the imidazole ring.

After annealing to 130K the OH radicals trapped in the ice crystallites are lost irreversibly. The spectra of the nitroimidazole compound containing samples were again very similar. The esr spectra of all three nitroimidazole samples contain the features of DNA primary radicals (Figure 5-3.ii), however these are significantly

114

reduced in comparison to those observed in the DNA control. Computer subtraction of the spectrum of misonidazole prepared in D_2O / CD_3OD glass enabled the reduction in DNA primary radical yield to be quantified as being *ca.* 40%. This appeared to be predominantly due to the reduction in DNA radical anion centre C^-/T^- yields, as a consequence of the high degree of electron capture by the nitroimidazole compounds, the G^+ yields appeared to remain unaltered. Double integration of the spectra of the sample containing nitroimidazole compounds and the spectrum of the DNA control enabled the comparison of total radical yield in each of the samples. These were found to equivalent within the errors of such integration. Demonstrating that electron capture by the nitroimidazole compounds competes efficiently with electron capture by the pyrimidine base residues of the DNA, resulting in reduced DNA radical anion centre formation. This is in good agreement with previous reported studies[13].

This is further supported by the appearance of clearly defined triplet features assigned to the nitroimidazole radical anions, where spin is centred largely on the N-atom of the nitro-substituent of the nitroimidazole group, which are observed in the esr spectra (Figure 5-3ii).

Further annealing reveals that the reduction in DNA radical anion yield in the samples containing nitroimidazole compounds is reflected in significantly reduced TH radical yields. This reduction being *ca.* 95% in comparison to the DNA control at 210K. The initial reduction in DNA radical anion yield does not account completely for this large reduction in TH yield suggesting that DNA radical anions C^-/T^- are scavenged by the electron affinic nitroimidazoles before TH formation takes place.

FIG 5-3.i.

3220 G

20 G

$m_I = -1 [^{14}N]$

$m_I = 0 [^{14}N]$

$m_I = +1 [^{14}N]$
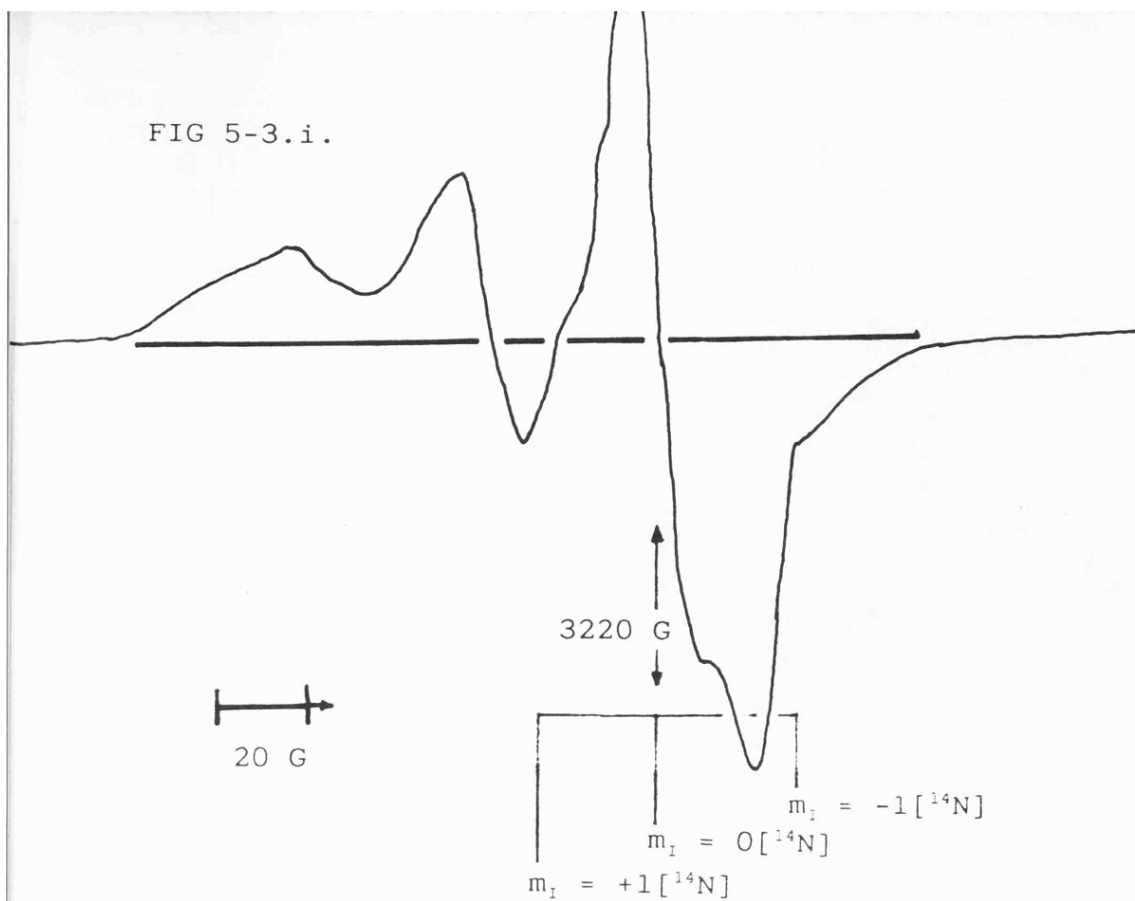
DNA(1° radicals)

FIG 5-3.ii.
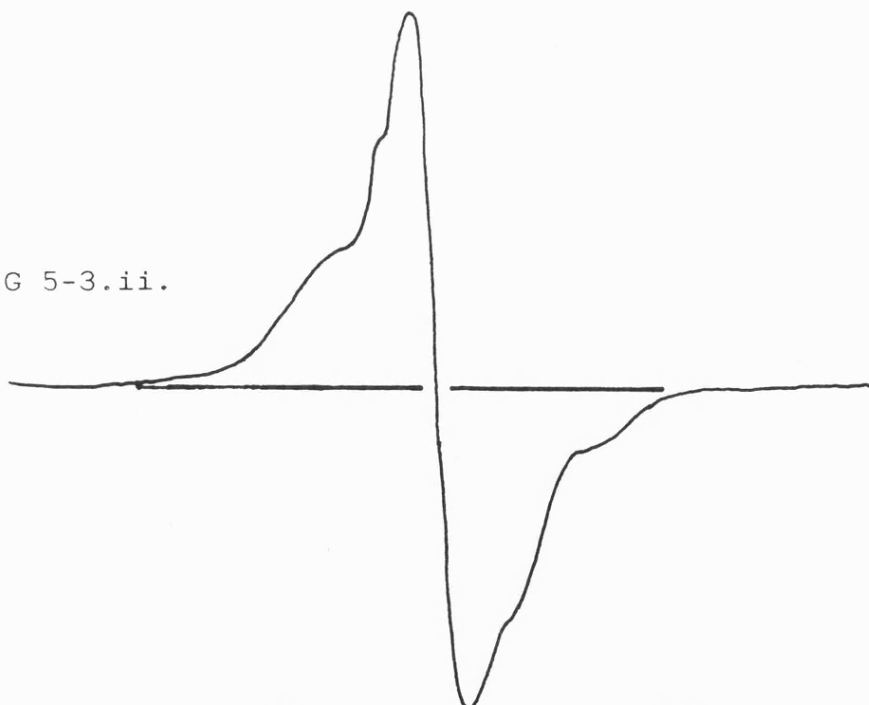
Figure 5-3. First derivative X–band esr spectrum of AM–1229 1:20 DNA pairs at 77K (i), and after annealing to 130K (ii). both contain features assigned to DNA primary radicals and to the electron capture product, $imz-NO_2^-$ radical anions.

116

$$T^- + imz-NO_2 ----> T + imz-NO_2^-$$
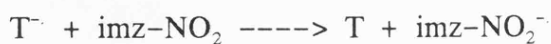
TH radical yield in these samples is illustrated by plots of the radical yields versus temperature (Figure 5-4).
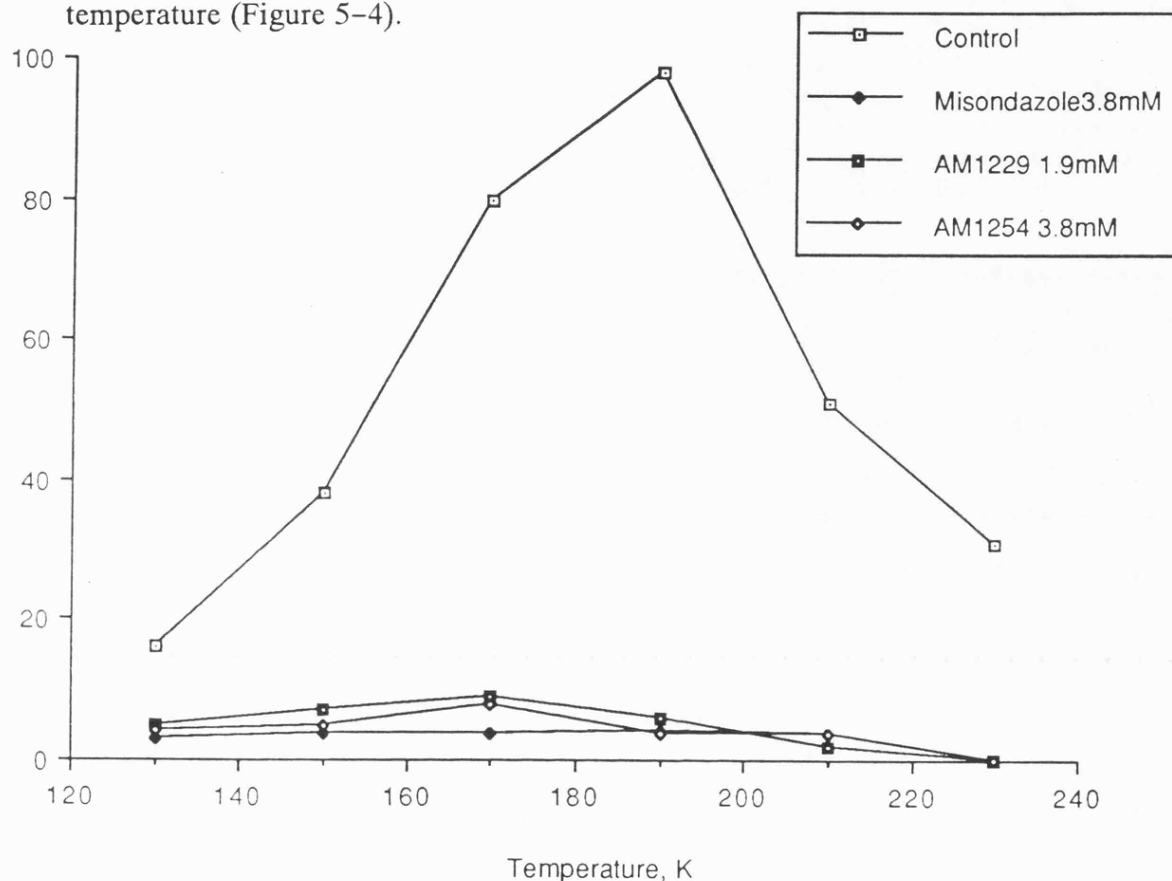
Figure 5-4. Plot of TH radical yield versus temperature for 1.9mM AM-1229, 3.8mM AM-1254, 3.8mM misonidazole and DNA control samples, illustrating the reduction in TH radical yield in the nitroimidazole containing samples.

Clearly at these concentrations electron capture by the nitroimidazoles occurs so efficiently that little can be gauged from these results concerning the influence of electrostatically binding the nitroimidazole compounds to the DNA.

Thus a further series of 50 mg ml^{-1} samples were prepared with AM 1254 and misonidazole concentrations of 1.52 mM, and AM 1229 concentration of 0.76 mM,

117

giving nitroimidazole group to DNA base pair ratios of 1:50. Also prepared, for

further comparison, together with a DNA control, was a sample containing a spermine

concentration of 0.152 mM. Spermine is a naturally occuring polyamine, and similarly

to AM 1229 and AM 1254 possesses three amine groups (Figure 5-2.iii.). These

samples were thoroughly degassed with respect to oxygen, frozen and irradiated as

described in Chapter 2.

At 77K the spectra of the samples containing AM 1229, AM 1254 and spermine all

appeared to be identical to that of the DNA control, consisting of only features

assigned to the DNA primary radicals and OH radicals. Only the spectrum of the

misonidazole sample contained the high field $M_l = -1$ feature assigned to the

nitro-group centred electron capture product, $imz-NO_2^-$. After annealing to 130K it

became clear that electron capture by the compounds AM 1229 and AM 1254 was

significantly less than by misonidazole. Computer subtraction of the spectrum of the

DNA control at this temperature from the spectra of the AM 1229 and AM 1254

samples revealed significantly less intense triplet features of the respective $imz-NO_2^-$

radicals (Figure 5-5.). The yields of these electron capture products were found to be

ca. 8% that of the misonidazole electron capture product.

The yield of DNA primary radicals, in the spermine sample was equal to that of the

DNA control, the yield in the AM 1229 and AM 1254 samples were also found to be

very similar to that of the control. The misonidazole sample however demonstrated a

reduction in DNA primary radical yield of ca. 20% in comparison with that of the

DNA control. This appeared to almost wholly consist of reduction in the yield of anion

centres, presumably the result of competition for electron capture. The relative yields

of DNA primary radicals versus temperature for these samples are represented in

Figure 5-6.

3220 G

20 G

$m_I = 0 [^{14}N]$

$m_I = +1 [^{14}N]$

$m_I = -1 [^{14}N]$
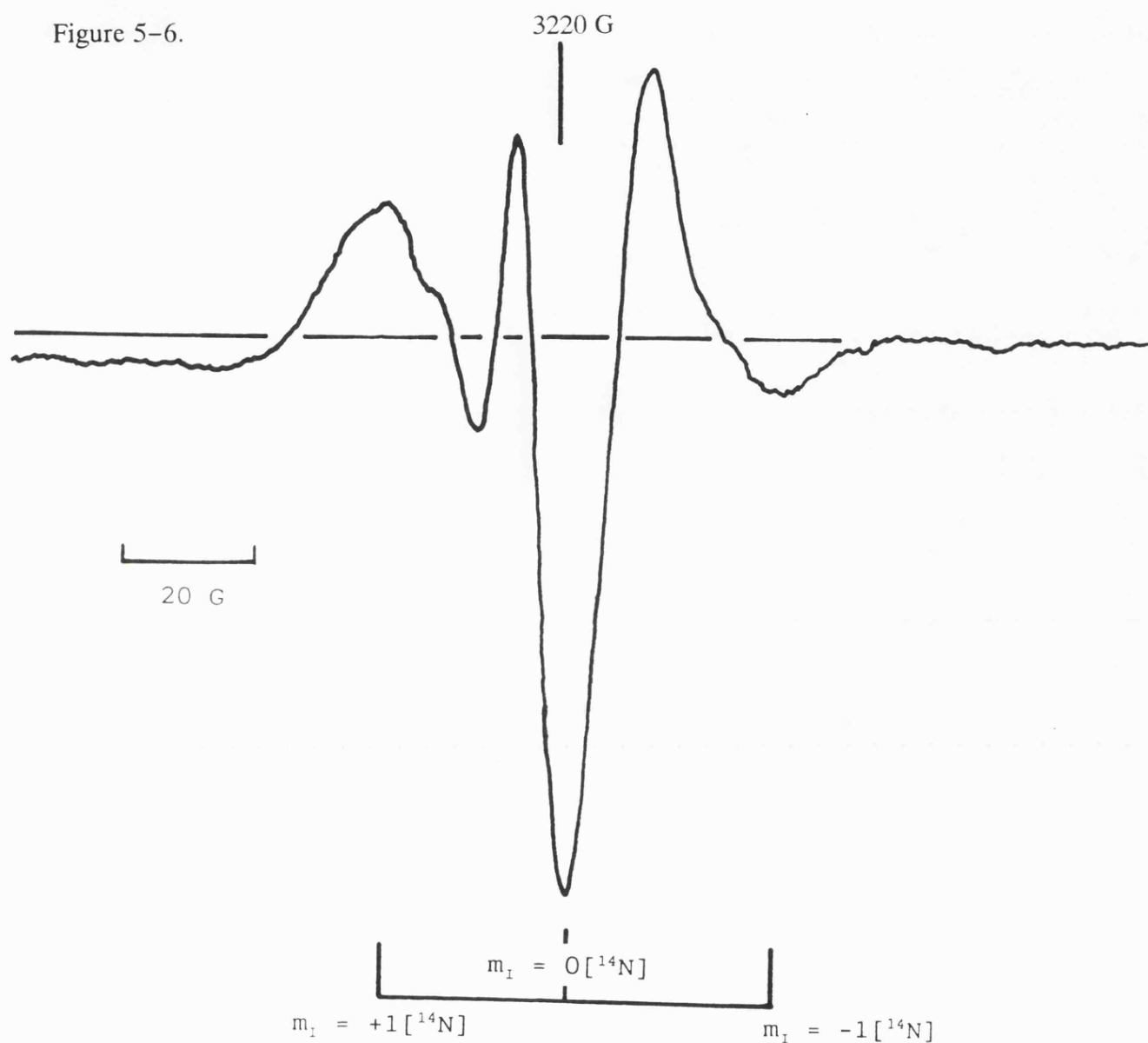
Figure 5-5. The resulting spectrum obtained by subtracting the spectrum of the DNA control from that of the AM-1254 1:50 DNA pairs sample after annealing to 130K. The spectrum contains weak features assigned to imz-NO_2^- radicals.

On further annealing, the spectrum of the misonidazole sample contained

prominent triplet feature assigned above to the electron capture product. However only

trace amounts of TH radicals were detected, even at 210K. This suggests that misonidazole not only reduces the yield of DNA primary radical anions, but also scavenges the electron capture centres of the DNA on annealing, even at this relatively low concentration, thus further reducing the TH radical yield.
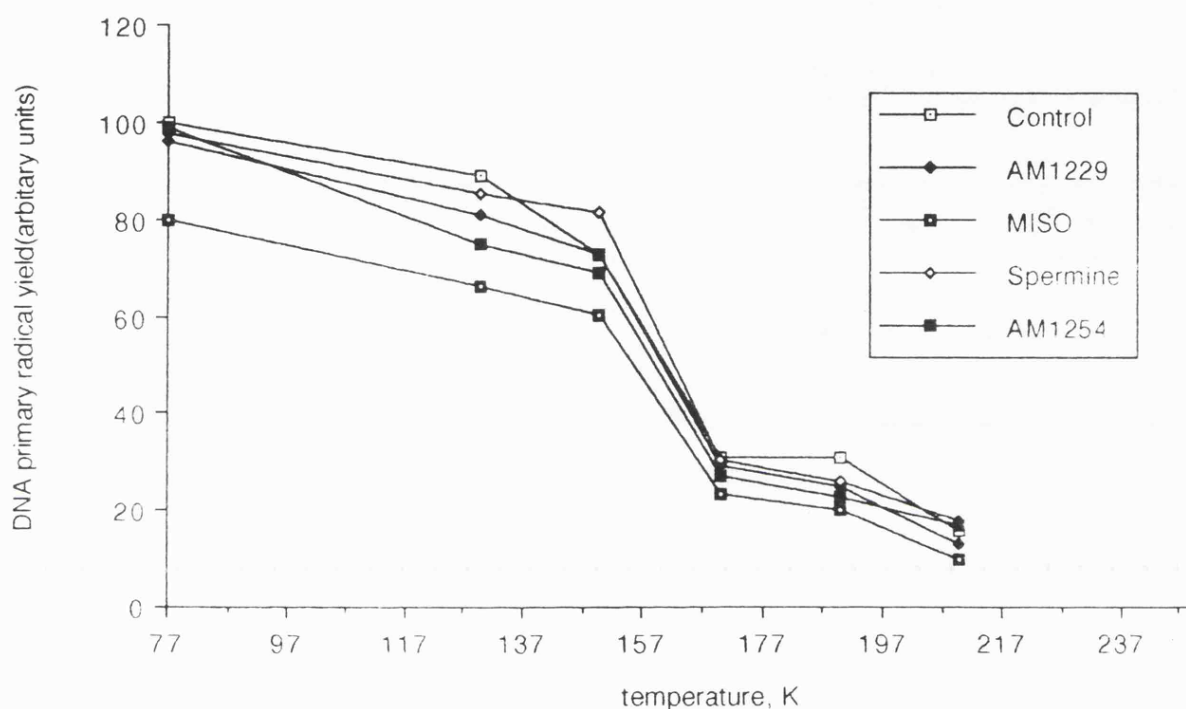
Figure 5-6. Relative yields of DNA primary radicals versus temperature for 0.76 mM AM-1229, 1.52 mM AM-1254, 1.52 mM misonidazole, 1.52 mM spermine and DNA control samples.

Startlingly, considering the very small reduction in DNA primary radical anion yield, a large reduction in TH yield is also observed in the spectra of the AM 1229 and AM 1254 samples in comparison with the yield of the control. In both cases the triplet features of the $imz-NO_2^-$ electron capture product are lost from the spectra after annealing to 150K. This reduction in TH yield was quantified at 210K and was

found to be 80 and 84% for AM 1254 and AM 1229 respectively compared with that of the control.

A reduction in TH was also observed for the spermine sample however this was not so great, giving a 68% reduction at 210K.

These effects are best illustrated by a plot of TH yield versus temperature for the four samples and the control (Figure 5-7).
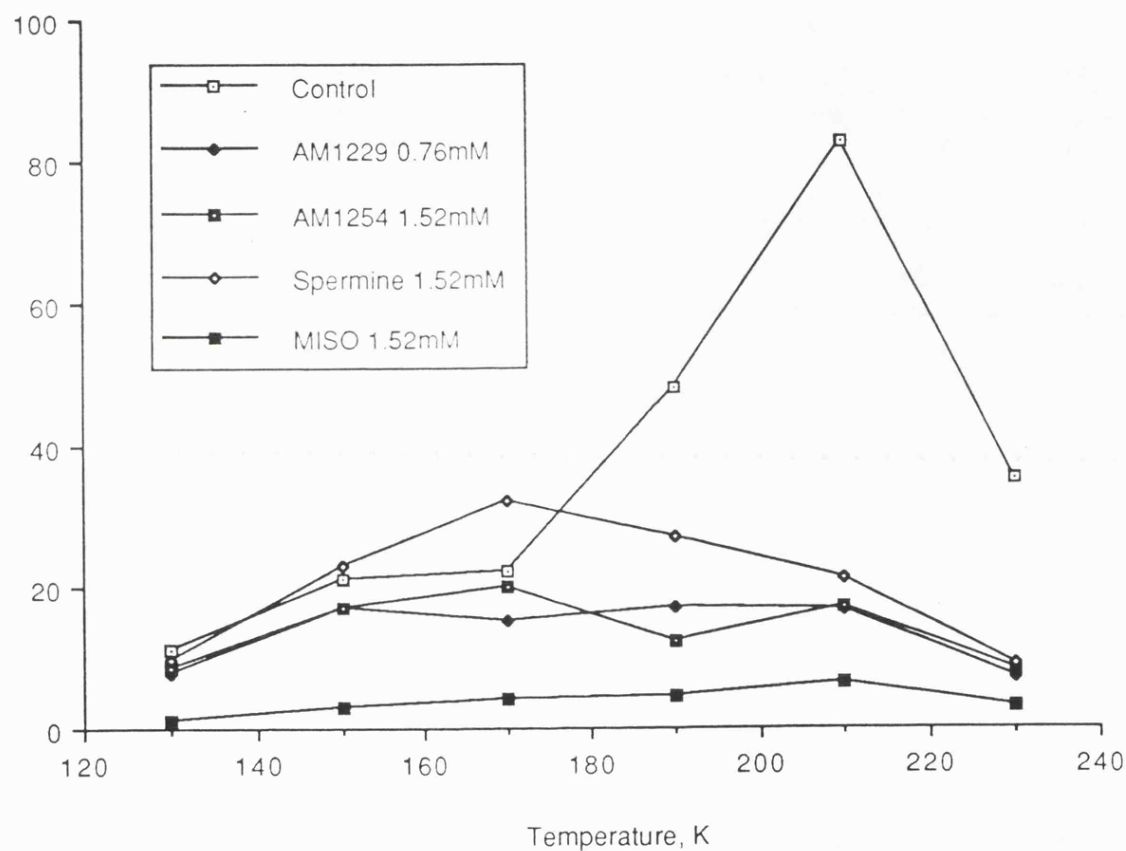
Figure 5-7. Plot of TH radical yield versus temperature for 0.76 mM AM-1229, 1.52 mM AM-1254, 1.52 mM misonidazole, 1.52 mM spermine and DNA control samples, illustrating varying reduction in TH radical yields in comparison with the control.

121

5.3. Discussion.

The large reduction in TH yield in the misonidazole case is easily resolvable in the light of the high degree of electron capture. However, the large reduction in TH in the AM 1254 and AM 1229 is less easily explained, since only relatively small yields of their relative electron capture products were detected.

Spermine was also found to reduce TH yield, though less effectively than the nitroimidazole polyammonium cations, AM 1229 and AM 1254. This suggests that in some way the polyammonium cationic species prevent TH formation, possibly by scavenging the DNA radical anion centres. However, polyamines have been shown to be poor electron scavengers, and have been shown to react slowly even with OH radicals[22]. Thus radical anion scavenging by spermine does seem unlikely and the mechanism by which this suppression in TH yield occurs is unresolved.

It is likely that this unknown mechanism of protection at least partially responsible for the reduction in TH yields observed in the AM 1229 and AM 1254 samples. However there was a greater reduction in yield in these cases particularly. This suggests that the nitroimidazole components also give radioprotective effects. A possible mechanism for this is, that the nitroimidazole components of these compounds may scavenge the DNA radical anions, given their close proximity to the DNA this seems possible. The resulting anion may be sufficiently mobile to progress along the DNA (whilst remaining bound) and return the electron to a 'hole' centre. The anion not being trapped and therefore not observed.

References for Chapter 5.

1. J.D. Chapman, A.O. Reuvers, J. Borsa and C.L. Greenstock., *Radiat. Res.*, 1973, **56**, 291–306.

2. A. Tallentine, N.L. Schiller and E.L. Powers., *Int. J. Radiat. Biol.*, 1969, **14**, 397.

3. G.E. Adams and M.S. Cooke., *Int. J. Radiat. Biol.*, 1969, **15**, 457.

4. M. J. Ashwood-Smith, J. Barnes, J. Huckle and B.A. Bridges, *"Radiation Protection and Sensitization"*, eds: E. Moroson and M. Quintiliani, 1970, London, p.183.

5. J.D. Chapman, R.G. Webb and J. Borsa., *Int. J. Radiat. Biol.*, 1971, **19**, 561.

6. 5-5. J.D. Chapman, R.G. Webb, J. Borsa, A.Petkau and D.R. McCalla., *Cancer Res.*, 1972, **19**, 575.

7. A.C. Begg, P.W. Sheldon and J.L. Foster., *Brit. J. Radiol.*, 1974, **47**, 474.

8. D.I. Edwards., *J. Antimicrob. Chemother.* 1975, **5**, 499.

9. G.E. Adams, E.D. Clark, I.R. Flockhart, R.S. Jacobs, D.S. Sehmi, I.J. Stratford, P. Wardman, M.E. Watts, J. Parrick, R.G. Wallace and C.E. Smithen., *Int. J. Radiat. Biol.*, 1979, **35** (2), 133–150.

10. R.C. Knight, D.A. Rowley, I.S. Kolimowski and D.I. Edwards., *Int. J. Radiat. Biol.*, 1979, **36** (4), 367–377.

11. R. Willson, B.C. Gilberts, P.D.R. Marshall and R. Norman., *Int. J. Radiat. Biol.*, 1974, **26**, 427.

12. P.B. Ayscough, A.J. Elliot and P. Neta., *Int. J. Radiat. Biol.*, 1975, **27**, 603.

13. P.J. Boon, P.M. Cullis, M.C.R. Symons and B.W. Wren., *J. Chem. Soc. Perkin Trans. II.*, 1985, 1057–1061.

14. G.E. Adams. *"Radiation Chemistry of Aqueous Solutions"*, 1968, Interscience Pub., New York, London, Sydney.

15. B.W. Wren. *Ph.D. Thesis*, Leicester. 1985.

16. P.J. Boon, P.M. Cullis, M.C.R. Symons and B.W. Wren., *J. Chem. Soc. Perkin Trans. II.*, 1984, 1393.

17. D. Evans, unknown source.

18. D.R. Morris and L.J. Marton., *"Polyamines in Biology and Medicine"*, 1981, Marcel Dekker, New York.

19. R.A. Campbell, D. Bartos, D.R. Morris, G.B. Daves and F. Bartos., *"Advances in Polyamine Research"*, 1978, Wiley, New York.

20. D. Morris and J.J. Harada., *"Polyamines in Biomedical Research"*, 1980, Wiley, New York.

21. S. Besley. *Ph.D. Thesis*, Leicester, 1991.

22. W. Bors, C. Langebartels, C. Michel and H. Sandermann Jr., *Biochemistry*, 1989, **28**(6), 1589–1595.

CHAPTER 6– The effects of AM1229 a 2–nitroimidazole polyammonium cationic compound on radiation induced DNA double strand breaks in Chinese Hamster V79 cells.

6.1. Introduction.

Neutral (pH 9.6) filter elution is now used extensively to monitor radiation induced DNA double strand breaks both in whole cells and in isolated nuclei. This technique, originally developed by Bradley and Kohn[1], allows the quantification of radiation induced damage to DNA at biologically relevant doses and thus allows direct comparison with cell survival studies. Whilst not being devoid of criticism a growing volume of evidence exists establishing the accuracy and precision of the technique[2-6].

The aim of the studies presented in this chapter, were to elucidate the effect of condensing the 2–nitroimidazole compound, AM1229 (Figure 5–2) into close proximity to cellular DNA prior to radiation induced DNA double strand breaks as measured by neutral filter elution under conditions of hypoxia.

As noted above, the site of action within the cell of nitroimidazole radiosensitizers, is believed to be the DNA. Thus the ability to target such radiosensitizers to their site of potential action might offer great advantages in clinical applications.

Neutral (pH 9.6) filter elution was used in the studies presented here to measure the relative yield of gamma–radiation induced DNA double strand breaks in Chinese Hamster V79 cells under conditions of hypoxia in the presence and absence of nitroimidazole radiation response modifying compounds. The aim of these studies

was to determine the influence polyamine substituents may have upon the radiation modifying effects of 2–nitroimidazoles.

It must be stressed that the system used in these studies (described in Chapter 2) only demonstrated relative radiation effects, since it was not calibrated to give absolute double strand break yields. For reference, such calibrations may be performed by using ^{125}I–dUrd–labelled cells, based on the observation that each ^{125}I decay yields on average one DNA double strand break[2].

6.2. Results.

As described in chapter 2, two identical fractions of Chinese Hamster V79 cell suspensions were prepared, one fraction was retained as a control, the second fraction being dosed with the required compound. These fractions were incubated for 40 minutes while cooling on ice, and then placed again on ice in a continuously purged nitrogen/CO_2 atmosphere for a further 90 minutes to generate hypoxic conditions. After irradiation filter elution was carried out and the results expressed as elution profiles in which the fraction of retained DNA was plotted against the eluted volume.

In order to allow the direct comparison of these elution profiles, the relative strand scission factors for each plot were calculated. The relative strand scission factor being defined as:

$$\text{relative strand scission} = -\log_{10}[F_x / F_o]$$

where; F_x = the fraction of DNA retained after 21ml of eluted

volume of the irradiated sample.

F_o = the fraction of DNA retained after 21ml of eluted

volume of the relative unirradiated control.

Previously the 2-nitroimidazole compound misonidazole has been shown to enhance radiation induced DNA double strand breaks in mouse cells under conditions of hypoxia at concentrations of 10mM[2]. In the same study this dose modifying effect was shown to correlate linearly with radiation induced cell killing. Metronidazole (a

5-nitroimdazole, Figure 5-1), has also been shown to give similar radiosensitizing effects in terms of radiation induced cell killing under hypoxic conditions[3]. For this reason an initial experiment was carried out, the test fraction of cells being dosed with 10mM metronidazole. The metronidazole dosed and control aliquots were irradiated at 0, 20, 40 and 80 Gy.

The elution profiles for the control and test fractions are shown in Figure 6-1. To allow direct comparison, these results are also expressed in a relative strand scission factor versus dose plot (Figure 6-4). The yield of DNA double strand breaks in the 10mM metronidazole treated cells is enhanced relative to the control cells, the relative sensitization in strand scission factor being 1.86. Radiosensitizing dose modifying effects by metronidazole have been shown only to occur in oxygen deficient conditions, thus this marked senitization effect demonstrates that hypoxic conditions were achieved. These results also demonstrate that the system used here is sufficiently sensitive to monitor such effects.

However, when the experiment was repeated at doses of 0, 5, 10 and 15 Gy, the scatter in the data was too great to be meaningful. Thus it was felt that the system was only sufficiently sensitive to measure double strand breaks accurately at doses of 20 Gy and above.

Control fractions and test fractions treated with 5mM AM1229 were irradiated at doses of 0, 20, 40, 60 and 80 Gy under identical conditions. 5mM AM1229 concentration giving an equivalent nitroimidazole group concentration to that used in the metronidazole reported above. The elution profile for the AM1229 test cells is given in Figure 6-2. A plot of relative strand scission factors is given in Figure 6-4, each point being the mean of three experiments. The measured strand scission factor

at 60 Gy was 0.43 that of the control, demonstrating a marked radioprotective effect under these conditions.

In order to gauge any influence the polyamine substituent of AM1229 might have control fractions and test fractions treated with 5mM spermine were irradiated at doses of 0, 20, 40, 60 and 80 Gy under identical conditions. Spermine having a similar structure to the polyamine substituent of AM1229. The elution profile of the spermine treated fractions is given in Figure 6-3, and the relative strand scission factors (the mean of three experiments) are expressed in Figure 6-4. The measured strand scission factor at 60 Gy was 0.66 that of the control.
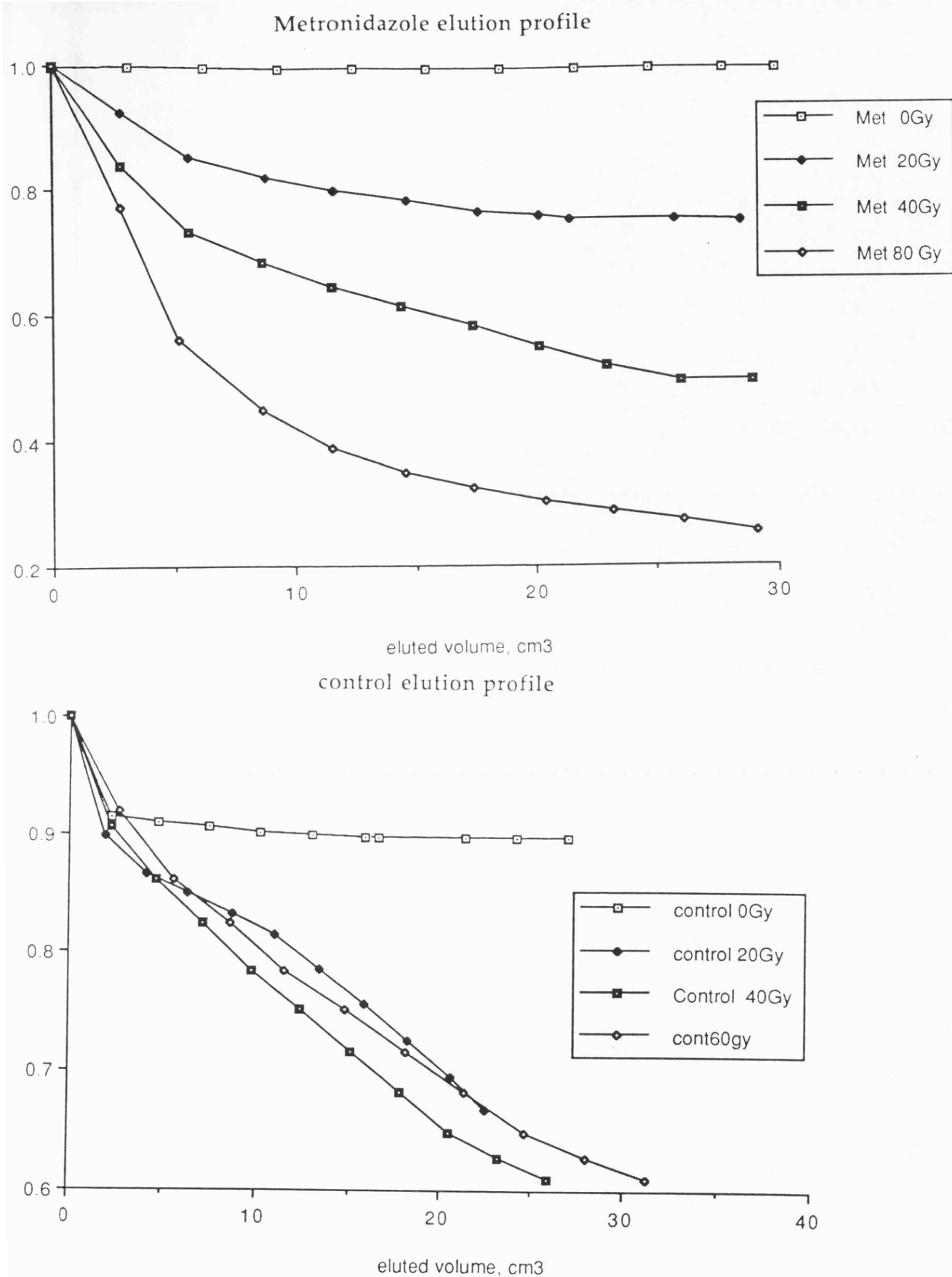
Figure 6-1. pH 9.6 neutral filter elution profile of chinese hamster V79 cells gamma-irradiated under hypoxic conditions.
i) control fraction. ii) 10mM metronidazole.

131
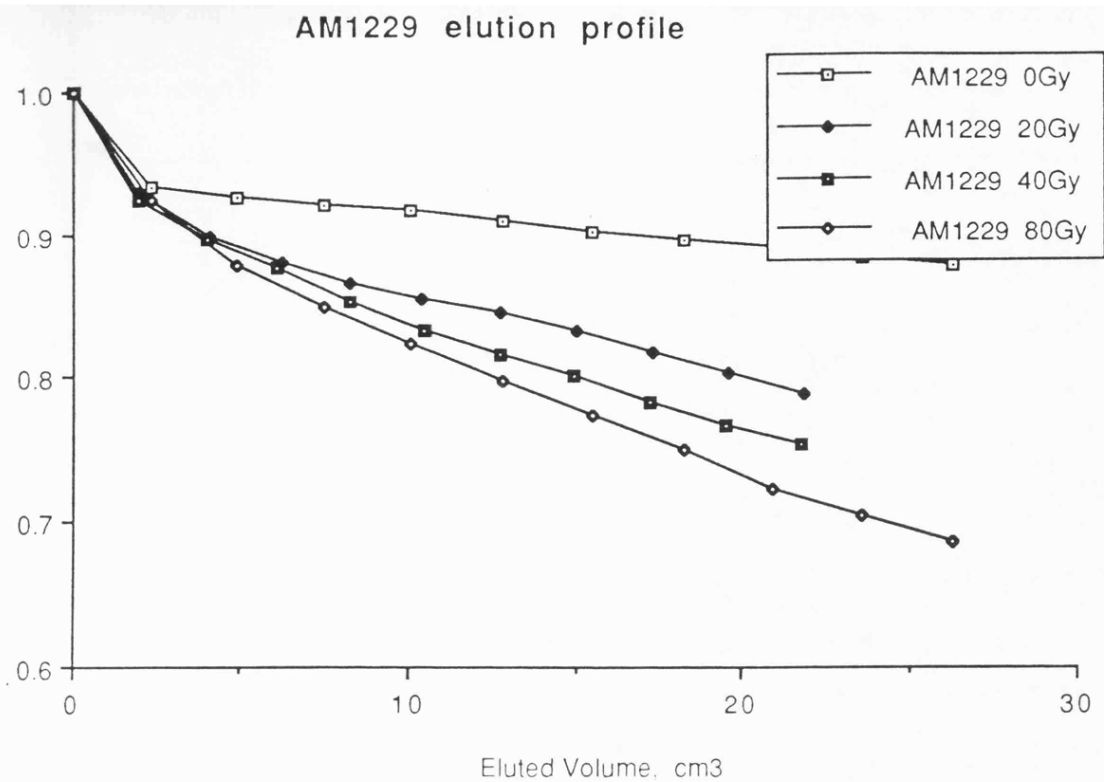
Figure 6-2. ph 9.6 neutral filter elution profile of chinese hamster V79 cells gamma irradiated under hypoxic conditions dosed with 5mM AM-1229.
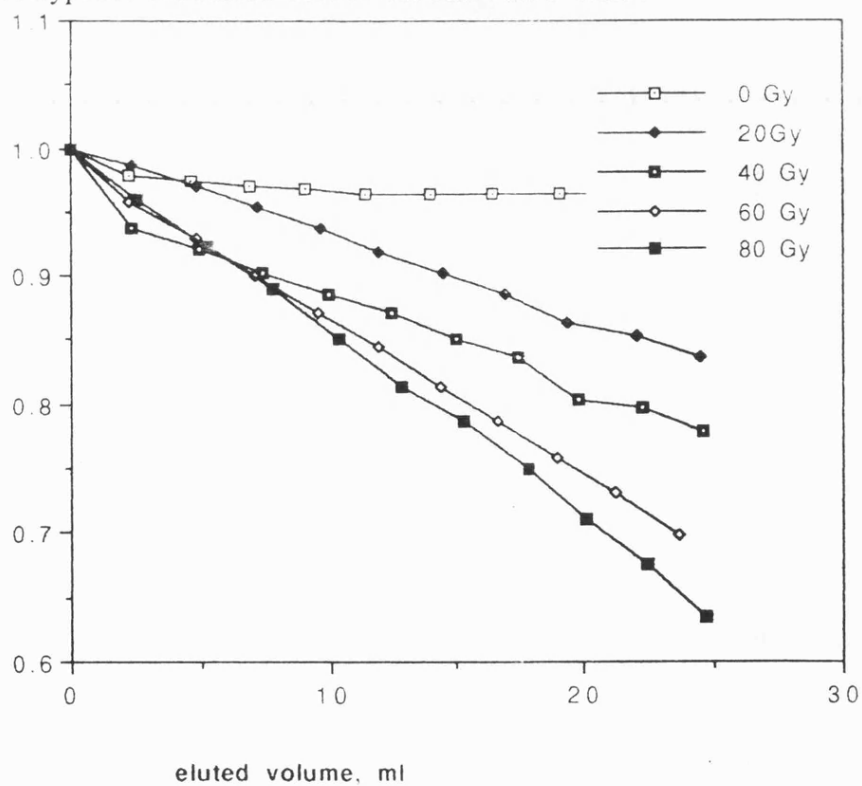
Figure 6-3. pH 9.6 neutral filter elution profile of chinese hamster V79 cells gamma-irradiated under hypoxic conditions dosed with 5mM Spermine.

132
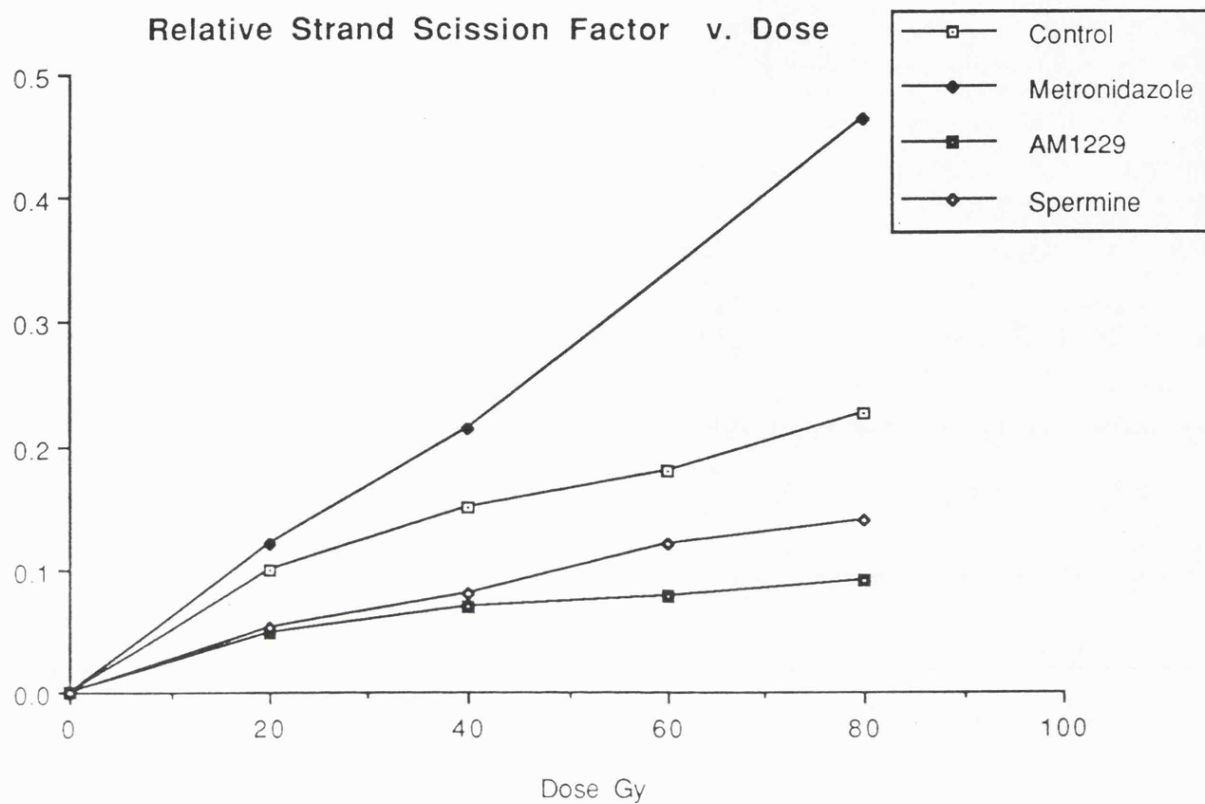
Figure 6–4. A plot of relative strand scission factor versus dose.

6.3. Discussion.

Clearly at these concentrations, AM1229 does not give radiosensitizing dose modifying effects in terms of radiation induced DNA double strand breaks under hypoxic conditions, as metronidazole does in these studies and misonidazole have been shown to in previous studies[2]. Instead AM1229 and also spermine give radioprotective dose modifying effects relative to untreated controls under these conditions. The strand scission factor (SSF) at 60 Gy and the sensitization relative to the controls are presented in Table 6-1.

Table 6-1.

	SSF at 60 Gy	Rel. Sensitization.
Control	0.181	1.00
Metronidazole (10mM)	0.337	1.86
AM1229 (5mM)	0.078	0.43
Spermine (5mM)	0.120	0.66

Thus the effect of electrostatically binding a nitroimidazole compound to DNA in terms of DNA double strand breaks appears to overcome the radiosensitizing action previously observed in studies with these compounds.

Spermine, a polycationic species at physiological pH, also induced radioprotective dose modifying effects. Although to a lesser degree.

These radioprotective effects may be due to hydroxyl radical scavenging by both spermine and AM1229, since a substantial concentration of these DNA binding

compounds might be expected in close proximity to the DNA. AM1229 being a much more efficient OH radical scavenger by virtue of the two nitroimidazole substituents. In previous studies polyamines have been shown to scavenge hydroxyl radicals[7]. However the rate constants for such scavenging are relatively very low, and in biological systems polyamines have been shown to be poor hydroxyl radical scavengers[8-10].

In the previous chapter under conditions of direct damage to DNA, both spermine and AM1229 were shown to significantly reduce the formation of TH radicals. As discussed in Chapter 1, TH radicals are believed to be possible precursors of DNA strand breaks. AM 1229 was observed to give the greater effect.

This suggests that, whilst hydroxyl radical scavenging by these compounds may occur, this may not solely responsible for the observed radioprotective effects. In the proceeding chapter it was also suggested that because of electrostatic binding to DNA, that the nitroimidazole component of AM1229 might scavenge trapped anion centres on the DNA formed as a result of direct ionization, and be sufficiently mobile to facilitate electron return to hole centres. Thus DNA bound electron affinic compounds may give rise to repair by facilitating charge recombination, providing they are sufficiently mobile. In room temperature ^{23}Na and ^{1}H nmr studies polyammonium cations have been shown to bind to DNA whilst remaining mobile[11].

The effect of binding a compound known to give radiosensitizing effects, to its expected site of action should simply to enhance such radiosensitizing effects or to at least result in similar radiosensitization. This clearly does not occur here. There is evidence that under hypoxic conditions that some reductive chemical modification of nitroimidazoles takes place, the products of which have been shown to result in

radiosensitizing dose modification effects[12]. Electrostatically binding nitroimidazoles

to DNA may remove the imidazole compound from the metabolic processes that result

in such reduction, thus preventing radiosenstization. Whilst being a possible reason for

the reduction or loss of ability to radiosensitize in terms of DNA double strand breaks,

this does not, explain the observed radioprotective effects of AM1229.

In criticism of these experiments additional information may be provided about the

mechanism of radioprotection by both AM1229 and spermine by repeating them in

oxic conditions. This would also allow an oxygen enhancement ratio measurement of

the effects of metronidazole allowing further comparison with other studies and a

more accurate assessment of the hypoxic conditions generated here.

References to Chapter 6.

1. M.O. Bradley and K.W. Kohn, *Nucl. Acids Res.*, 1979, **7**, 793.

2. I.R. Radford., *Int. J. Radiat. Biol.*, 1985, **49**, 45–54.

3. J.C. Fox and N.J. McNally., *Int. J. Radiat. Biol.*, 1988, **54**, 1021–1030.

4. T.M. Koval and E.R. Kazmar., *Int. J. Radiat. Biol.*, 1988, **54**, 869–890.

5. K.M. Prise, S. Davies and B.D. Micheal., *Int. J. Radiat. Biol.*, 1989, **56** (6), 943–950.

6. I.R. Radford., *Int. J. Radiat. Biol.*, 1988, **54**, 45–54.

7. A.C. Begg, P.W. Sheldon and J.L. Foster., *Brit. J. Radiol.*, 1974, **47**, 474.

8. D. Morris and J.J. Haraden. *"polyamines in Biomedical Research. "*, 1980, Wiley, New York.

9. G. Drolet, E.B. Dumbroff, R.L. Legge and J.E. Thompson., *Biochemistry*, 1986, **25** (2), 367–371.

10. W. Bors, C. Langebartels, C. Michel and H. Sandermann Jr., *Biochemistry*, 1989, **28**(6), 1589–1595.

11. K.D. Held and S. Awad., *personal communication.*

12. S. Besley., *Ph.D. Thesis*, Leicester, 1991.

13. R.C. Knight, D.A. Rowley, I.S. Kolimowski and D.I. Edwards., *Int. J. Radiat. Biol.*, 1979, **36** (**4**), 367–377.

Effects of Ionising Radiation on Deoxyribonucleic Acid

Part VI. —Effects of Hydroxyl Radical Scavengers on Radiation Damage to DNA

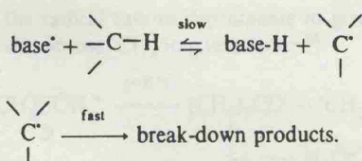**Paul M. Cullis, Steven Langman, Ian D. Podmore and Martyn C. R. Symons***
Department of Chemistry, The University, Leicester LE1 7RH, UK

Exposure of dilute aqueous DNA to ionizing radiation at ambient temperatures results in indirect damage to the DNA, major reactions being the addition of ˙OH radicals to DNA bases and abstraction of C—H hydrogen atoms from deoxyribose units. In order to concentrate on direct damage processes, we have studied frozen aqueous solutions, but it remains possible that some damage is still caused by ˙OH radicals generated close to DNA molecules.

In order to check this, we have used two ˙OH radical scavengers, dimethyl sulphoxide (DMSO) and t-butyl alcohol (TBA). For both, in low concentrations ($\leqslant 1:1$, base-pair), the damage is confined to DNA and exactly corresponds to normal damage in the absence of scavengers. In a second series of experiments, solid solutions containing hydrogen peroxide were photolysed with UV light at 77 K. This gave a poorly defined sextet assigned to sugar radicals or possibly to thymine ˙OH-radical adducts, which was not detected in the absence of hydrogen peroxide, or during γ-radiolysis. We conclude that hydroxyl radical attack is not important for fully hydrated frozen DNA.

The nature and significance of a range of other radicals detected in DNA solutions more concentrated in DMSO and TBA are also discussed, together with the identification of a species giving a broad singlet in the hydrogen peroxide studies.

It is commonly thought that cell death on exposure to ionizing radiation arises primarily as a result of DNA damage. It is therefore important to try to understand the mechanism of radiation damage to DNA. There are clearly two limiting overall mechanisms for primary damage, one being direct interaction between radiation quanta and DNA, the other being indirect damage *via* attack by water radicals generated by the radiation. In the latter case, damage by hydroxyl (˙OH) radicals is thought to be of major significance. Because most studies have been with dilute aqueous solutions in the liquid state, the latter has been far more widely studied than the former. It was originally supposed that ˙OH attack was predominantly on the deoxyribose units, especially since this leads to a nice explanation for strand-breaks (SB), but it has been shown recently that, at least with model compounds, addition of ˙OH to bases constitutes the major part of ˙OH radical attack.[1-3] It is suggested that this may be followed by hydrogen-atom transfer from a neighbouring sugar unit, as we postulated originally as part of the direct damage mechanism[4,5] (fig. 1). We stress that our justification for such reactions, which are probably endothermic, was that the C—H hydrogen atoms are 'poised' close to the reaction centre, and that after transfer [reaction (1)] the reactive sugar radicals can react further, thus forcing the equilibrium to completion [reaction (2)]:

$$\text{base}^\cdot + -\overset{|}{\underset{|}{C}}-H \underset{}{\overset{slow}{\rightleftharpoons}} \text{base-H} + \overset{|}{\underset{|}{C}}^\cdot$$

$$\overset{|}{\underset{|}{C}}^\cdot \xrightarrow{fast} \text{break-down products.}$$

It is unlikely that the direct mechanism is of much importance for fluid aqueous DNA, but it may be of considerable importance for DNA in chromatin for two reasons: (i) this is so highly organised and tightly packaged that there is not much room for water so that water damage becomes much less important; (ii) nuclear water comprises concentrated solutions of a wide range of organic compounds all of which are reactive towards water radicals. Hence the only radicals

$$\text{TH}^\cdot + \text{H}-\text{C}{\Large\lessgtr} \longrightarrow (\text{R})\text{TH}_2 + {}^\cdot\text{C}{\Large\lessgtr}$$
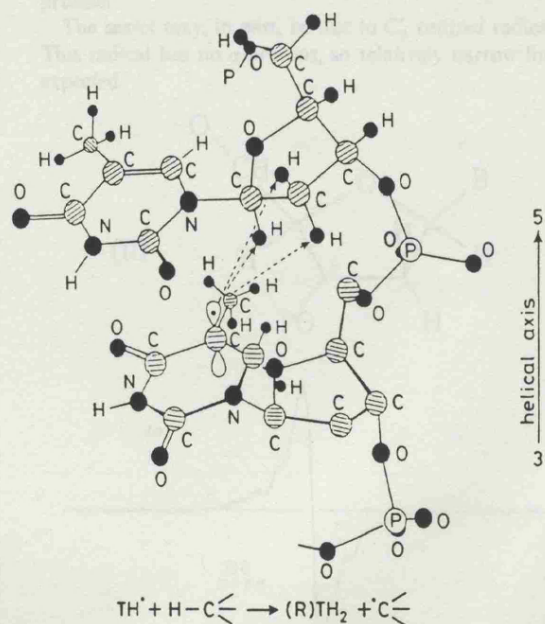
Fig. 1. Local structure around a ˙TH radical showing how a 'poised' hydrogen can be transferred to give a sugar-centred radical.

likely to attack DNA are those generated close to DNA. This greatly limits the effective aqueous target volume, thereby again reducing the probability of indirect damage. Therefore, direct damage needs to be considered. Our approach, following that of Gregoli and co-workers,[6,7] has been to use frozen aqueous solutions of DNA.[8-11] Others have used either dry DNA or partially hydrated DNA, and in particular, Gräslund, Hüttermann and their co-workers[12] have used stretched DNA ribbon, which is largely oriented along the long axis, in order to obtain better EPR information than can be obtained from the frozen solutions.

The frozen solutions that we have used have the advantage that the DNA is fully solvated. Also, it is easy to incorporate additives designed to modify the course of DNA damage. On

freezing, pure ice crystals grow out until a 'glassy' DNA phase solidifies. Additives are totally rejected by the ice, and usually remain in the DNA phase and hence are close to the DNA. This convenient system breaks down if a third phase, comprising pure or hydrated additive, also crystallises out.

Dimethyl sulphoxide (DMSO) is of great importance as an additive to cellular systems, since it acts as a cryoprotector. It is also found to be a radioprotector in that it suppresses radiation-induced cell transformation *in vitro*.[13] It is widely used as an ˙OH radical scavenger in radiation-chemical studies, since it reacts at near diffusion rates to give the sulphuranyl radical adduct (I), which readily loses a methyl radical.[14,15] It is used extensively in biological radiation studies
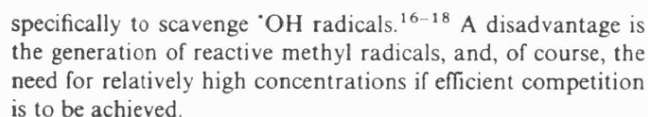
OH
|
˙S —— CH₃
(I) |
O   CH₃

specifically to scavenge ˙OH radicals.[16-18] A disadvantage is the generation of reactive methyl radicals, and, of course, the need for relatively high concentrations if efficient competition is to be achieved.

DMSO reacts slowly with solvated electrons $(k = 1.7 \times 10^6 \text{ mol}^{-1} \text{ s}^{-1})$,[19] but in the pure solid, reaction with ejected electrons occurs to give methyl radicals, the expected radical-anions being apparently too unstable to be detected[20,21]

$$Me_2SO + e^- \rightarrow [Me_2\dot{S}O^-] \rightarrow Me^{\cdot} + MeSO^- \quad (3)$$

Electron loss gives the radical cation. This species has been prepared unambiguously in CFCl₃ at 77 K and has been characterised by a septet EPR spectrum and large g-value variation.[22] In pulse radiolysis studies a transient with $\lambda_{max} = 600$ nm was identified as the parent radical cation, or as a breakdown product therefrom.[19] In the present work we have found that the parent cation formed in CFCl₃ at 77 K has an intense violet colour, indicating an absorption band close to 600 nm. Hence we are able to confirm that the species detected in the liquid state was indeed the parent cation.

t-Butyl alcohol is also favoured as an ˙OH radical scavenger by radiation chemists.[23,24] Its reaction with solvated electrons is unimportant, but it reacts very rapidly to give ˙CH₂—C(Me₂)OH with ˙OH radicals. In the solid-state it reacts with 'dry' electrons to give t-butyl radicals,

$$(CH_3)_3COH + e^- \rightarrow (CH_3)_3C^{\cdot} + OH^- \quad (4)$$

and the radical cations deprotonate to give H₂ĊC(Me₂)OH radicals, or lose ˙CH₃ to give acetone.[25]

$$\left(CH_3\right)_3\dot{C}OH^+ \xrightarrow{(-H^+)} (CH_3)_3CO^{\cdot} \rightarrow {}^{\cdot}CH_3 + (CH_3)_2CO$$
$$\quad\quad\quad\quad\quad \rightarrow H_2\dot{C}(CH_3)_2OH \quad (5)$$

In our previous study of the action of hydrogen peroxide on DNA,[11] no significant changes were detected in the absence of radiation, but on exposure to ⁶⁰Co γ-rays at 77 K the yields of DNA radicals were reduced and HO₂˙ radicals, together with species identified as sugar radicals, were detected.[11] In the present work we have used UV light to generate ˙OH radicals exclusively, thereby avoiding the competing generation of DNA radicals by the direct mechanism. This was one of the first techniques used to generate matrix

isolated radicals for EPR study,[26,27] and remains a powerful method for studying reactions of ˙OH radicals.

Results and Discussion

DNA + Hydrogen Peroxide

Using light from a high-pressure mercury lamp (mainly 313 + 365 nm) there was no significant DNA damage in the absence of hydrogen peroxide. However, in its presence, spectra in the free-spin region grew in (fig. 2), which at high microwave powers showed a low-field doublet characteristic of HO₂˙ radicals (b). The central features comprise a broad singlet together with a poorly defined 15 G sextet.

Despite the liquid-phase results, which strongly indicate preferential addition of ˙OH radicals to the bases of DNA, our results seem to favour H-atom abstraction from the deoxyribose units for solid systems at low temperatures. Thus, EPR spectra for most possible ˙OH radical DNA base adducts have been reported (table 1),[28-31] but we have found no evidence for any of these adducts, which are all expected to be stable at 77 K despite their rapid reactions at room temperature. The only reasonable candidate is the thymine ˙OH adduct for which we obtained a 20 G quintet in the solid-state (table 1). This differs sufficiently from the 15 G features of fig. 2(a) that we consider that it cannot be a major product.

The sextet may, in part, be due to C₃' centred radicals (II). This radical has no α-protons, so relatively narrow lines are expected.

O
\
CH₂   O   B
H   \   / \   H
(II)   ˙   H
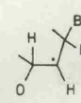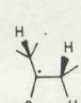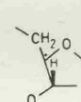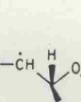H   H
PO   H

Fig. 2. First derivative X-band EPR spectra for a hydrogen peroxide–DNA solution photolysed at 77 K, (a) at low microwave power, showing features assigned to a sugar radical (six lines) + a central singlet, and (b) at high power, showing features assigned to HO₂˙ radicals.

Table 1. Radicals formed from DNA bases and deoxyribose units by 'OH radical attack

| radical | hyperfine coupling/G^{a,b} | | comment |
	$A[\alpha H]$	$A[\beta H]$	
(TOH)	—	3H ≈ 20^c 1H ≈ 20	quintet (20 G) expected
('COH)	(1H ≈ 20)	(1H ≈ 20)	triplet (20 G) expected
('GOH or 'AOH)	—	1H ≈ 33^{c,d}	('GOH)^{14}N(‖) ≈ 21 G ∴ major doublet with extra parallel features ['AOH is expected to be similar]
'C$_1$	—	1H ≈ 23^e 1H ≈ 45	quartet (≈23 G) expected
'C$_2$	1H ≈ 22	1H ≈ 48^e 1H ≈ 6	quartet (≈25 G) expected
'C$_3$	—	1H ≈ 13^f 1H ≈ 45 1H ≈ 15	sextet (≈15 G) expected
'C$_4$	—	1H ≈ 15^f 1H ≈ 33 1H ≈ 0	quartet (≈16 G) expected
'C$_5$	1H ≈ 20	1H ≈ 5	doublet (20 G) expected

^{a} 1 G = 10^{-4} T; ^{b} data in parentheses are expectation values only; ^{c} ref. (32); ^{d} ref. (30); ^{e} ref. (33); ^{f} ref. (34).

A stick diagram, using the data given in table 1 (included in fig. 2) shows that this assignment is reasonable, but we do not consider that it is fully established. Also, there may be other anisotropic features present from other sugar radicals which are largely concealed by the sextet and singlet. It is, of course, difficult to identify the broad singlet which is always present in the spectra. None of the radicals discussed above is expected to give such a spectrum. There is a contribution from the 'perpendicular' features for HO$_2$' radicals [fig. 2(c)] but another centre is also present. Guanine cations (G$^{•+}$) give rise to a very similar singlet (same average g value and same width), and we tentatively suggest that these cations may be formed from 'OH radicals under our conditions. (They are not formed on photolysis in the absence of H$_2$O$_2$.) Guanine has a low ionization potential (8.24 eV†), and 'OH radicals have a high electron affinity. If some 'OH radicals are formed close enough to G for electron-transfer to be reasonable (<20 Å), but too far away from any reactive unit to permit

† 1 eV ≈ 1.602 × 10^{-19} J.

direct attack, then the following reaction may occur by electron tunnelling

$$G + {}^{•}OH \rightarrow G^{•+} + OH^-. \qquad (6)$$
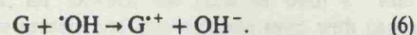
At present, we have no other suggestions for the structure of the species responsible for this central feature.

Absence of high yields of 'OH radical base-adducts probably reflects the inaccessibility of the bases at 77 K. The most mobile species under these conditions are electrons, which can travel considerable distances along the DNA spine.[35] Protons can also migrate, but 'OH radicals are likely to be trapped or to react with their near neighbours. There is no clear evidence for trapped 'OH radicals, but we stress that, in glassy media, their EPR features are not well defined.[36] We suggest that they react with their near neighbours, which are expected to be H$_2$O$_2$ molecules (giving HO$_2$') and the outer regions of the DNA, which are mainly deoxyribose units.

One of the most exposed C—H groups is C$_3$—H, and this may explain why the 'C$_3$ radical appears to be of importance in this study. The absence of this centre in the radiolysis of

DNA reinforces our conclusion that 'OH radical attack is not of major importance under these conditions.

DNA–DMSO System

In our studies of electron-donor and -acceptor additives, there have been clear reductions in the yields of the major DNA damage centres (G^{++} and T^{--}/C^{--}) for additive: base-pair ratios of ca. 1:50.[7-12,35] However, for DMSO systems, even at ratios of 1:1 the $[G^{++}]$ and $[T^{--}/C^{--}]$ are almost unchanged. (Although we and others have previously assumed that the major e^--capture centre is 'T^{--}', there is growing evidence that 'C^{--}' is also important.[37-40] This result also supports the contention that 'OH radical reactions are not an important source of DNA damage under our conditions.)

However, there are interesting effects for higher [DMSO]. Increasing the DMSO: base-pair ratio to ca. 10:1 results in a clear loss of DNA radicals, and the appearance of signals from 'CH$_3$ and H$_2$ĊSO(CH$_3$) radicals (fig. 3). The EPR

resembles that obtained from concentrated aqueous DMSO solutions after exposure at 77 K, but the large reduction in [DNA'] radicals means that these do not simply arise as a result of damage to a separate H_2O–DMSO phase. Since the ionization potential of DMSO (9.1 eV) is greater than that of G^{++} (8.24 eV) hole transfer should not favour DMSO damage.

The problem is, not the appearance of DMSO radicals, since these must surely be formed at high concentrations of DMSO, but the decrease in DNA radicals, when DMSO is so ineffective at low concentrations [fig. 3(b)]. Probably several factors contribute: (i) the decrease in [H_2O] in the DNA zone may facilitate electron return thus decreasing $[G^{++}]$ and $[T^{--}/C^{--}]$; (ii) the reaction of H_2O^{++} to give, ultimately, G^{++}, may become less favourable than reaction with DMSO to give DMSO^{++}; (iii) DMSO molecules may intercept electrons before they reach T or C or before these units have time to relax to form protonated units. Also, electron-transfer between DMSO molecules may help to remove e^- from the vicinity of DNA.

DNA–t-Butyl Alcohol

As with DMSO, at relative concentrations up to ca. 1:1 (TBA: base-pairs) there is almost no effect on the concentration of DNA radicals or their behaviour on annealing. Despite the relatively high concentration of TBA, there is no detectable yield of TBA radicals. Even 'CH$_3$ and (CH$_3$)$_3$C', which can be detected in very low concentrations because of their narrow features even at 77 K,[25] were not detectable.

This result accords with those from the DMSO and hydrogen peroxide studies, showing that, in marked contrast to the liquid-phase, attack by 'OH radicals formed by γ-radiolysis, must be insignificant.

Results at higher [TBA] contrast significantly with those for DMSO. Yields of TBA radicals ['CH$_3$, (CH$_3$)$_3$C' and H_2ĊC(CH$_3$)$_2$] remain very low, but yields of DNA radicals (G^{++}, T^{--}/C^{--} and 'TH) increase, rather than decrease (fig. 4). Thus TBA appears to act as a radiosensitiser, whereas DMSO acts as a poor radioprotector.

This curious contrast can be understood in the following way. In both cases, the aquated cosolvent molecules are forced into the vicinity of the DNA, thereby potentially increasing the DNA target volume. (This volume effect is well defined for inert salt systems, and will be elaborated separately.) In the case of TBA, electron-capture [eqn (4)] and hole-capture [eqn (5)] are clearly very inefficient, so that both electrons and holes are mobile and can reach the DNA, thereby increasing the yields of DNA radicals.

However, for DMSO, the rates of both e^- and hole capture are greater and can compete even with capture by DNA so that DMSO radicals dominate at high concentrations.

Strand-breaking Studies

In most of our previous work we have correlated the EPR data with measurements of strand breaks after annealing to room temperature.[8-12] In the present work, only TBA systems have so far been studied.[41] We note that, in this case, TBA in the low concentration range has very little effect on the number of strand-breaks, in accord with the EPR results, whilst in fluid solution marked protection was observed.
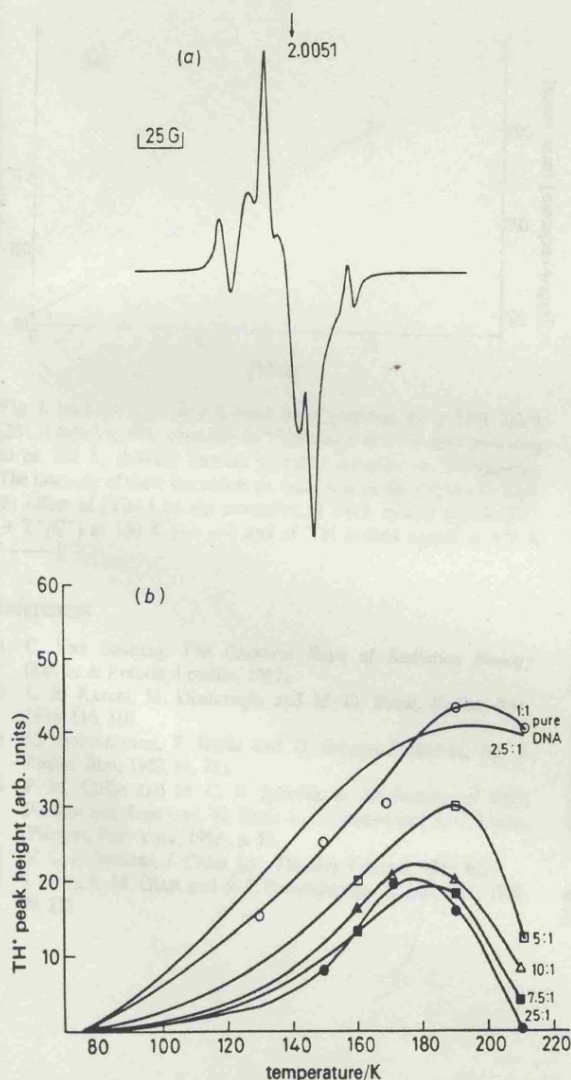
Fig. 3. (a) First derivative X-band EPR spectrum for a DMSO–DNA solution (10:1) after exposure to ^{60}Co γ-rays at 77 K and annealing to ca. 135 K to remove signals from 'OH radicals in ice crystals, showing features assigned to methyl radicals and H$_2$ĊS(O)CH$_3$ radicals. (b) Temperature profile for the gain and loss of 'TH radicals. Note that this remains similar to the change in the absence of DMSO up to the 1:1 solution. Loss of G^{++}/T^{--} radicals shows a similar trend.
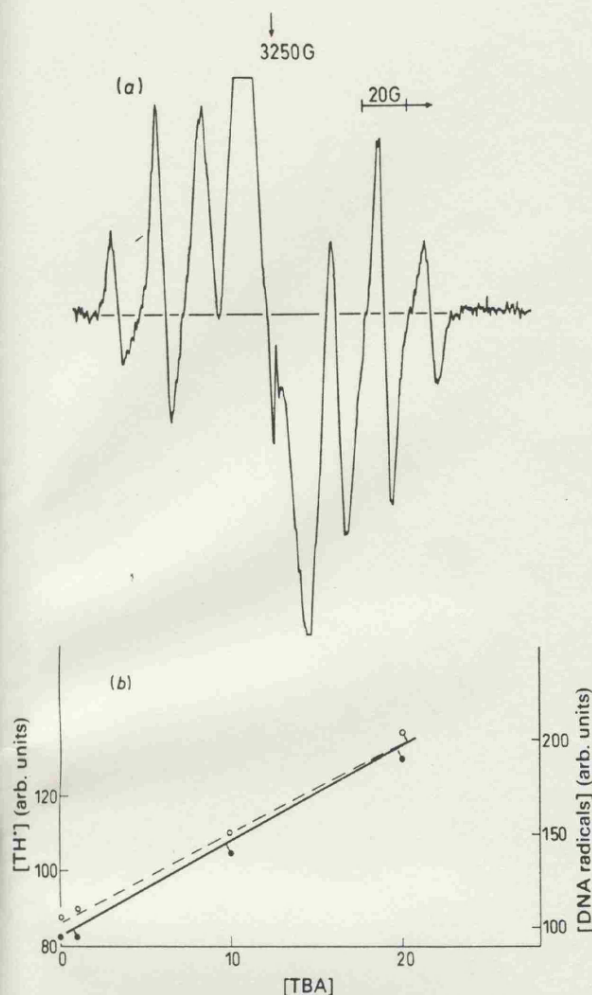
Fig. 4. (a) First derivative X-band EPR spectrum for a TBA–DNA (20 : 1) solution after exposure to ^{60}Co γ-rays at 77 K and annealing to ca. 208 K, showing features primarily assigned to ˙TH radicals. The intensity of these features is ca. twice that in the absence of TBA. (b) Effect of [TBA] on the intensities of DNA radical signals (G˙$^+$ + T$^-$/C$^-$) at 150 K (– – – –) and of ˙TH radical signals at 170 K (———).

References

1 C. Von Sonntag, *The Chemical Basis of Radiation Biology* (Taylor & Francis, London, 1987).
2 L. R. Karam, M. Dizdaroglu and M. G. Simic, *Radiat. Res.*, 1988, **116**, 210.
3 M. Adinarayana, E. Bothe and D. Schulte-Frohlinde, *Int. J. Radiat. Biol.*, 1988, **54**, 723.
4 P. M. Cullis and M. C. R. Symons, in *Mechanisms of DNA Damage and Repair*, ed. M. Simic, L. Grossman and A. C. Upton (Plenum, New York, 1985), p. 29.
5 M. C. R. Symons, *J. Chem. Soc., Faraday Trans. 1*, 1987, **83**, 1.
6 S. Gregoli, M. Olast and A. J. Bertinchamps, *Radiat. Res.*, 1982, **89**, 238.

7 M. G. Ormerod, *Int. J. Radiat. Biol.*, 1965, **9**, 291.
8 P. J. Boon, P. M. Cullis, M. C. R. Symons and B. W. Wren, *J. Chem. Soc., Perkin Trans. 2*, 1984, 1393.
9 P. J. Boon, P. M. Cullis, M. C. R. Symons and B. W. Wren, *J. Chem. Soc., Perkin Trans. 2*, 1985, 1057.
10 P. M. Cullis, M. C. R. Symons and B. W. Wren, *J. Chem. Soc., Perkin Trans. 2*, 1985, 1819.
11 P. M. Cullis, M. C. R. Symons, M. C. Sweeney, G. D. D. Jones and J. D. McClymont, *J. Chem. Soc., Perkin Trans. 2*, 1986, 1671.
12 A. Gräslund, A. Rupprecht, W. Köhnlein and J. Hüttermann, *Radiat. Res.*, 1981, **88**, 1.
13 A. R. Kennedy and M. C. R. Symons, *Carcinogenesis*, 1987, **8**, 683.
14 B. C. Gilbert, R. O. C. Norman and R. C. Sealy, *J. Chem. Soc., Perkin Trans. 2*, 1975, 308.
15 G. Meissner, A. Henglein and G. Beck, *Z. Naturforsch.*, 1967, **226**, 13.
16 L. G. Littlefield, E. E. Joiner, S. P. Colyer, A. M. Sayer and E. L. Frome, *Int. J. Radiat. Biol.*, 1988, **53**, 875.
17 M. J. Ashwood-Smith, *Int. J. Radiat. Biol.*, 1961, **3**, 41.
18 J. D. Chapman, S. D. Doern, A. P. Gillespie, A. Chatterjee, E. A. Blakely, K. C. Smith and C. A. Tobias, *Radiat. Environ. Phys.*, 1979, **16**, 29.
19 A. M. Koulkes-Pujo, L. Gilles, B. Lesogne and J. Sutton, *J. Chem. Soc., Chem. Commun.*, 1971, 749.
20 K. Nishikida and M. C. R. Symons, *J. Am. Chem. Soc.*, 1974, **96**, 4781.
21 M. C. R. Symons, *J. Chem. Soc., Perkin Trans 2*, 1976, 908.
22 D. N. R. Rao and M. C. R. Symons, *Chem. Phys. Lett.*, 1982, **93**, 495.
23 *Radiation Chemistry*, ed. Farhataziz and M. A. J. Rogers, (VCH Publishers, Inc., 1987).
24 H. Schuessler and E. Jung, *Int. J. Radiat. Biol.*, 1989, **56**, 423.
25 M. C. R. Symons and K. V. S. Rao, *Radiat. Phys. Chem.*, 1977, **10**, 35.
26 J. F. Gibson, M. C. R. Symons and M. G. Townsend, *J. Chem. Soc.*, 1959, 269.
27 J. F. Gibson, D. J. E. Ingram, M. C. R. Symons and M. G. Townsend, *Trans. Faraday Soc.*, 1957, **53**, 914.
28 S. Gregoli, M. Olast and A. Bertinchamps, *Radiat. Res.*, 1976, **65**, 202.
29 S. Gregoli, M. Olast and A. Bertinchamps, *Radiat. Res.*, 1974, **60**, 388.
30 S. Gregoli, M. Olast and A. Bertinchamps, *Radiat. Res.*, 1977, **72**, 201.
31 W. H. Nelson, E. O. Hole, E. Sagstuen and D. M. Close, *Int. J. Radiat. Biol.*, 1988, **54**, 963.
32 K. Hildenbrand, G. Belvus, D. Schulte-Frohlinde and J. N. Herek, *J. Chem. Soc., Perkin Trans. 2*, 1989, 283.
33 H. Riederer, J. Hüttermann and M. C. R. Symons, *J. Phys. Chem.*, 1981, **85**, 2789.
34 M. Fitchett, B. C. Gilbert and R. L. Wilson, *J. Chem. Soc., Perkin Trans 2*. 1988, 673.
35 P. M. Cullis, J. D. McClymont and M. C. R. Symons, *J. Chem. Soc., Faraday Trans. 1*, 1990, **86**, 591.
36 H. Riederer, J. Hüttermann, P. J. Boon and M. C. R. Symons, *J. Magn. Reson.*, 1983, **53**, 54.
37 W. A. Bernhard, *J. Phys. Chem.*, 1989, **93**, 2187.
38 J. Hüttermann, *Free Rad. Res. Commun.*, 1989, **6**, 103.
39 P. M. Cullis, I. Podmore, M. Lawson, M. C. R. Symons, B. Dalgarno and J. D. McClymont, *J. Chem. Soc., Chem. Commun.*, 1989, 1003.
40 M. C. R. Symons, *Int. J. Radiat. Biol.*, 1990, in press.
41 B. W. Wren, *Ph.D. Thesis* (Leicester University, 1985).